**Title**
500 kW DCHX PILOT PLANT EVALUATION TESTING



**Authors**
Hlinak, A.
Lee, T.
Lobach, J.
et al.

**Publication Date**
1981-10-01

LBL-13339
UC-66d

# Lawrence Berkeley Laboratory

UNIVERSITY OF CALIFORNIA

## EARTH SCIENCES DIVISION

# 500-kW DCHX PILOT-PLANT EVALUATION TESTING

A. Hlinak, T. Lee, J. Lobach, K. Nichols, R. Olander, S. Oshmyansky, G. Roberts, and D. Werner



October 1981



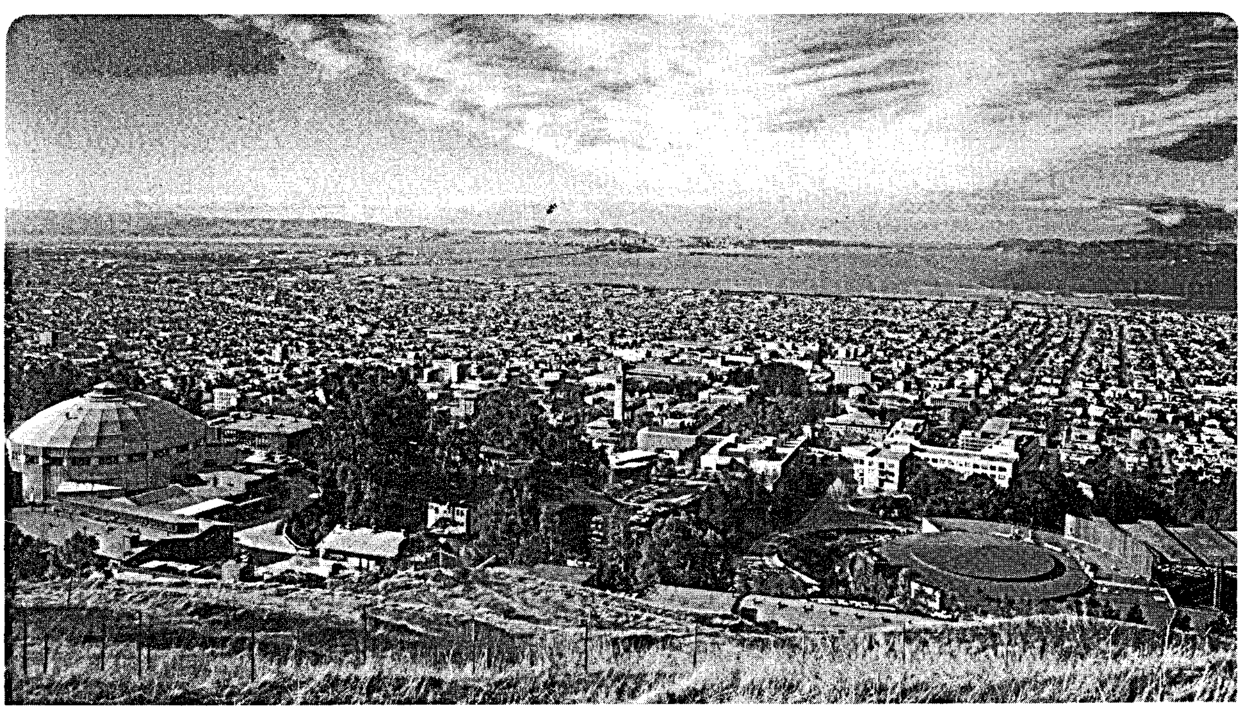

Prepared for the U.S. Department of Energy under Contract DE-AC03-76SF00098

## DISCLAIMER

**Printed in the United States of America**
**Available from**
**National Technical Information Service**
**U.S. Department of Commerce**
**5285 Port Royal Road**
**Springfield, VA 22161**
**Price Code: A06**

LBL-13339
UC-66d

DISCLAIMER



# 500 kW DCHX PILOT PLANT

# EVALUATION TESTING

LBL--18339

DE82 012328

A. Hlinak, T. Lee, J. Lobach, K. Nichols,
R. Olander, S. Oshmyansky, G. Roberts, D. Werner

October 1981

Barber-Nichols Engineering
6325 West 55th Avenue
Arvada, Colorado 80002

for

Lawrence Berkeley Laboratory
University of California
Berkeley, CA 94720

Contract 4504010

This work was supported by the Assistant Secretary for Conservation and Renewable Energy, Office of Renewable Technology, Division of Geothermal and Hydropower Technologies of the U.S. Department of Energy under Contract DE-AC03-76SF00098.

# TABLE OF CONTENTS

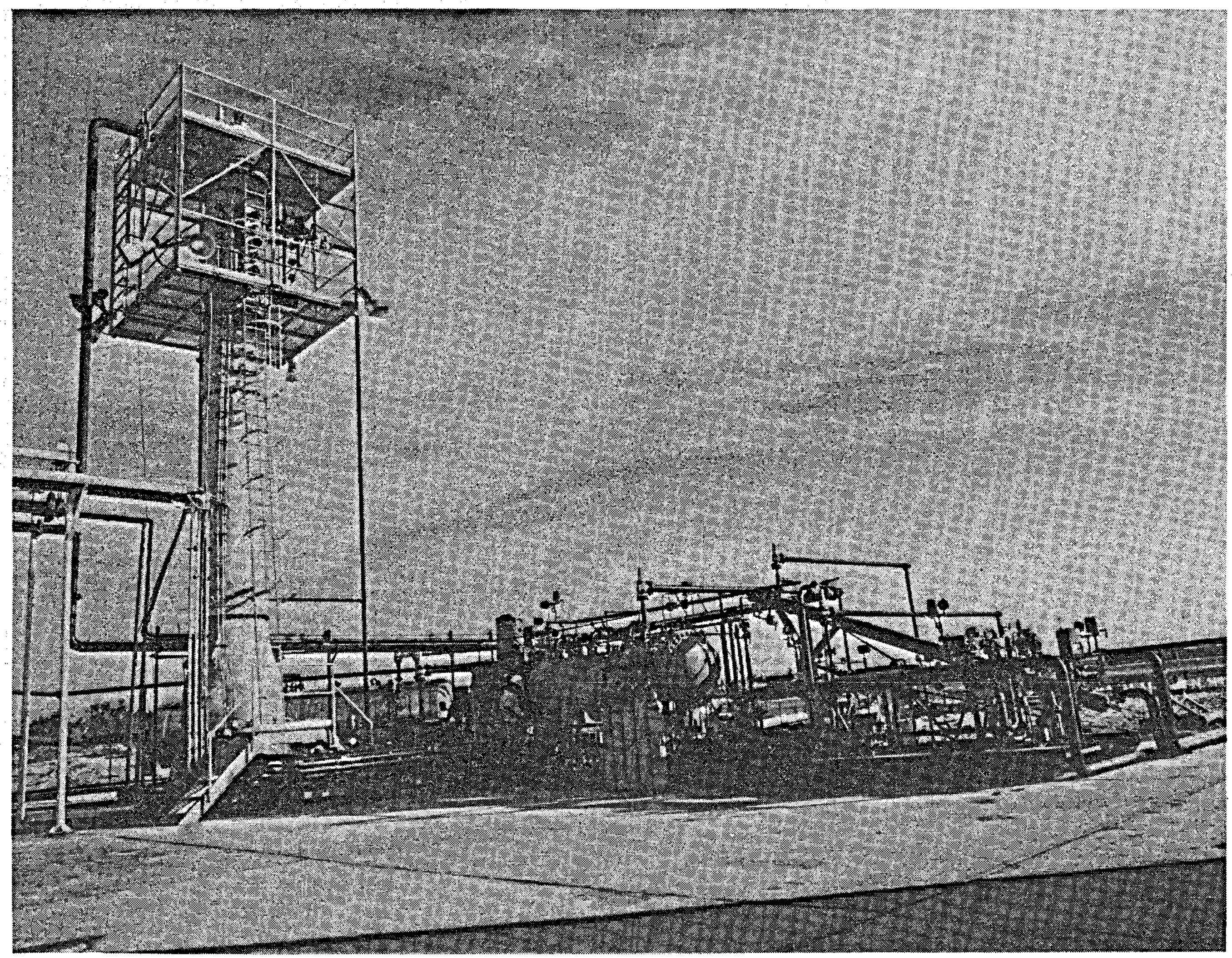

500 kW Direct Contact Pilot Plant - East Mesa, California XBC 807-8247

## 1.0 INTRODUCTION

This report covers field test results obtained with the 500 kW pilot plant at the East Mesa Geothermal Component Test Facility. The effort was performed for the Lawrence Berkeley Laboratory (LBL) and the United States Department of Energy (DOE) under LBL Contract No. 4504010. The testing was performed during the period between April 1980 and May 1981.

These results are a continuation of a DOE effort to explore the performance potential of direct contact heat exchange and to determine relative cost and operating advantages as compared to standard shell-and-tube configurations. Equipment unique to the direct contact cycle to provide for non-condensible gas handling and working fluid recovery has been designed and fabricated, and test results are reported herein.

The pilot plant was configured to accomplish two objectives: first, to evaluate the overall performance potential of direct contact power plants and second, to provide design criteria and parameters for much larger direct contact plants. The pilot plant includes all of the process functions that would be incorporated in a large plant. Incoming brine is processed to control undissolved and dissolved gases, pumped through the direct contact heat exchanger (DCHX), and then sent to a recovery system for removal of the dissolved working fluid. The working fluid is isobutane ($IC_4$). The working fluid loop includes a radial inflow turbine with generator, condensers, hotwell reservoir, and a feed pump. A downwell pump was installed in geothermal well 6-2 at East Mesa to supply the plant with unflashed brine.

The program was started in late 1977 with a design definition phase (Ref. 1). Plant construction and baseline tests were completed in early 1980 (Ref. 2). Field tests conducted during 1980 and 1981 have accomplished the following primary objectives for the pilot plant:

1. Cycle design basis for the pilot plant has been verified.
2. Performance objectives for the plant and equipment have been achieved with the exception of the turbine prime mover.
3. Direct contact performance parameters and sizing criteria have been quantified.
4. Non-condensible gas handling has been demonstrated and effects on system performance determined.
5. One method of working fluid recovery has been demonstrated and the effect on the economics of plant operation quantified.
6. The effect of scale accumulation on plant hardware was determined and a method of control demonstrated.
7. A preliminary evaluation of direct contact plant operating costs and power availability was determined.

The remainder of this report presents results obtained in the 1980 and 1981 tests.

## 2.0 SUMMARY

Field tests with the 500 kw Direct Contact Pilot Plant were conducted utilizing brine from well Mesa 6-2. The tests were intended to develop comprehensive performance data, design criteria, and economic factors for the direct contact power plant. The tests were conducted in two phases. The first test phase was to determine specific component performance of the DCHX, turbine, condensers and pumps, and to evaluate chemical mass balances of non-condensible gases in the $IC_4$ loop and $IC_4$ in the brine stream. The second test phase was to provide a longer term run at nearly fixed operating conditions in order to evaluate plant performance and identify operating cost data for the pilot plant. During these tests the total accumulated run time on major system components exceeded 1180 hours with 777 hours on the turbine prime mover.

Direct contact heat exchanger performance exceeded the design prediction. Greater brine cooling than design was achieved in the heat exchanger with measured exit brine temperatures in the range of 128$^{\circ}$F to 135$^{\circ}$F compared to a design goal of 149$^{\circ}$F. An average volumetric heat transfer coefficient of 4500 Btu/hr-ft$^3$-$^{\circ}$F was measured, which is some 20% higher than predicted by the small scale model correlations. Operating characteristics of the DCHX column were quite suitable throughout the test, although a fluctuating vapor flow from the DCHX was observed. Turbine output power was found to vary $\pm$ 10% with a typical period of 10 minutes. A temperature plateau was also found to exist in the column about 10 feet above the $IC_4$ distributor plate. The temperature in this region varied from 150$^{\circ}$F to 200$^{\circ}$F with no discernable pattern. This plateau is not understood at this time but does not appear to affect performance. Based on the measured brine cooling, a good approximation to counterflow heat transfer was achieved in the DCHX, and no indication of back-mixing of the flows was evident.

Turbine performance was evaluated during plant performance

testing. Structural problems with the turbine early in the test program prevented performance measurement with the original design. The design was subsequently modified to improve integrity and has been operated successfully about 777 hours. Turbine output power was determined by measuring the gross alternator output and adding the gearbox parasitics and alternator inefficiencies. Available expansion energy for the working fluid was calculated for the $IC_4$ including the saturated steam fraction. Flow rate was measured to the turbine using an in-line Venturi meter. The value of turbine efficiency measured in this fashion was 72-74%. Predicted design efficiency for the turbine prime mover is 83% and unanticipated disc windage losses are thought to be the cause of the discrepancy. A new turbine rotor of different design is being fabricated, and improved plant output is anticipated. If the design efficiency goal of 83% is attained for the turbine, plant utilization will exceed the design goal.

A flash extraction technique for removing the dissolved $IC_4$ from the brine exiting the DCHX was evaluated. The extracted vapors were cooled under pressure to separate the condensing $IC_4$ from the non-condensible $CO_2$ before the $CO_2$ was was discharged from the plant. Extraction reduced $IC_4$ levels in the exiting brine from 225 ppm to less than 10 ppm. The separation step was hampered by excessive levels of $CO_2$ present in the 6-2 brine, causing about 50% of the extracted $IC_4$ to leave with the discharged $CO_2$. Modifications to the recovery system have been recommended that are estimated to increase the total recovered $IC_4$ fraction to over 90%.

## 3.0 SYSTEM TEST RESULTS AND DATA ANALYSIS

The 500 kw pilot plant was designed to produce 500 net kilowatts of electricity using a direct contact heat exchanger (DCHX) with a geothermal brine resource. The geothermal resource selected for testing the plant was well Mesa 8-1 located at the Geothermal Component Test Facility at East Mesa, California. The well was anticipated to produce brine at a temperature of 340°F. The thermodynamic cycle and working fluid were selected during the design definition phase early in the program (Ref. 1). The cycle utilizes isobutane ($IC_4$) as the working fluid and has a peak cycle temperature of 225°F). Cycle state points and predicted performance are shown in Figure 3.1. The calculated cycle efficiency is 8.9% and, with a 94° condenser (64°F wet bulb), the source production factor is 5.1 watt-hrs/lb of brine flow.

The process flow diagram and selected cycle state points are shown in Figure 3.2. The incoming brine passes through a combination sand trap and carbon dioxide separation vessel. The boost pump then increases the brine pressure to 453 psia for injection into a spray column DCHX. The brine is cooled to 149°F in the DCHX and, after passing through an $IC_4$ recovery system, is returned to a facility pond for reinjection. The $IC_4$ working fluid is pumped from the hotwell to a pressure of 485 psia for injection to the bottom of the DCHX. As the $IC_4$ droplets rise to the top of the DCHX, they are heated to 255°F and taken off the top of the heat exchanger as a superheated vapor. This vapor, along with some water vapor, passes through a single-stage radial inflow turbine to the condenser where the mixture is condensed at 94°F and returned to the hotwell. The hotwell separates the condensed water and $IC_4$ liquid phases. The water fraction is directed to the recovery system, and the $IC_4$ returns to the feed pump, completing the cycle.

The design parameters for system power and parasitic loads are shown in the following table.

TABLE I

DESIGN PARAMETERS FOR SYSTEM POWER AND PARASITIC LOADS

| Component | Efficiency | Load, kw |
|---|---|---|
| Condenser motors | | 77.7 |
| Organic feed pump | $\eta_p = .75$ | |
| and motor | $\eta_m = .90$ | 96.7 |
| Brine boost pump | $\eta_p = .76$ | |
| and motor | $\eta_m = .90$ | 54.4 |
| Brine discharge pump | $\eta_p = .70$ | |
| and motor | $\eta_m = .98$ | 2.1 |
| Recovery system | | 15.0 |
| | Total electrical | 245.9 |
| Gearbox and | $\eta_{gb} = .97$ | |
| alternator | $\eta_{al} = .85$ | 61.0 |
| | Total parasitic | 306.9 |
| Power turbine | $\eta = .83$ | 776.7 |
| Hydraulic turbine | $\eta = .81$ | 30.2 |
| | Total output | 806.9 |
| | Net output | 500.0 kw |

Baseline tests were performed with brine from well Mesa 8-1. Performance obtained during these tests was reported in Reference 2. These tests demonstrated the ability of pilot plant components to meet the overall design objectives. However, the maximum brine temperature encountered with Mesa 8-1 was about 326°F. The test program was then extended to operate with brine from Mesa 6-2 which provided data closer to the 340°F brine for which the plant was designed. This section of the report describes tests with brine from Mesa 6-2 and covers the DCHX performance parameters, non-condensible handling, condenser performance, working fluid recovery, and overall plant performance. Operating experience with the 500 kw plant is also described.

## 3.1 DIRECT CONTACT HEAT EXCHANGER PERFORMANCE

### 3.1.1 Description and Design Parameters

The brine-to-$IC_4$ heat exchanger is a spray tower direct contact DCHX configuration (see Figure 3.3). The heat transfer zone is a column 40 inches in diameter by 30 feet tall. Heat exchange occurs between the $IC_4$ distributor plate and the brine injection level with preheating requiring about 27 feet and boiling and superheating occurring in the top 3 feet of the heat exchange zone. The $IC_4$ distributor plate is a perforated carbon steel plate 36 inches in diameter with 0.078 inch holes spaced 0.281 inches on staggered centers. The estimated droplet diameter is 0.125 inches. Nitric acid surface treating was used on the plate to reduce the hydrocarbon wettability and improve droplet formation. Brine is injected 12 inches below the controlled liquid level through a 2 inch diameter pipe. A flat plate covers the end of the pipe providing for radial injection of brine into the column. Isobutane and water vapor are taken from the top of the column through a horizontal demister. The demister consists of a four inch thick stainless steel mesh pad followed by chevron baffles to provide an impact-type eliminator. View ports are provided at the top of the preheater and boiler sections for visual observation. Fourteen temperature probes extending about 12 inches into the column are provided to determine temperature profiles in the preheat section. The column is flanged into two center sections 14.5 feet long so a shorter column could be tested, if desired.

DCHX heat transfer load is defined by the cycle and plant power level. The total heat load is $18.0 \times 10^6$ Btu/hr with 60% of the total heat transfer occurring in the preheater and 40% vaporizing the working fluid. The water vapor mass fraction (1.4%) was predicted for equilibrium conditions at the top of the column. The column diameter was selected to provide 90% of the flooding capacity at design flow conditions. A pinch or minimum temperature difference between the $IC_4$ and brine of $7^oF$ was predicted.

Volumetric heat transfer coefficients ($U_v$, Btu/hr-ft$^3$-$^oF$) were predicted to be 3800 in the preheater, 9375 in the boiler, and 1920 in the superheater. Respective lengths of 27 feet, 2.5 feet, and 0.5 feet result. These parameters and dimensions are based on the correlations provided in Reference 5.

### 3.1.2 Measured Heat Exchanger Performance

DCHX performance met or exceeded the design goal in all tests. The unit was tested at brine flows ranging from 100 gpm to 220 gpm and column pressures from 300 psig to 450 psig. Design and greater heat transfer rates were achieved in the DCHX while brine exit temperatures of less than design were observed. Typical values achieved were 128$^oF$ to 135$^oF$, which were significantly lower than the 149$^oF$ predicted. The larger-than-design temperature drop in the brine through the heat exchanger means that greater energy is available to the power loop and higher utilization factors (watt-hrs/lb of brine flow) can be achieved.

A typical heating curve obtained near design conditions is shown in Figure 3.4. As noted in the figure, brine inlet and exit temperatures were measured as well as $IC_4$ inlet and discharge temperatures. The $IC_4$ preheating curve was calculated assuming a pure fluid. The minimum temperature difference between the brine and $IC_4$ occurs in the preheat section. Pinch temperatures ranging from 1$^oF$ to 7$^oF$ were measured in this section, with the majority of data between 4$^oF$ and 5$^oF$. Based on these performance curves, a reasonable approximation to counter-current heat transfer is being achieved in the DCHX, which would indicate that there is not a significant amount of back-mixing occurring in the column.

Because the preheater has lower heat transfer coefficients than the boiler and a greater heat load, the preheater length is much greater than the length required for boiling. For example, Figure 3.5 shows the ratio of calculated boiler length to liquid length as a function of column presusre. The proportion of boiler length becomes much less as the pressure level approaches critical pressure. Above critical pressure the entire column could be considered a preheater.

Pilot plant data was used to evaluate heat transfer performance of the preheater. For purposes of this evaluation the preheater volume ($V_p$) was determined by subtracting the estimated boiler volume from the total volume. The boiler volume was estimated from the total heat required to boil, the calculated logarithmic mean temperature difference for the boiler, and an estimated volumetric heat transfer coefficient of 9375 Btu/hr-ft$^3$-$^o$F (Ref. 9, 12).

A length-weighted mean temperature difference for the preheater was calculated using the following procedure. The preheater volume was divided into 20 zones and the heat transferred and mean temperature difference calculated for each zone. Then the total mean temperature difference was calculated from:

$$\overline{lmtd} = \frac{\dot{m}_{IC_4}(h^{sat}_{IC_4} - h_{IC_4})}{\sum_{i=1}^{20}\left(\frac{q_i}{lmtd_i}\right)}$$

and
$$Q_{PH} = \dot{m}_{IC_4}(h^{sat}_{IC_4} - h^{in}_{IC_4})$$

where $q_i$ is the heat transferred in the $i^{th}$ increment and $lmtd_i$ is the lmtd of the $i^{th}$ increment. $Q_{ph}$ is the total heat transferred in the preheater. Finally, the preheater volumetric heat transfer coefficient was calculated from:

$$U_V = \frac{Q_{PH}}{V_p\,\overline{lmtd}}$$

Data from a number of runs is shown in Figure 3.6. As may be noted, at a brine flow of 200 gpm the majority of data shows average values of heat transfer coefficient of about 4500, which is about 20% higher than design. The very low pinch temperature differences shown in the figure may have some small error due to inaccuracies of the temperature instrumentation, estimated at ± 0.5$^o$F.

Heat transfer performance has not been evaluated in terms of the Woodward or Letan-Kehat correlations which define heat transfer as a function of holdup. Attempts made during early testing to measure holdup were not successful and an accurate technique has not yet been devised.

Operating experience with the pilot plant has shown a fluctuating output flow from the DCHX. This is evidenced by a periodically varying turbine output power with constant input flows of $IC_4$ and brine into the DCHX. Turbine output power varies $\pm$ 10% with a typical period of about 10 minutes. While the cause of this variation has not been identified, it has no discernible adverse effects on overall plant operation.

Characteristic temperature versus length profiles are shown in Figure 3.7. Data sets were obtained both 1 foot from the wall and with probes extending to the center line of the vessel. Both data sets gave similar results. An unexplained temperature plateau occurs in the column approximately 10 feet above the $IC_4$ distributor plate. The temperature in this region varies from about 150$^{o}$F to about 200$^{o}$F with no discernible pattern. This temperature plateau does not seem to affect the counterflow nature of heat transfer occurring in the vessel.

Water vapor produced by the DCHX was monitored by measuring the water flow after separation in the hotwell. Data obtained is shown in Figure 3.8. At a peak temperature of 255$^{o}$F, the measured water fraction averaged 2.1% by mass, which was about 50% larger than predicted (see Appendix A). Since the water flow is a small fraction of the total flow, this difference in flow amounts to less than a 2% increase in system output as compared to the design prediction.

This analysis of the DCHX performance is based on an assumption of complete immiscibility of the brine and isobutane working fluid. An alternative approach to the analysis of the spray tower performance has been studied at LBL by P. Rapier (Ref. 4). He has predicted the thermodynamic properties of the isobutane-water mixture and used these to establish the DCHX's boiling point elevation and vaporization efficiency. While the end-point thermodynamic state conditions predicted by both methods are the same, the mixture properties more accurately predict the water vapor content of the DCHX exit vapor stream. The approach taken by Rapier becomes more important as the relative miscibilities of the working fluid and brine increase.

The test series with the DCHX was considered very successful. The heat exchanger operated as expected, and no problems were encountered with startup or operation. On several occasions the vessel was shut down abruptly by closing the inlet and exit valves with no significant changes in vessel pressure. Stable column operation has been consistently maintained without undue difficulties.

Advantages of direct contact heat exchange were demonstrated in terms of heat transfer performance with reasonable size and low first cost as compared to conventional shell-and-tube exchangers. As reported in Section 3.6 of this report, no problems with carbonate or silica scale in the DCHX were observed through the test series.

Additional tests are planned with the DCHX to investigate brine inlet geometry, shorter column lengths, and possible flow straighteners in the column. These tests are intended to improve the measurement of heat transfer coefficients and investigate flow fluctuations in the column.

Subsequent to the design of the DCHX, additional work has been done to understand the heat and mass transfer characteristics of direct contact heat exchangers. These studies have focused on a mass transfer model (Ref. 5), heat transfer during droplet formation (Ref. 6), and the comparison between a spray tower and a tray tower (Ref. 7). The results of these studies will be used to analyze the planned future tests.

## 3.2 $CO_2$ EFFECTS ON SYSTEM PERFORMANCE

In the direct contact process non-condensible gases are stripped from the brine by the $IC_4$ and are carried to the condenser. These gases tend to reduce power production and system efficiency due to increased turbine back pressure. Although the heat transfer process is enhanced by the large surface area generated by the $IC_4$ droplet swarm rising in the brine stream, the process promotes the mass transfer of non-condensible gases dissolved or entrained in the incoming brine into the working fluid stream. After passing through the power turbine, the non-condensing gases separate from the working fluid in the condenser where the concentration builds until the gases redissolve in the liquid working fluid and an equilibrium condition in the loop is established. The non-condensible buildup elevates the pressure in the condenser, reducing turbine output power and resource utilization. This effect is shown quantitatively in Figure 3.9. While trace amounts of $N_2$, $CH_4$, and $H_2S$ can be found in the brine used, by far the most significant non-condensible is $CO_2$.

A major effort was undertaken during this test phase to 1) correlate quantitatively the pressure elevation in the condenser with the dissolved $CO_2$ level in the incoming brine, and 2) demonstrate a viable approach to control this pressure elevation to acceptable levels.

### 3.2.1 Design Approach

Control of the condenser pressure elevation due to non-condensibles can be achieved by flashing the incoming brine from the well into a tank (sand trap) to control the quantity of non-condensibles remaining in the brine injected into the DCHX. Flashing is accomplished by spraying brine into the vessel through two spray nozzles to provide single-stage flash separation of $CO_2$ and other dissolved gases. The steam-$CO_2$ vapor mixture produced is vented from the sand trap and directed to a shell-and-tube heat exchanger where thermal energy is recovered by preheating and vaporizing a small sidestream of $IC_4$. Detailed component descriptions can be found in Reference 2. Early analysis of $CO_2$ equilibrium in the process loop indicated that reduction of dissolved $CO_2$ to 50 ppm in the incoming brine would reduce $CO_2$ buildup in the condenser to approximately 2 psi. For non-condensible levels of 800 ppm, typical of brine from East Mesa well 8-1, this corresponds to a total flash of about $5^{o}F$. For the 2000 ppm levels found in well 6-2, a total single-stage flash of about $20^{o}F$ is required.

### 3.2.2 Plant Operating $CO_2$ Levels

$CO_2$ levels were monitored in the brine out of the primary flash tank (B2, see Figure 3.2), in the $IC_4$ in and out of the DCHX (WF1 or WF2), and in the condensate vapor phase in the condenser exit manifold over a range of flash conditions. Details of the measurement process and sampling locations are covered in Appendix B.

At equilibrium, $CO_2$ released from the brine at the top of the DCHX is replaced by $CO_2$ injected into the column with the $IC_4$. There is an insignificant amount of $CO_2$ dissolved in water leaving the hotwell and a minor amount returning to the hotwell from the recovery system; therefore, brine leaving the DCHX has the same level of $CO_2$ as when it enters. Likewise, the compositions of the working fluid in and out of the DCHX (WF5 and WF1) must be the same (except for the water fraction) when the system is at equilibrium.

The measured concentration of dissolved $CO_2$ leaving the sand trap is shown in Figure 3.10 along with a comparative theoretical prediction. The prediction is based on classical flash calculations and values of Henry's law constant for $CO_2$ in saline solutions reported by Ellis and Golding (Ref. 8). A derivation is shown in Appendix C. While some deviation from the predicted value is apparent, reasonable agreement is shown.

The measured total pressure in the sand trap is the sum of the saturation pressure of water and the partial pressure of non-condensible gases released during the flash. Assuming the non-condensible fraction is essentially $CO_2$ and using the measured sand trap discharge temperature to determine the saturation pressure of the brine, the Ellis and Golding data allows a calculation of the dissolved $CO_2$ remaining in the brine (see Appendix C). Figure 3.11 shows a comparison of this calculated value and the measured $CO_2$ level (Appendix B) out of the sand trap. The very good agreement suggests sand trap pressure and temperature measurements provide a good estimate of dissolved $CO_2$ entering the DCHX.

The measured concentration of $CO_2$ in the working fluid stream as a function of DCHX brine inlet concentration is shown in Figure 3.12. The data suggests the $CO_2$ is concentrated in the working fluid loop by a factor of about 7.9 and agrees well with the factor of 9 used for the pilot plant design.

A correlation of the pressure elevation in the condenser, as a function of dissolved $CO_2$ entering the DCHX, is shown in Figure 3.13. The pressure elevation is obtained by subtracting the sum of the saturation pressures of $IC_4$ and $H_2O$ at the measured condensate temperature from the measured total pressure of the condensers. The pressure elevation, therefore, includes the effect of other non-condensibles (principally propane found in the $IC_4$ feedstock) and any subcooling of the condensate. The indicated theoretical line is based on a concentration factor of 7.9 across the DCHX, a residual elevation due to other non-condensibles of 2.5 psi (estimated from G.C. analysis) and an estimated $3.5^{o}F$ of condensate subcooling (see Appendix D).

### 3.2.3 Effect on Condenser and Plant Performance

Flashing the brine to reduce dissolved $CO_2$ levels resulted in reduced pressure elevation due to $CO_2$ accumulation in the condenser. Extensive flashing, however, adversely effects the electrical generating potential of the resource by reducing the temperature of the brine sent to the DCHX. While this effect is minimized by recovering the latent and sensible energy of the steam/non-condensible mixture generated, determination of the optimum flash conditions required comparing the improvement due to condenser pressure reduction to the loss in system output due to the lower brine inlet temperature.

The results of such a comparative analysis for a single-stage flash are shown in Figure 3.14. Here the empirically determined effect of $CO_2$ concentration in the brine on the condenser pressure elevation (Figure 3.13) and the corresponding heat recovery system performance (Figure 3.15) were used to calculate the expected generating performance (expressed as watt-hrs/lb brine) as a function of flash pressure. While an apparent optimum exists in the vicinity of 115 psia (corresponding to 8°F of flash and a $CO_2$ level entering the DCHX of 205 ppm), the generating performance test data displays only modest sensitivity to flash pressure, indicating the improvement in condenser pressure elevation was largely offset by the resulting brine inlet temperature loss.

### 3.2.4 Heat Recovery System Performance

Flashing the brine to remove $CO_2$ produced a steam/$CO_2$ mixture which was vented to the binary heat exchanger where the thermal energy in the mixture was transferred to a sidestream of $IC_4$. The $IC_4$ flow rate was controlled so that saturated $IC_4$ vapor was produced. Instrumentation limitations restricted our ability to measure the heat balance across the heat exchanger. An evaluation of the data indicated that there was a reasonable heat balance and therefore the performance presented in Figure 3.15 is a good representation of the heat recovered.

## 3.3 CONDENSERS

The condenser module consists of four separate Baltimore Air Coil evaporative condensers modified for the specific application. Each condenser unit requires a 450 gpm recirculating water pump and three axial flow fans which provide a combined air flow of 79,000 cfm. Condenser modifications included explosion-proof motors and oversized fans. The condensers are elevated to provide a vertical liquid barometric leg between the condensate exit and the hotwell. Additionally, the hotwell is vented to the vapor inlet of the condensers to prevent hotwell vapor buildup and facilitate condenser liquid drainage.

### 3.3.1 Design Approach

Table II summarizes the condenser module design point interface conditions. The design entering air wet bulb temperature of 64°F was selected from comparisons of condenser size, cost, cycle performance and East Mesa weather conditions. Design working fluid inlet pressure is 70 psia, and the nominal condensate temperature is 94°F. The working fluid composition is estimated to be 27.2 lb/sec isobutane vapor, 0.39 lb/sec water vapor and 0.012 lb/sec $CO_2$. The water vapor is saturated with an 88.3% quality. The design condenser heat load is 17.0 x $10^6$ Btu/hr assuming no liquid subcooling. The predicted electrical parasitic load of the fans and pumps is 75 kw at design.

### 3.3.2 System Operation and Field Experience

Condenser performance, expressed as the difference between saturated condensing temperature and entering air wet bulb temperature, is presented in Figure 3.16. The data indicates the condenser field performance exceeds predicted performance over a range of wet bulb temperatures from 47 to 56°F. Predicted performance was extrapolated from the manufacturer's tested design performance.

The condensing temperature of a condensing vapor/non-condensible gas mixture is not isothermal. As the vapor is condensed, the mixture becomes richer in non-condensibles, and the $IC_4$ partial pressure and condensing temperature decrease accordingly. Thus, condenser performance was plotted using a weighted average condensing temperature.

TABLE II

CONDENSER DESIGN CONDITIONS

| | |
|---|---|
| Entering Air Wet Bulb Temperature | $64^{o}F$ |
| Entering Air Dry Bulb Temperature | -- |
| Nominal Working Fluid Inlet Pressure | 70 psia |
| Condensate Temperature | $94^{o}F$ |
| Working Fluid: | $IC_4$, 27.2 lb/sec |
| | $H_2O$, 0.39 lb/sec |
| | $CO_2$, 0.012 lb/sec |
| Entering $H_2O$ quality | 88.3% |
| Temperature of Entering Working Fluid | $142^{o}F$ |
| Heat Load | $17 \times 10^6$ Btu/hr |
| Electrical Requirements | 75 kw, 440 v, 3 Ø |
| Makeup Water | 80 gpm at 30 psi |
| Blowdown | 40 gpm (maximum) |

This weighted average temperature was calculated by adding two-thirds of the difference between the initial and final condensing temperatures to the final condensing temperature. The initial condensing temperature is equal to the saturation temperature of the $IC_4$ at its entering partial pressure as determined from measured entering condenser pressure and $CO_2$ concentration. Final condensing temperature for this analysis was calculated by adding a constant value of $3^oF$ to account for subcooling to the measured exit condensate temperature. This procedure was used to approximate a length weighted average condensing temperature. Based on theoretical calculations, using the method of Colburn and Hougen to predict the non-condensible effect on condenser performance, the approximation is reasonable for the non-condensible concentration encountered in testing.

### 3.3.3 Scale Accumulation

Limited carbonate scale accumulation has been observed on the evaporative water side (outside) top two rows of condenser tubes. The deposits are typically white or rust-colored calcium carbonate approximately 0.13 inches thick. The accumulated scale was removed with an 800 psi water spray or by wire brushing after every 200 to 300 hours of operation.

The initial design approach for eliminating exterior tube fouling focused on treating the recirculated cooling water. Based on previous experience carbonate scale formation could be minimized by maintaining the water pH level near 7.0, and the total dissolved solids (TDS) concentration below 13,000 ppm. The water treatment unit was designed to control and monitor pH and TDS, and to inject a biocide at predetermined intervals to prevent biological fouling. The consumption rate of the treatment chemicals was monitored during the 500 hour endurance test. Based on this test a cost of 5 mills/kw-hr is estimated for a plant using makeup water with a TDS of approximately 2300 ppm.

Although the limited scale formation had no discernible effect on condenser performance, the required maintenance interval of 200 to 300 operating hours was not acceptable. The scaled tubes experienced the highest operating temperatures and, accordingly, the greatest cooling water evaporation rates. The cooling water did not keep the surface of these tubes wet, which allowed the carbonate to precipitate and harden. This condition occurred most often when the hot $IC_4$ flow bypassed the power turbine.

An isobutane spray desuperheater was added to the turbine exhaust line after 500 hours of plant operation. The desuperheater sprays liquid isobutane into the superheated vapor in the exhaust line ahead of the condensers. This liquid spray lowers the temperature of the entering vapor, but because of the increased flow rate, does not reduce the heat load on the condenser. After an additional 500 hours of operation the tubes had no apparent additional scale accumulation.

## 3.4 WORKING FLUID RECOVERY

Intimate mixing in the direct contact heat exchanger promotes some degree of mass transfer of the $IC_4$ working fluid into the brine. Actual loss ratios experienced (in lieu of recovery system) may be affected by the salt content of the brine used, the presence of non-condensibles, the DCHX operating pressure, and the residence time. In addition to the diffusion of working fluid into the brine, huge losses occur if the brine entrains whole droplets emerging from the distributor plate and carries them out the bottom of the DCHX. This carryunder condition is avoided by proper selection of the column design (Ref. 9), which determines the operating limits with respect to brine throughput. A loss of 250 ppm of $IC_4$ represents an economic penalty of $\$1.2 \times 10^6$/yr for a 50 MW plant based on current prices.

Major goals of the extended test phase included 1) determination of loss rates of dissolved $IC_4$ leaving the DCHX, 2) testing for limiting carryunder conditions at high brine throughputs, and 3) investigation of the potential for a simple recovery system utilizing vacuum extraction of dissolved $IC_4$.

### 3.4.1 Recovery Approach

Various methods have been proposed (Ref. 9, 10, 11) for recovering working fluid in DCHX cycles. These include vacuum extraction, gas stripping, absorbents, and salt addition. A system based on vacuum extraction was included in the design of the pilot plant to provide a performance reference with which to compare other approaches. The spent brine from the DCHX flashed twice before being rejected from the plant - initially to a pressure of about 2 atmospheres in the tailstock vessel and finally to a moderate vacuum (5-7 psia) in the recovery tank. The vapors generated during each flash contain dissolved $IC_4$, water vapor, and varying amounts of $CO_2$ and minor non-condensible gases present in the brine. These vapors are compressed and cooled to condense the $IC_4$ fraction which is then returned to the hotwell. The remaining gas phase, rich in $CO_2$, is vented to the atmosphere. A detailed description of the recovery system design can be found in Reference 2.

The recovery performance of this type of system is strongly influenced by the amount of $CO_2$ and other non-condensible gases that must be handled along with the $IC_4$. Since a relatively fixed fraction of the gas phase eventually vented is $IC_4$, more of the working fluid is lost at the higher vent flows required with increased non-condensible handling. The recovery system was originally designed to process spent brine from East Mesa well 8-1 after an initial $5^{o}F$ flash in the sand trap, resulting in an estimated dissolved $CO_2$ level of 50 ppm. For this $CO_2$ level the system is expected to extract 95% of the incoming dissolved $IC_4$ (estimated at 200 ppm) from the brine and return 84% of this amount to the hotwell, resulting in an overall recovery efficiency of 80%.

### 3.4.2 Working Fluid Recovery Performance

The contact time for $IC_4$ absorption by the brine is inversely proportional to the brine flow rate. The measured $IC_4$ concentration in the brine leaving the DCHX is plotted as a function of DCHX pressure in Figure 3.17a and as a function of flow rate in Figure 3.17b. A complete description of measurement technique is included in Appendix B. Measurements of the gas composition in the head space above the stripped brine and those inferred from the measured composition and the flow rate from the compressor, along with various degrees of the theoretical saturation limit of $IC_4$ dissolution in water are shown in Figure 3.17a for comparison. The range in brine flow rate shown in Figure 3.17b represents a range in residence time of from 8 to 12 minutes. While a certain amount of scatter is apparent with both techniques, the data indicates 1) the brine exits the DCHX with dissolved $IC_4$ levels of 10-50% of the maximum saturation limit and 2) this level shows little dependence on the residence time of contact between the $IC_4$ and brine streams in the DCHX.

While not included in Figures 3.17a or 3.17b, several of the brine samples collected at the DCHX exit showed $IC_4$ levels in excess of the saturation limit at flow rates as low as 83 x $10^3$ lb/hr (the stripping technique was not available when the lower flow rates shown in Figure 3.17b were run). In each of these cases, however, no appreciable increase was observed in the $IC_4$ levels measured exiting the recovery compressor, contradicting the liquid sample analysis and suggesting no significant carryunder of liquid $IC_4$ was occurring. Further sampling has been proposed to resolve this apparent discrepancy. Corresponding samples of the brine leaving the recovery tank showed consistently low residual $IC_4$, indicating that any liquid phase $IC_4$ exiting the DCHX was effectively extracted by the recovery system.

From continuity considerations, the difference between the total $IC_4$ leaving the DCHX and that returned to the hotwell by the recovery system must show up as a level change in the hotwell. This level change and the total returned by the recovery system were measured, and the average concentration in the brine leaving the DCHX was calculated. The resulting value, 247 ppm, agrees well with the data obtained by the other techniques described.

Figure 3.18 shows the measured residual $IC_4$ leaving the recovery system. This GC data was obtained using both the stripping technique and complete liquid sample injection techniques as described in Appendix B. Because of the problems with $IC_4$ detection using the liquid sample injection technique, the stripping data is considered to be significantly more accurate. The representative ranges of measured $IC_4$ entering the recovery system in the brine are shown (shaded region) for reference. The low residual values indicate that vacuum extraction effectively removes the dissolved $IC_4$ from the brine over a range of recovery tank pressures. Theoretical residual limits based on an equilibrium assumption are in the 1 to 3 ppm range for the operating conditions represented. A model for the single stage recovery flash system may be found in Appendix E.

The measured performance of the recovery system as a function of the dissolved $CO_2$ level is shown in Figure 3.19. The three data points are based on an estimated average $IC_4$ level exiting the DCHX of 250 ppm. The original design goal of recovering 80% of the $IC_4$ with a $CO_2$ level of 50 ppm in the brine (assuming a recovery condenser pressure of 90 psia) and the experienced recovery performance are shown for comparison. Preflashing to remove $CO_2$ from the brine dramatically improves the performance of this type of recovery system.

## 3.5 OVERALL PLANT PERFORMANCE

Pilot plant performance has been evaluated in terms of brine utilization. This parameter is defined as the net plant output (watts) divided by the brine flow rate (lb/hr). The net plant output was determined by deducting electrical parasitic losses for the plant including condenser power requirements, $IC_4$ and brine pumping power, and recovery system power from the gross turbine output. Temperature limits for the power generation cycle are bounded by the geothermal resource at the high end and, using evaporative condensers, ambient wet bulb temperature at the low end. Maximum brine utilization cycle performance is achieved when the plant output is a maximum for a given brine flow rate.

Because of high resource costs, a maximum utilization also yields a near cost-optimum cycle, so long as reasonable temperature differences are maintained for the heat exchange equipment. For example, the 500 kw pilot plant was designed for a 7.0°F pinch temperature difference in the DCHX, and a 30°F difference (condensing temperature minus wet bulb) for the evaporative condensers. With these constraints, 500 kw cycle design conditions were selected at a peak temperature of 255°F, resulting in a cycle utilization of 5.1 watt-hrs/lb. Increasing the boiling temperature above 250°F produces a slight gain in source utilization (Ref. 1), but it also causes the absolute pressure level in the system to rise, resulting in higher system costs. An increase in the system pressure level also makes both brine and $IC_4$ pump performance more critical to the achievement of overall performance goals.

Field tests have essentially verified the performance prediction and, with the exception of the power turbine, all components are performed as expected. The predicted electrical parasitic power was 246 kw. Based on field tests, the measured loss was between 250 and 260 kw including plant service equipment such as air compressors, which verifies the above prediction. The remainder of this section presents data obtained during this test series.

### 3.5.1 System Utilization

Figure 3.20 shows measured plant utilization as a function of boiling temperature for the 500 kw pilot plant. Data shown was taken near design brine flow rate and was corrected to a constant 54°F wet bulb temperature, since the actual data points were taken at a range of ambient wet bulb temperatures (45°F to 54°F). The correction involved estimating condensing pressure and adjusting the turbine available energy to determine the gross turbine output. Measured parasitic losses were then deducted to calculate the net plant power production. The maximum utilization appears to be between 4.5 and 4.7 watt-hrs/lb of brine flow at an $IC_4$ boiling temperature of 250°F.

Wet bulb or condensing temperature has a strong influence on plant utilization. For example, increasing wet bulb from 54$^{o}$F to 64$^{o}$F results in a predicted increase in condensing temperature of about 7$^{o}$F. This would, in turn, reduce plant utilization from the value of 4.7 at 54$^{o}$F to 4.3 watt-hrs/lb of brine flow at an ambient wet bulb temperature of 64$^{o}$F.

### 3.5.2 Turbine Performance

The turbine prime mover for the 500 kw pilot plant is a radial inflow design operating at a speed of 25,000 rpm. The impeller is 7.75 inches in diameter, and the predicted efficiency is 0.83 at the design conditions specified in Section 3.0. The turbine is equipped with variable nozzles that give an adjustable throat area. At a constant inlet pressure, flow rates from 60 to 120% of design can be accommodated with small changes in turbine efficiency. Turbine shaft speed is reduced to 1800 rpm to drive a synchronous alternator using a double reduction gearbox.

Turbine efficiency was evaluated during these tests by measuring the gross electrical power out of the alternator. Manufacturer's data for alternator efficiency (79% + 18 kw fixed loss) was used to determine alternator input power and, using a gearbox loss estimate of 21 kw, the turbine shaft output power was calculated. Turbine flow rate was measured with a Venturi meter located upstream of the turbine and the available energy calculated using the MBWR equation of state for isobutane and including the expansion energy for the saturated steam fraction. Previous tests of a 10 kw power system using direct contact heat exchange and an axial flow turbine were evaluated in the same fashion (Ref. 12). Turbine performance data reasonably matched predicted performance, and confidence was established in predicting $IC_4$ and water available energy with this 10 kw system.

Figure 3.21 shows the variation of 500 kw turbine efficiency obtained over a continuous run during the endurance testing. The decrease in efficiency over time shown in the figure is the result of changing plant conditions during the run and not degradation. Volumetric flow rate decreased, which resulted in the observed drop in efficiency. The value of turbine efficiency varies from 72% to 67% and matches performance data obtained during other runs at the same conditions. A new turbine rotor of different design is being fabricated in an attempt to improve overall plant output. Assuming that the design efficiency of 83% is achieved in tests, the gross plant output will improve from about 680 kw at design brine flow rate and 64°F wet bulb temperature to 773 kw. With 260 kw electrical parasitic loads, the projected net plant output is 513 kw, which will exceed the design goal.

### 3.5.3 Performance Comparison to Design

As shown in the preceeding section, the pilot plant was operated over a range of brine flow rates and ambient conditions. Table III shows the measured performance compared to design. The DCHX and condensers exceed design performance. With the exception of the turbine, the remainder of the hardware is achieving design goals. Even with increased $CO_2$ levels encountered with Mesa 6-2 brine, the plant's tested performance meets design performance objectives if the low turbine performance is accounted for.

## 3.6 PLANT OPERATION EXPERIENCE

### 3.6.1 General Plant Performance

The Direct Contact Heat Exchanger and the basic power plant configuration have proven to be simple to operate and inherently dependable. The DCHX is readily started and shutdown and thermal shock is not a concern (as it is with tube and shell units). Starting a cold DCHX does require that a simple startup procedure be executed, but once the DCHX is up to temperature, the plant can be started by bringing both brine and $IC_4$ flow immediately up to the required levels.

From a safety, as well as an operation standpoint, the plant

# TABLE III

## 500 KW PLANT DESIGN TEST PARAMETERS

| DCHX | Design | Range of Test Conditions |
|---|---|---|
| Brine flow, gpm | 216 | 100 - 215 |
| Brine in temp, $^oF$ | 340 | 336 - 340 |
| Brine exit temp, $^oF$ | 149 | 128 - 135 |
| Pressure, psia | 450 | 300 - 450 |
| $IC_4$ in temp, $^oF$ | 95 | 70 - 85 |
| $IC_4$ exit temp, $^oF$ | 255 | 230 - 260 |
| $IC_4$ flow, gpm | 367 | 160 - 365 |
| **Power Generation** | | |
| Utilization, w-hr/lb | 5.1 | 4.5 - 5.0 |
| Gross power, kw | 750 | 700 |
| Net power, kw | 500 | 450 |
| Turbine efficiency | 83% | 67 - 72% |
| **Condenser** | | |
| Heat load, Btu/hr x $10^6$ | 16.9 | 9 - 20 |
| Wet bulb, $^oF$ | 64 | 45 - 63 |
| Condenser temp, $^oF$ | 94 | 65 - 80 |
| **Flash System** | | |
| Brine out temp, $^oF$ | 335 | 335 - 310 |
| $\Delta T$, $^oF$ | 5 | 0 - 25 |
| $CO_2$ inlet, ppm | 850 | 2000 |
| $CO_2$ exit, ppm | 50 | 300 - 800 |
| **Recovery System** | | |
| $IC_4$ in brine out of DCHX, ppm | 200 | 150 - 300 |
| $IC_4$ in brine exiting plant, ppm | 10 | $<10$ |

can be shut down completely, instantly and without any post-operational concern or action required. Safety is a prime consideration in the plant due to risks inherent in using $IC_4$ as the working fluid. The current plant configuration meets the objective of high safety standards.

The plant controls are not designed for completely automatic operation; however, once the operating flow rates have been established these flows can be held automatically and the plant will run indefinitely without any adjustment. Parametrically it is possible to add a minimum of control hardware, preset the desired operating point, and have the plant seek and hold the setting.

In general, operational problems have been hardware related except for carbonate scaling problems and the poor reliability of the downwell pumps. The equipment failures were typical pilot plant type failures and were not related to the geothermal or DCHX process. The scaling problems were solved by injection of a scale-inhibiting additive, supplied by Pfizer Central Research, into the incoming brine. A more detailed discussion of scale-related effects is given in Section 3.6.2. The recovery compressor used in the plant is the only major component that experienced repeated failures. The seals in the compressor were not performing, allowing water to enter the crankcase and resulting in bearing failure. Modifications are proposed to eliminate these failures. The experience to date with the plant indicates that the basic configuration which was developed can be readily scaled up to commercial plant applications with power levels in the 5 to 50 megawatt range.

### 3.6.2 Scale Accumulation and Effects

One of the major problems encountered in geothermal power plants is the formation of calcium carbonate scale. Scale deposits on rotating machinery, valve seats and in piping have a measurable effect on plant performance and are one of the most common causes of plant shutdown.

To minimize the effect of non-condensible pressure buildup in the condenser, $CO_2$ is stripped from the incoming brine by flashing the brine into the free space of a pressure vessel. The vessel pressure is maintained to achieve a $5^{o}F$ brine flash. Removing too much of the $CO_2$ can result in carbonate scale deposition. The sand trap/flash tank was designed to provide adequate residence time and a large deposition surface for the calcium precipitates. Based on limited prior experience with this approach, it was postulated that detrimental scale formation should be confined to the sand trap/flash tank and that there should be no severe scaling problems in the high pressure brine downstream of the boost pump.

The sand trap/flash tank design configuration was determined by the functions it is required to perform. First, as the name implies, it is intended to provide a retention area for entrained solids to settle out of the incoming brine. The second function is to strip free $CO_2$ from the brine stream by flashing. The vessel was sized to provide sufficient residence time for the $CO_2$/flashed brine mixture to come to equilibrium. The third design consideration is to provide a large surface area for carbonate deposition. This was accomplished by the addition of expanded metal baffles which have a large surface area and direct the flow longitudinally through the tank to help increase the residence time.

During the first year of operation, the plant experienced continuous scale buildup problems within the flash tank and piping between the flash tank and DCHX. Problems first occurred in the automatic and manual bypass valves around the boost pump. These valves required maintenance approximately every 70 hours of operation due to valve sticking. The automatic valves failed due to a light film buildup which occurred on the close clearance parts. The manual valve problems were due to carbonate buildup on the valve seats.

Other scale related failures in the inlet brine piping included partial blockage of the bypass flow orifice and failure of the DCHX inlet brine flow switch. The wellhead flowmeter also failed when blocked by carbonate deposits. These were single occurrences and, in general, did not affect plant performance.

The 14-stage brine boost pump used to transfer brine from the flash tank to the DCHX exhibited a decrease in flow capacity after 110 hours of operation. Inspection revealed considerable scale buildup in the bowls and impellers. Five of the 14 carbon graphite bearings were worn out because of scale buildup, and the 17-4 PH pump shaft was worn at the bearing surfaces. The pump was rebuilt with 17 stages using a 416 stainless steel shaft and bronze replacement bearings. This was the only boost pump failure to occur while using brine from well Mesa 8-1.

Brine production was shifted to well Mesa 6-2 after 123 hours of plant operation. Scaling and related failures were expected to increase because of the higher $CO_2$ concentration in the brine from 6-2. The operating life of the brine boost pump decreased, as expected, after changing the brine source. There were eight pump failures directly attributable to calcium carbonate scaling with an average time of 65 hours between failures. To minimize pump damage in disassembling the scaled-up assemblies, it became standard procedure to soak the pump in inhibited muric acid to dissolve as much $CaCO_3$ as possible. Following reassembly, an acid solution was circulated through the brine system to reduce scale buildup elsewhere in the system.

Prior to starting the second year of operation, two modifications were made to the brine handling system. The original brine boost pump was replaced after 700 operating hours and a brine antiscalant injection unit was installed. The unit, supplied by Pfizer Central Research, Inc., was designed to inject chemical additive Flocon 247 into the brine line upstream of the sand trap. This additive is maleic acid containing a polymeric scale inhibitor. Use of the Pfizer treatment measurably reduced scale accumulation in the system (Ref. 13). Scale buildup on the sample coupon located in front of the brine boost pump was reduced by a factor of 100 with a 2.0 to 4.5 ppm dosage of Flocon 247 and, more significantly, the new boost pump has had no failures during the 580 hours of operation since the addition of the Pfizer treatment unit.

Analysis by gas chromatography indicates that the Pfizer treatment does not alter the chemical balance of the direct contact column; however, a physical effect of the additive was observed in the column. The upper viewports showed an accumulation of particulates which appeared as soft wax suspended in the brine. Initial speculation assumed that the suspended particles were the result of residual scale removal; however, the amount has not decreased with continued plant operation and appears to be associated with action of the additive in the column.

The scale deposits found in the sand trap were analyzed before and after the introduction of the Pfizer additive and contained the same primary constituents. Additionally, the brine was analyzed for total dissolved solids (TDS) at several points in the brine handling system. Measured TDS levels ranged from a maximum of 4644 ppm at the wellhead to 4153 ppm at the brine return pump.

Operating experience with the turbine indicated that the DCHX concept does not result in significant brine carryover or turbine scaling problems. Turbine inspections were made at 110 hours, 220 hours and 780 hours of operating time. A moderate amount of scale buildup was observed on the turbine blades and nozzles. The buildup was visually identical at each inspection regardless of exposure time or addition of scale inhibitors. Scale buildup was measured in all three inspections and ranged from a few thousandths of an inch to 0.015 inches, depending on the relationship of the surface to gas velocities and impingement. The smallest deposited amounts occurred where gas velocities were highest. A sample of the turbine scale was qualitatively analyzed using X-ray diffraction. Primary constituents of the sample were silicon dioxide, calcium silicate, calcium carbonate and elemental iron. Analysis of the condensed water vapor also indicated a low amount of brine carryover. The measured TDS level of the water separated in the hotwell was 200 ppm as compared to the average 4400 ppm TDS level measured in the brine system.

### 3.6.3 Continuous Operation Test

Part of the field testing of the 500 kw DCHX pilot plant included a period of continuous operation to demonstrate the plant's "on-line" potential. The objective of the test was to operate continuously for 500 hours, but because of personnel limitations the plant was operated in 5-day continuous intervals. The interrupted operation was a compromise, but possibly a tougher test due to the strain on components associated with starting and stopping.

Initial planning called for starting the plant at 7 a.m. on 4/6/81 and operating over a 4-week, 120-hours per week schedule with an extra 20-hour stint on a weekend to cover 500 hours. The 7 a.m. start on 4/6/81 was delayed by problems associated with reinstallation of the generator. As a result of the delay, the attempted operation time was reduced to a total of 475 hours. The plant startup at the beginning of each week consumed an average of 2 hours before the turbine could be put on the line; therefore, at least 8 hours of operation were lost that would not have been if the plant had run through the weekend. In the 475 hours of scheduled operation, 407.7 hours were accumulated on the $IC_4$ pump and 376.8 hours on the turbine generator.

There were eight unscheduled shutdowns during the 475 hours of operation. Four were associated with plant equipment and four were caused by utility power failures that shut down the downwell pump. The actual on-line availability for power was 79.3% of the total plant operating time. Excluding the lost time in scheduled weekly startups and the 24 hours due to an electrical phasing problem at the start of testing, on-line availability was 86%.

It is important to point out that none of the plant-originated shutdowns was associated with brine scaling or in any way associated with the fact that this is a geothermal plant. The major cause of plant operating problems in the earlier phases of testing was carbonate scaling. The carbonate scaling appears to be under control with the use of the Pfizer additive.

Another aspect of this endurance run was to obtain an accurate estimate of consumable supplies used to support plant operation. The run resulted in the following numbers (approximate):

| | |
|---|---|
| Water treatment chemicals for the condensers | 5 mills/kw-hr |
| Brine treatment, Flocon 247 | 0.78 mills/kw-hr |
| Purge gases | .64 mills/kw-hr |
| Turbine oil | .23 mills/kw-hr |
| $IC_4$ usage | 15.2 mills/kw-hr |

Some of the usage was higher than normal due to shutdowns and losses associated with plant failure. Of the two big cost items, the $IC_4$ use rate will be in the 1.4 mills/kw-hr range with a properly operating recovery system. At this time there has not been an evaluation of the condenser water treatment cost, and it is not known to what extent they can be reduced. The present condenser water treatment approach is the lowest cost one we are aware of that meets the strict EPA requirements. Sticking with the 5.0 mills for condenser water treatment and correcting the $IC_4$ loss to that for a properly operating recovery system, a cost of 7.5 mills for consumables can be projected. A further cost reduction to 6.0 mills is predicted for design plant operation.

A summary of the continuous test program is contained in Appendix F.

### 3.6.4 Downhole Geothermal Production Pump

While not a component of the original 500 kw Direct Contact Pilot Plant, a downhole production pump is necessary to supply unflashed pressurized geothermal brine to binary-cycle power plants utilizing either direct contact or surface heat exchangers. This requirement is especially important in a high-scaling carbonate system such as East Mesa.

After some development work using a DOE-funded Pump Test Rig, TRW-Reda has supplied a series of 80 hp, 220 gpm electrical submersible pumps that have been installed, first in well 8-1 and then in well 6-2. The reliability of these downhole pumps has not been good. Three pumps were installed in well 8-1. The first pump failed after fifteen days, the second pump accumulated almost six months of operating time, and the third pump operated for two months. Six pumps have been installed in 6-2. Of these, two have accumulated about three months total run time (each) and the remaining four each failed after less than a month of operation. The failures have primarily been electrical due to brine intrusion into the cable, pothead, packoff or motor.

Despite the problems during the 26 months beginning August, 1979, an East Mesa downhole pump has been available for operation over 60% of the time. The high cost of installation and removal of a downhole production pump make further improvements in operation lifetime a key factor in the commercialization of geothermal binary cycles.

## 4.0 CONCLUSIONS AND RECOMMENDATIONS

The testing performed under this contract has demonstrated that the DCHX binary power generation system is a viable concept for producing electrical energy from hydrothermal geothermal resources. The plant met or exceeded its design goals with the exception of turbine performance. The low turbine performance is believed to be the result of condensation between the back shroud and case which can be eliminated with a modified design. The pilot plant would meet its projected utilization factor of 5.1 watt-hrs/lb of brine with an 80% efficient turbine.

In the total operating time of 780 hours on the turbine, there is no evidence of excessive scaling or erosion problems resulting from the DCHX concept. Isobutane losses in the brine leaving the plant are minimal, and total $IC_4$ losses are estimated to cost approximately 2 mills/kw-hr. Non-condensible gases in the condenser can be managed without condenser venting. The use of small amounts of antiscalant in the brine upstream of the sand trap has eliminated carbonate scaling problems in the brine boost pump and the brine control valves. This additive is estimated to cost approximately .5 mills/kw-hr with proper plant performance.

The plant is easy to start up and control, and presents no unusual operating problems. During the last 30-day test there were no problems or shutdowns that were attributable to the fact that the plant operates from a geothermal source. Shutdowns that did occur were due to loss of grid power to the downwell pump and to nuisance hardware problems that can be corrected with experience. The system achieved an on-line availability of 86% in spite of these problems.

During this test program these objectives were met: evaluating DCHX component performance, determining $CO_2$ levels in the power loop, measuring $IC_4$ loss rates, and evaluating overall plant performance.

Future investigation with the pilot plant should include evaluation of changes to the DCHX brine inlet configuration in an attempt to eliminate some possible mixing in the top of the column and changes to improve the process used to separate the $IC_4$-$CO_2$ mixture recovered from the brine. Future work should include sizing of larger plants (both wellhead and gathering plants) complete with capital and operating cost estimates based on present verified design techniques.

## 5.0 REFERENCES


1. Barber-Nichols Engr. Co., "Design Definition of a 500 kW Direct Contact Geothermal Pilot Plant," Lawrence Berkeley Laboratory, Berkeley, California, Report No. UCID-8009.

2. Hlinak, A., et al, "Final Design, Installation and Baseline Testing of a 500 kw Direct Contact Pilot Plant at East Mesa," Lawrence Berkeley Laboratory, Berkeley, California, Report No. LBL-11153 UC-66d.

3. Jacobs, H. R. and Boehm, Robert, "Direct Contact Binary Cycles," University of Utah, Salt Lake City, Utah, Report No. UTEC-78-086.

4. Rapier, P. M., "Design Features and Equilibrium Flash Modeling of Direct Binary Fluid Heat Exchangers for Use with Geothermal Brines," presented at 20th ASME/AIChE National Heat Transfer Conference, Knoxville, Tennessee, August 1981, Lawrence Berkeley Laboratory Report No. LBL-12115, January 1981.

5. Knight, J. F. and Perona, J. J., "A Mass Transfer Model for a Spray Tower Direct Contact Heat Exchanger," presented at the 20th ASME/AIChE National Heat Transfer Conference, Milwaukee, Wisconsin, August 1981.

6. Culbreth, W., Johnson, G., and Marschall, E., "Heat Transfer and Hydrodynamics During Droplet Formation and Release in a Liquid-Liquid Direct-Contact Heat Exchanger," presented at the 20th ASME/AIChE National Heat Transfer Conference, Milwaukee, Wisconsin, August 1981.

7. Keller, A. S., Jacobs, H. R., and Boehm, R. F., "Comparison Between a Spray Column and a Sieve Tray Column Operating as Liquid-Liquid Heat Exchangers," presented at the 20th ASME/AIChE National Heat Transfer Conference, Milwaukee, Wisconsin,

August 1981.

8. Ellis, A. J., and Golding, R. M., American Journal of Science 261, pp. 45-60 (1963).

9. Jacobs, H. R., and Boehm, R. F., "Direct Contact Binary Cycles," chapter in Sourcebook on the Production of Electricity from Geothermal Energy, Joseph Kestin, Ed., U. S. Government Printing Office, Washington, D.C., DOE/RA/4051, March 1980.

10. I. Sheinbaum Co., Inc., "Stripping of Isobutane from Geothermal Brine,". Handout from DCHX Workshop, January 20-21, 1981 (unpublished).

11. Hoffman, E. J., "Isobutane Recovery from Spent Brine," report presented at DCHX Workshop, January 20-21, 1981, (unpublished).

12. Barber-Nichols Engr. Co., "Executive Summary Direct Contact Heat Exchanger 10 kw Power Loop Test Series, No. 1 and 2," LBL-7036, June 1979.

13. Auerbach, M. H., Reimer, R. A., et al, "A Calcium Carbonate Scale Inhibitor for Direct Contact Binary Geothermal Service," to be presented at the 1982 SPE International Symposium on Oil Field and Geothermal Chemistry, Dallas, Texas, January 1981.

ACKNOWLEDGMENT

This work was supported by the Assistant Secretary for Conservation and Renewable Energy, Office of Renewable Technology, Division of Geothermal and Hydropower Technologies of the U.S. Department of Energy under Contract DE-AC03-76SF00098.

FIGURE 3.1

PREDICTED PERFORMANCE AND SELECTED STATE POINTS

Superheated; Organic Pressure = 420.1 psia

| | | |
|---|---|---|
| Working Fluid: | Isobutane/$H_2O$ | |
| Brine Temperature in (F): | 335.0 | |
| Brine Pressure in (psia): | 175.0 | |
| DCHX Temperature (F): | 255.0 | |
| DCHX Pressure (psia): | 452.7 | |
| Condenser Temperature (F): | 94.0 | |
| Condenser Pressure (psia): | 70.0 | |
| Turbine Inlet Pressure (psia): | 442.7 | |
| Working Fluid Organic Fraction: | 0.986 | |
| Working Fluid $H_2O$ Fraction: | 0.014 | |
| Isentropic Analysis: | | |
| Turbine Exit Temperature (F): | 133.5 | |
| $H_2O$ Turbine Exit Quality (Pct): | 70.7 | |
| Enthalpy Drop Across Turbine (Btu/lb): | 32.1 | |
| Brine Temperature Drop (F): | 190.2 | |
| Working Fluid Flow Rate (lbs/sec-gpm): | 27.6- | 366.8 |
| Brine Flow Rate (lbs/sec-gpm): | 27.0- | 216.4 |
| Density of Organic Liquid at Condenser Temp. (lb/cf): | 33.83 | |
| Heat Transfer in DCHX (Btu/lb-Pct of Total): | | |
| Preheat Organic: | 112.6- | 59.4 |
| Vaporize Organic: | 60.6- | 32.0 |
| Superheat Organic: | 4.5- | 2.4 |
| Vaporize $H_2O$: | 12.1- | 6.4 |
| Total: | 189.7- | 100.0 |
| Heat Transfer in DCHX (MBtu/hr): | 18.88 | |
| Heat Transfer in Condenser (Btu/lb - MBtu/hr): | 169.4- | 16.86 |
| Energy Generated in System (kw-Pct of total generated): | | |
| Gas Turbine: | 776.7- | 96.3 |
| Hydroturbine: | 30.2- | 3.7 |
| Total: | 806.9- | 100.0 |
| Parasitic Losses (kw-Pct of total generated): | | |
| Gear Box and Alternator: | 61.0- | 7.6 |
| Condenser: | 77.7- | 9.6 |
| Organic Feed Pump: | 96.7- | 12.0 |

PREDICTED PERFORMANCE AND SELECTED STATE POINTS(CONT.)

| | | |
|---|---|---|
| Brine Boost Pump: | 54.4- | 6.7 |
| Brine Discharge Pump: | 2.1- | 0.3 |
| Recovery System: | 15.0- | 1.9 |
| Total: | 306.9- | 38.0 |
| Net Energy (kw-Pct of total generated): | 500.0- | 61.4 |
| Cycle Efficiency (Pct): | 8.9 | |
| Source Production Factor (kw-hr/lb brine): | 5.14 | (x.001) |
| Turbine Efficiency (Pct): | 33.0 | |
| Actual Turbine Exit Temperature (F): | 140.6 | |
| Actual $H_2O$ Exit Quality (Pct): | 85.6 | |
| Actual Enthalpy Drop Across Turbine (Btu/lb): | 26.7 | |
| Volumetric Flow Rate at Turbine Exit (cfs): | 39.9 | |

System Pressures (psia)--Refer to Figure 3.2

| Location | Pressure | Location | Pressure | Location | Pressure |
|---|---|---|---|---|---|
| 1 | 175.0 | 7 | 71.6 | 13 | 17.0 |
| 2 | 118 | 8 | 70.0 | 14 | 5.0 |
| 3 | 485.0 | 9 | 70.0 | 15 | 20.0 |
| 4 | 452.7 | 10 | 485.0 | | |
| 5 | 442.7 | 11 | 467.0 | | |
| 6 | 72.0 | 12 | 457.0 | | |

PROCESS FLOW DIAGRAM
500 KW DCHX PILOT PLANT

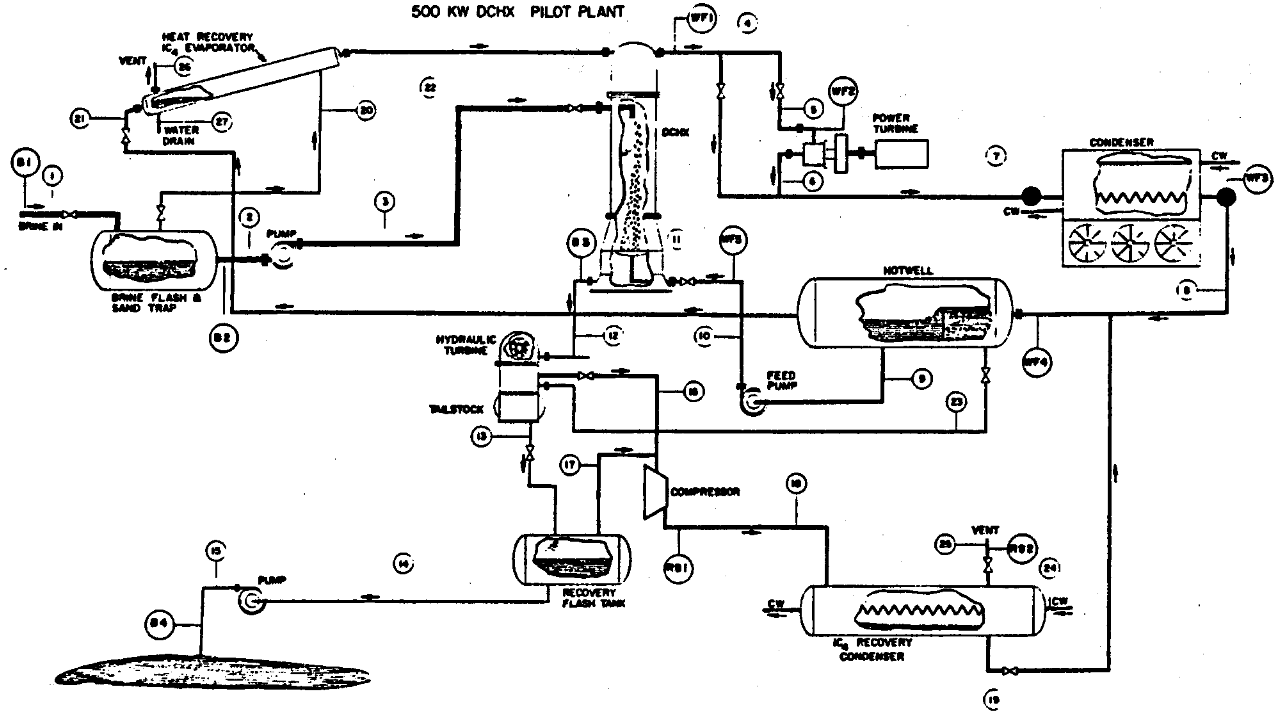


**MATERIAL BALANCE**

PROCESS STREAM NUMBER

| PARAMETER \ STREAM | 1 GEOTHERMAL BRINE SUPPLY | 2 GEOTHERMAL BRINE TO BOOST PUMP | 3 GEOTHERMAL BRINE TO DCHX | 4 ISOBUTANE VAPOR FROM DCHX | 5 ISOBUTANE VAPOR TO TURBINE | 6 ISOBUTANE VAPOR TO CONDENSER | 7 CONDENSER INLET | 8 ISOBUTANE CONDENSATE TO HOTWELL | 9 ISOBUTANE LIQUID TO FEED PUMP | 10 ISOBUTANE LIQUID FROM FEED PUMP | 11 ISOBUTANE LIQUID TO DCHX | 12 GEOTHERMAL BRINE FROM DCHX | 13 GEOTHERMAL BRINE FROM HYD TURBINE | 14 RETURN BRINE |
|---|---|---|---|---|---|---|---|---|---|---|---|---|---|---|
| FLOW RATE (lb/hr x $10^3$) | 97.8 | 97.2 | 97.2 | 99.4 | 99.4 | 99.4 | 99.4 | 99.4 | 98.0 | 98.0 | 95.4 | 95.8 | 97.2 | 97.2 |
| TEMPERATURE (°F) | 340 | 335 | 335 | 255 | 253.4 | 140.6 | 140.6 | 94.0 | 94.0 | 95.0 | 95.0 | 148.8 | 144.8 | 144.8 |
| PRESSURE (PSIA) | 175 | 118 | 485.0 | 452.7 | 442.7 | 72.0 | 71.6 | 70.0 | 70.0 | 485 | 467 | 457 | 17.0 | 5.0 |
| ENTHALPY (BTU/LBM) | 311.4 | 306.1 | 306.6 | 581.0 | 581.0 | -607.7 | -607.7 | -776.1 | -788.9 | -787.2 | -787.2 | 114.1 | 112.98 | 112.98 |
| DENSITY (LBM/FT$^3$) | 56.0 | 56.1 | 56.2 | 6.46 | 6.32 | 0.692 | 888 | 34.0 | 33.8 | 33.8 | 33.8 | 61.4 | 61.3 | 61.3 |

| PARAMETER \ STREAM | 15 RETURN BRINE | 16 VENT FROM TAILSTOCK | 17 VENT FROM RECOVERY FLASH TANK | 18 FLOW TO RECOVERY CONDENSER | 19 CONDENSATE FROM $IC_4$ RECOVERY CONDENSER | 20 STEAM & $CO_2$ TO EVAPORATOR | 21 $IC_4$ TO EVAPORATOR | 22 $IC_4$ FROM EVAPORATOR | 23 WATER CONDENSATE FROM HOTWELL | 24 COOLING WATER TO $IC_4$ RECOVERY CONDENSER | 25 $IC_4$ RECOVERY CONDENSER VENT | 26 $IC_4$ EVAPORATOR VENT | 27 $IC_4$ EVAPORATOR DRAIN |
|---|---|---|---|---|---|---|---|---|---|---|---|---|---|
| FLOW RATE (lb/hr x $10^3$) | 97.2 | .011 | 018 | 029 | 023 | 0629 | 2.6 | 2.6 | 1.4 | 16.0 | 006 | .140 | 489 |
| TEMPERATURE (°F) | 144.8 | 144.8 | 144.8 | 250 | 76 | 335 | 95 | 260 | 94 | 74 | 76 | 270 | 225 |
| PRESSURE (PSIA) | 20.0 | 17.0 | 5 | 90 | 90 | 95 | 485 | 460 | 17 | — | 90 | 95 | 95 |
| ENTHALPY (BTU/LBM) | 112.98 | — | — | — | — | 417.3 | -787.2 | -608 | 62.0 | 42.0 | — | — | — |
| DENSITY (LBM/FT$^3$) | 61.3 | — | — | — | — | .224 | 33.8 | 7.0 | 62.1 | 62.3 | — | — | — |

Figure 3.2

# FIGURE 3.3

DCHX CONFIGURATION

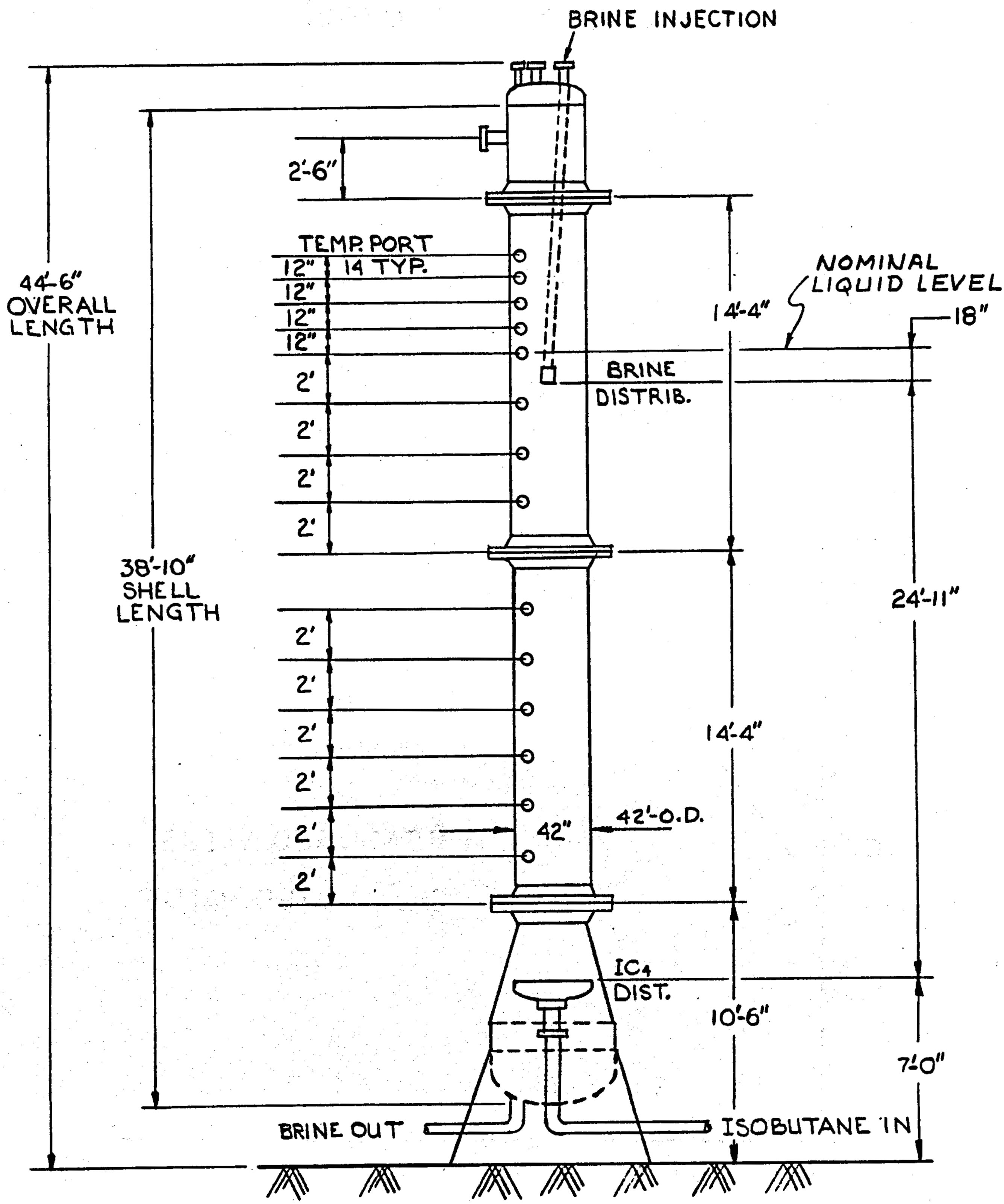

# FIGURE 3.4

TEMPERATURE VS % HEAT TRANSFER
FOR CONDITIONS ON
11-13-80 AT 9:45 A.M.
ESTIMATED PINCH=5.3°F

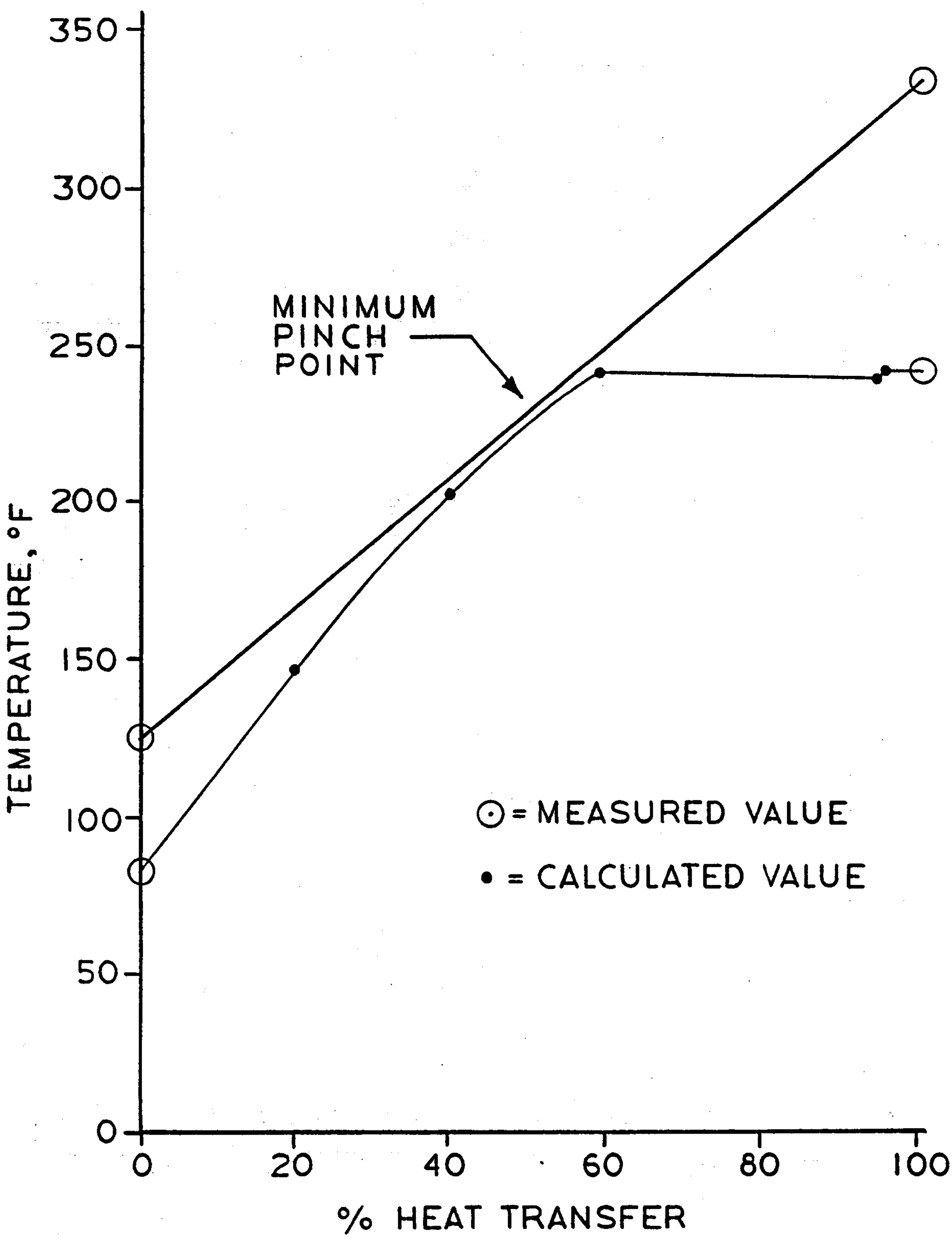

FIGURE 3.5

CALCULATED BOILER LENGTH
WITH DCHX PRESSURE.
FOR DECEMBER, 1980
TEST CONDITIONS

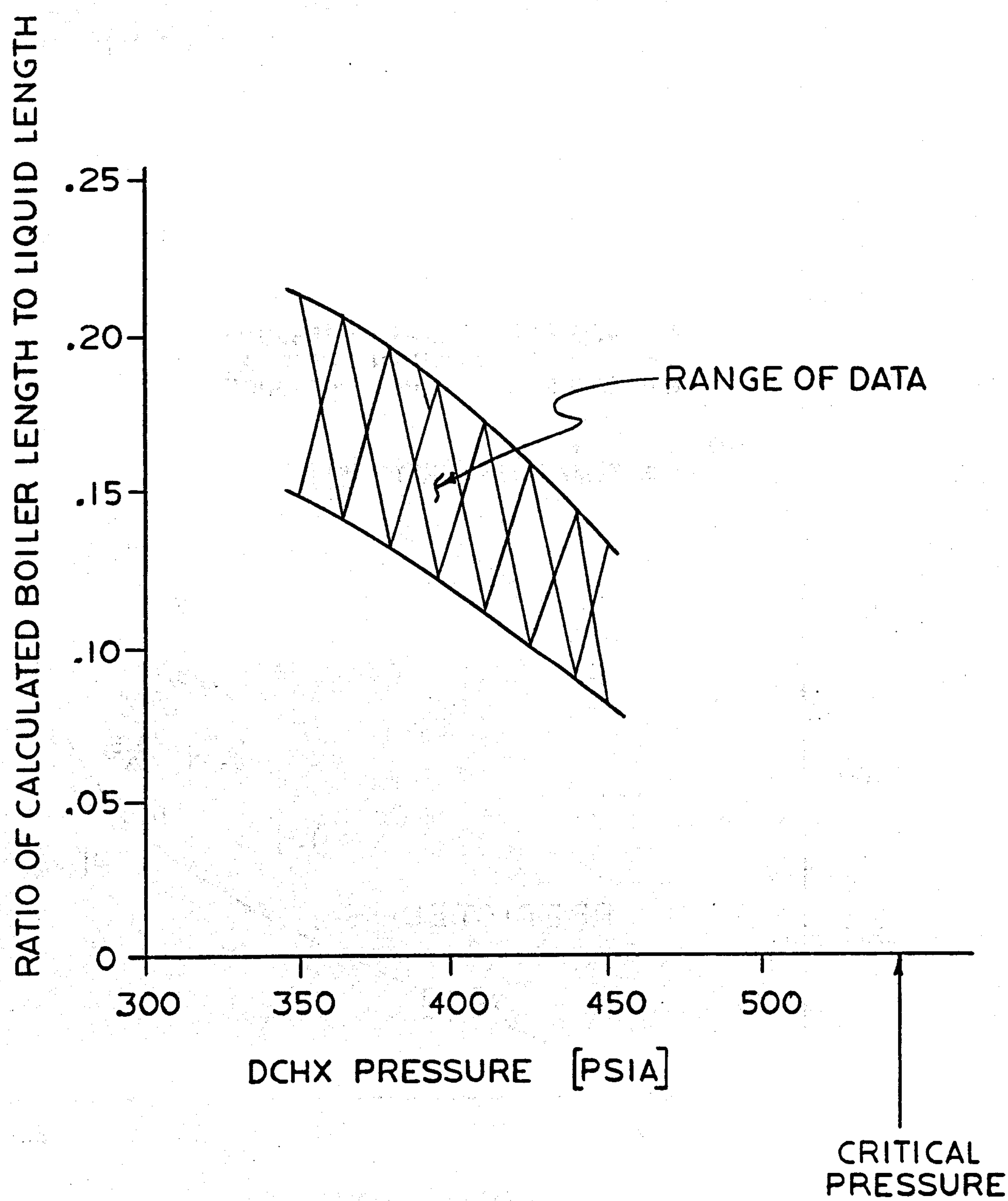

# FIGURE 3.6

## PREHEATER
## VOLUMETRIC HEAT TRANSFER VS BRINE FLOW
## DATA FROM DECEMBER, 1980

CALCULATED PREHEATER LENGTH ASSUMING $U_{BOIL} = 9{,}375 \frac{BTU}{FT^3\,HR\,^\circ F}$

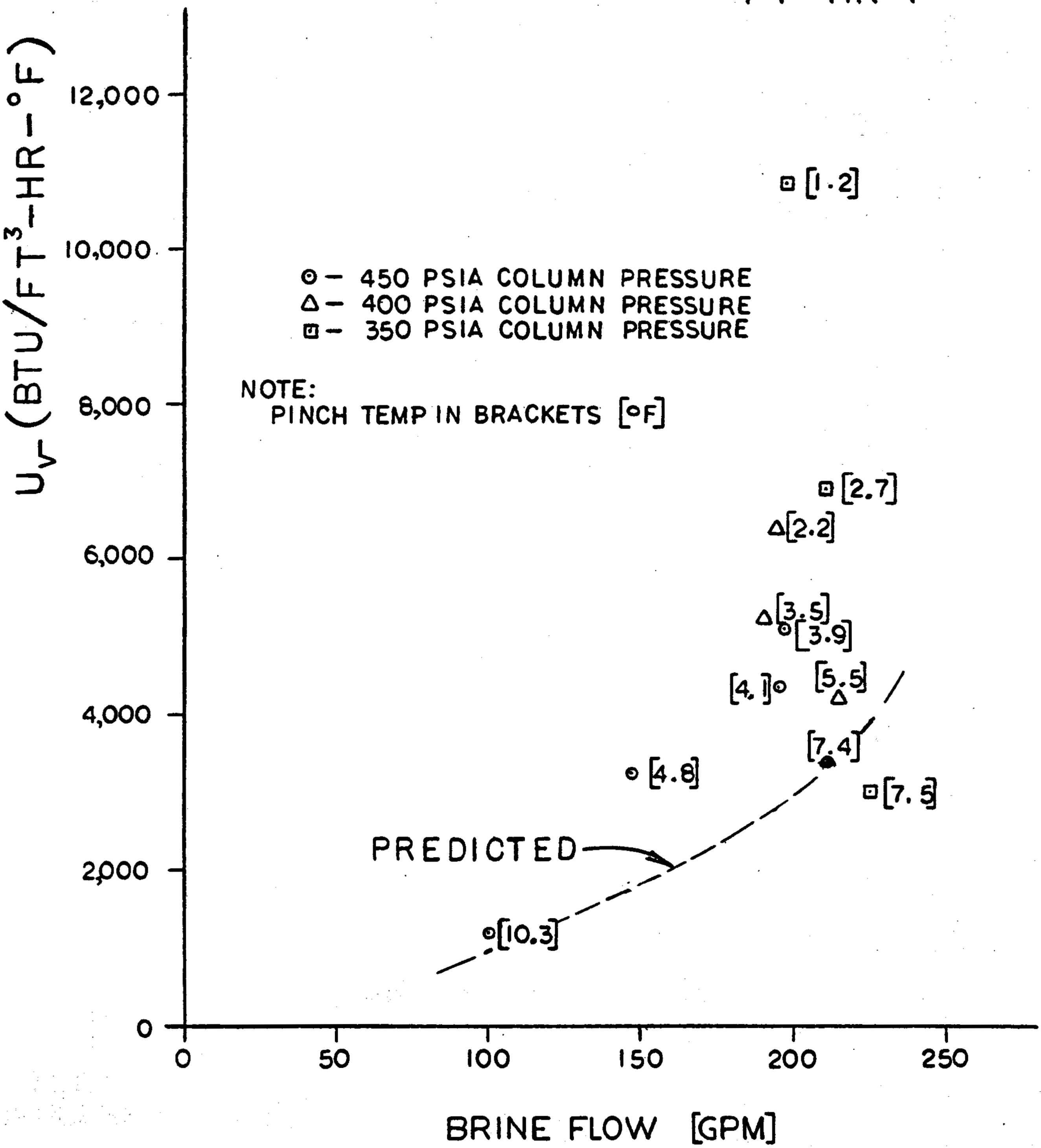

FIGURE 3.7

DCHX TEMPERATURE PROFILE

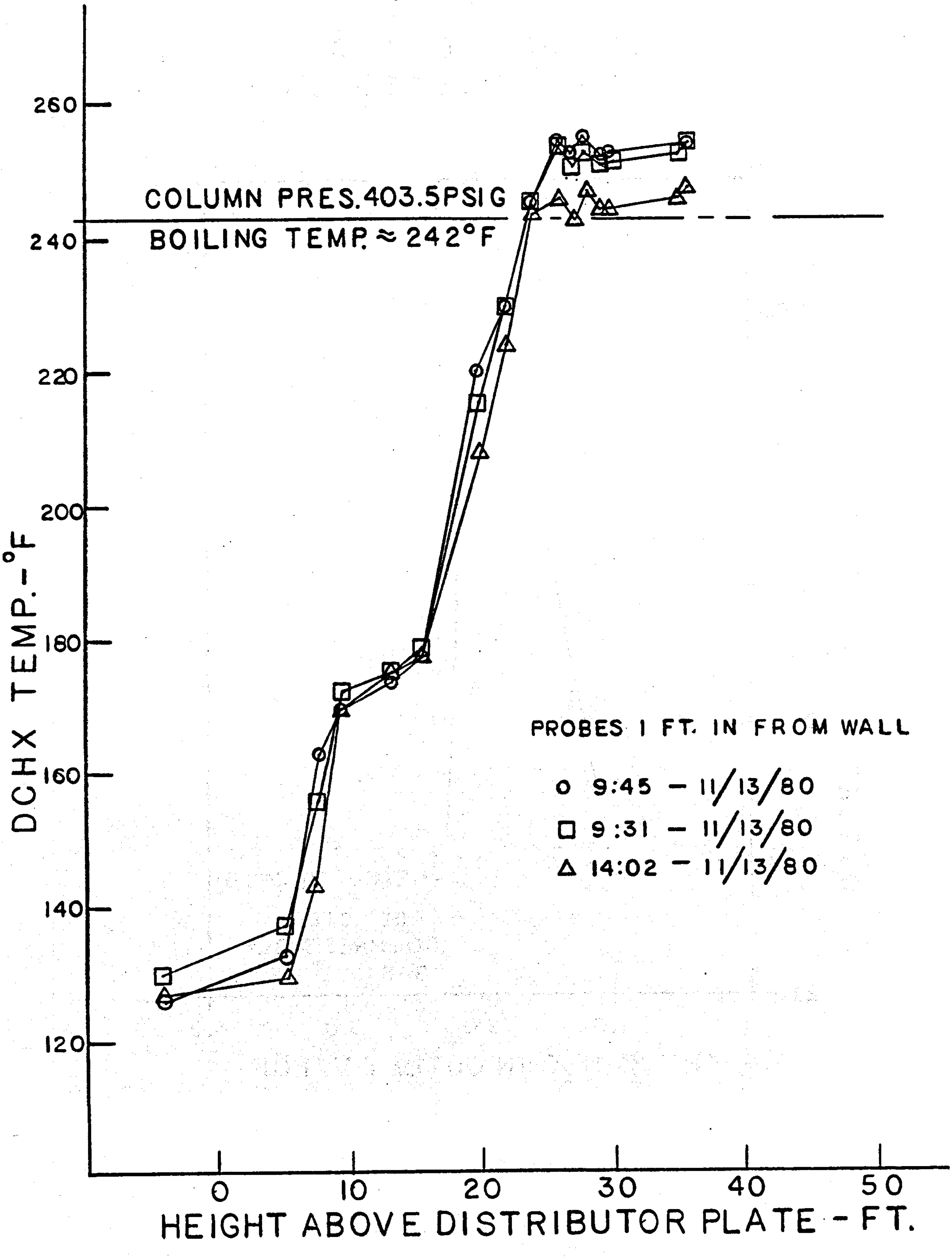

# FIGURE 3.8

WEIGHT % $H_2O$ IN DCHX OUTLET VAPOR Vs. OUTLET TEMP, °F

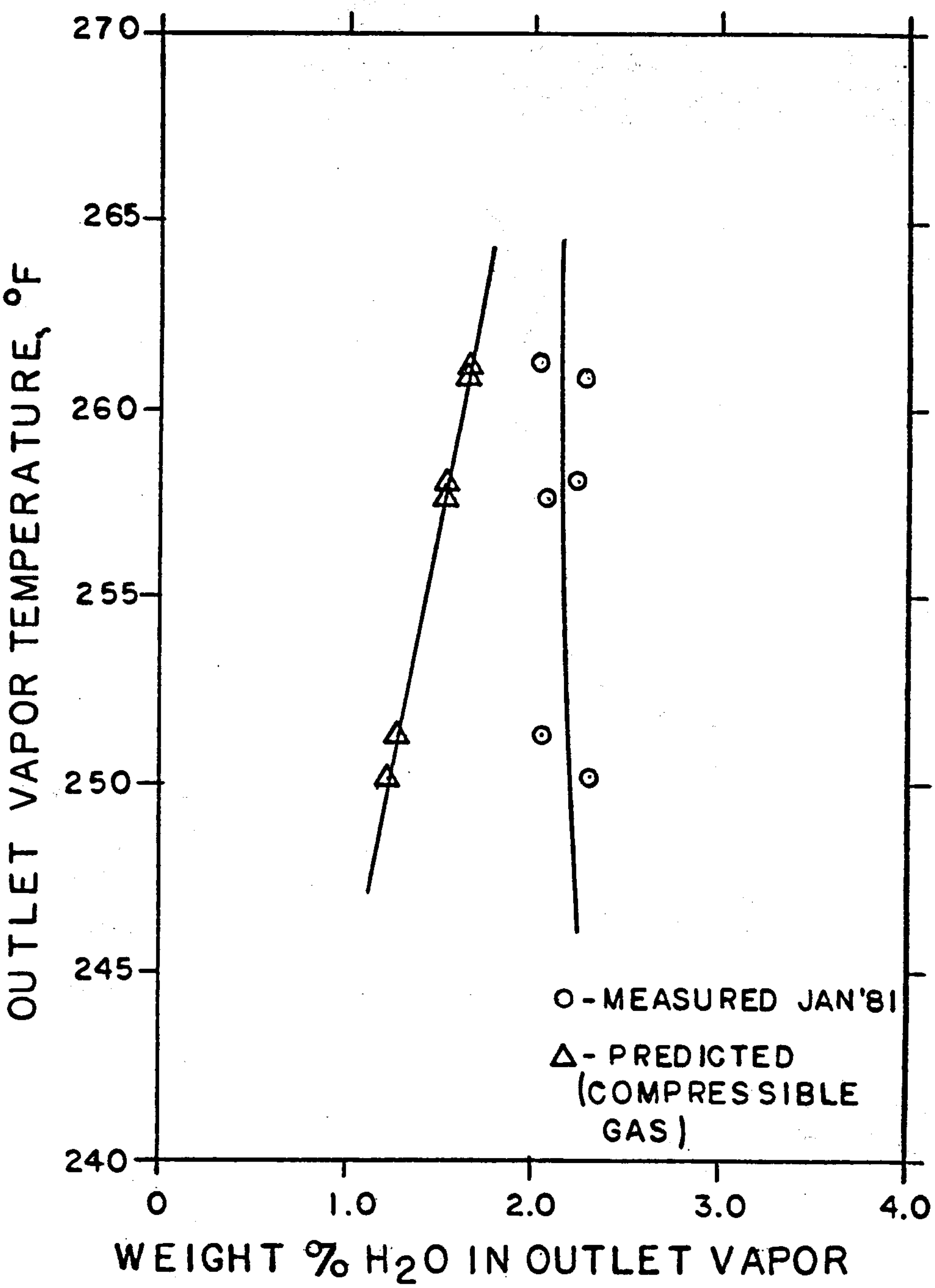

FIGURE 3.9

PLANT PERFORMANCE AS A FUNCTION OF NON CONDENSIBLE ACCUMULATION IN THE CONDENSER.

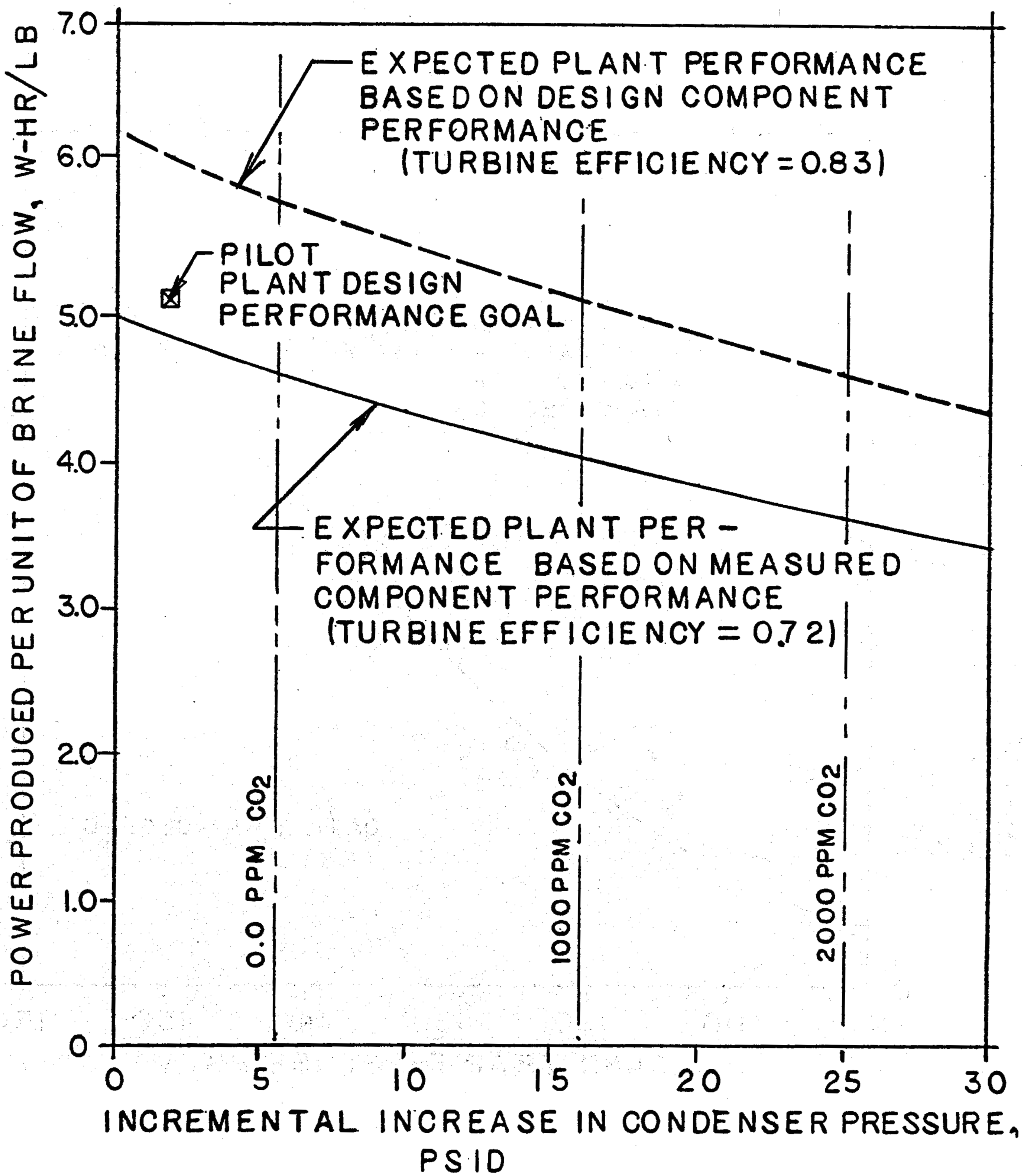

# FIGURE 3.10

CO2 CONCENTRATION IN BRINE LEAVING SAND TRAP AS A FUNCTION OF SAND TRAP PRESSURE.

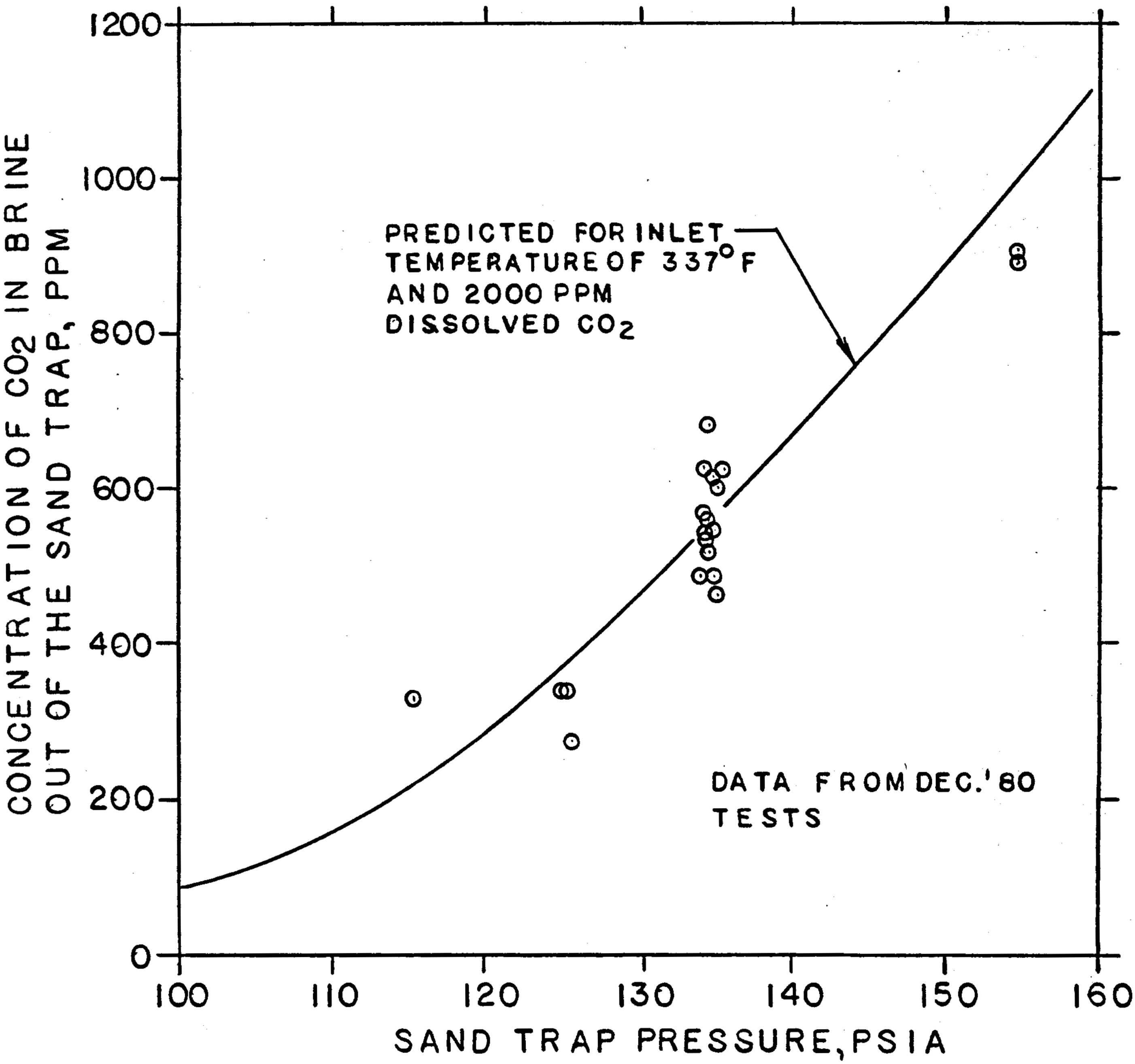

FIGURE 3.11

COMPARISON OF CALCULATED & MEASURED VALUES OF DISSOLVED $CO_2$ IN BRINE LEAVING SAND TRAP.

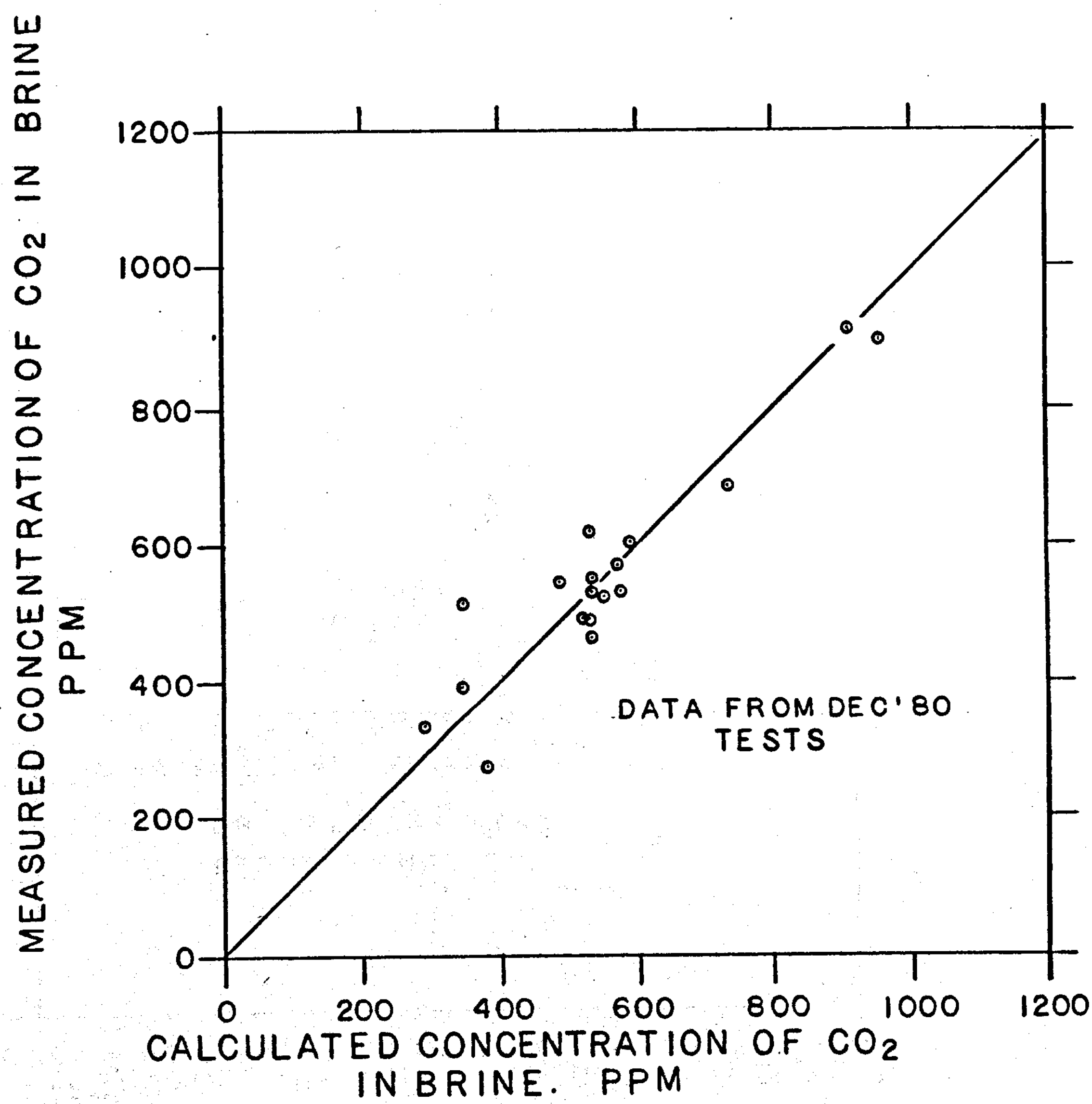

FIGURE 3.12
MEASURED CONCENTRATION OF $CO_2$ IN $IC_4$ LEAVING DCHX AS A FUNCTION OF INLET BRINE $CO_2$ CONCENTRATION.

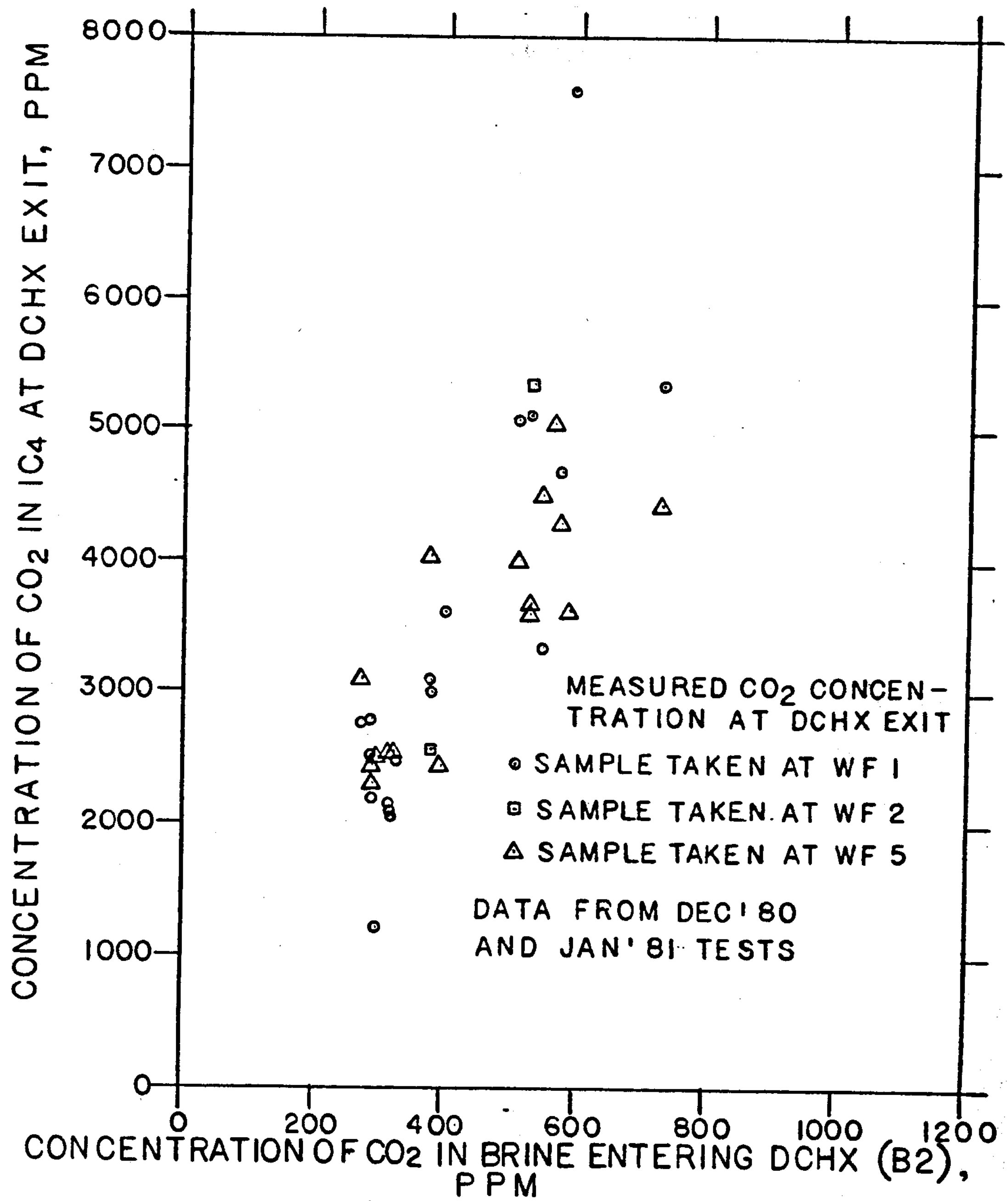

# FIGURE 3.13

EFFECT OF DISSOLVED $CO_2$ IN THE BRINE AT THE SAND TRAP EXIT ON EXCESS PRESSURE IN CONDENSER.

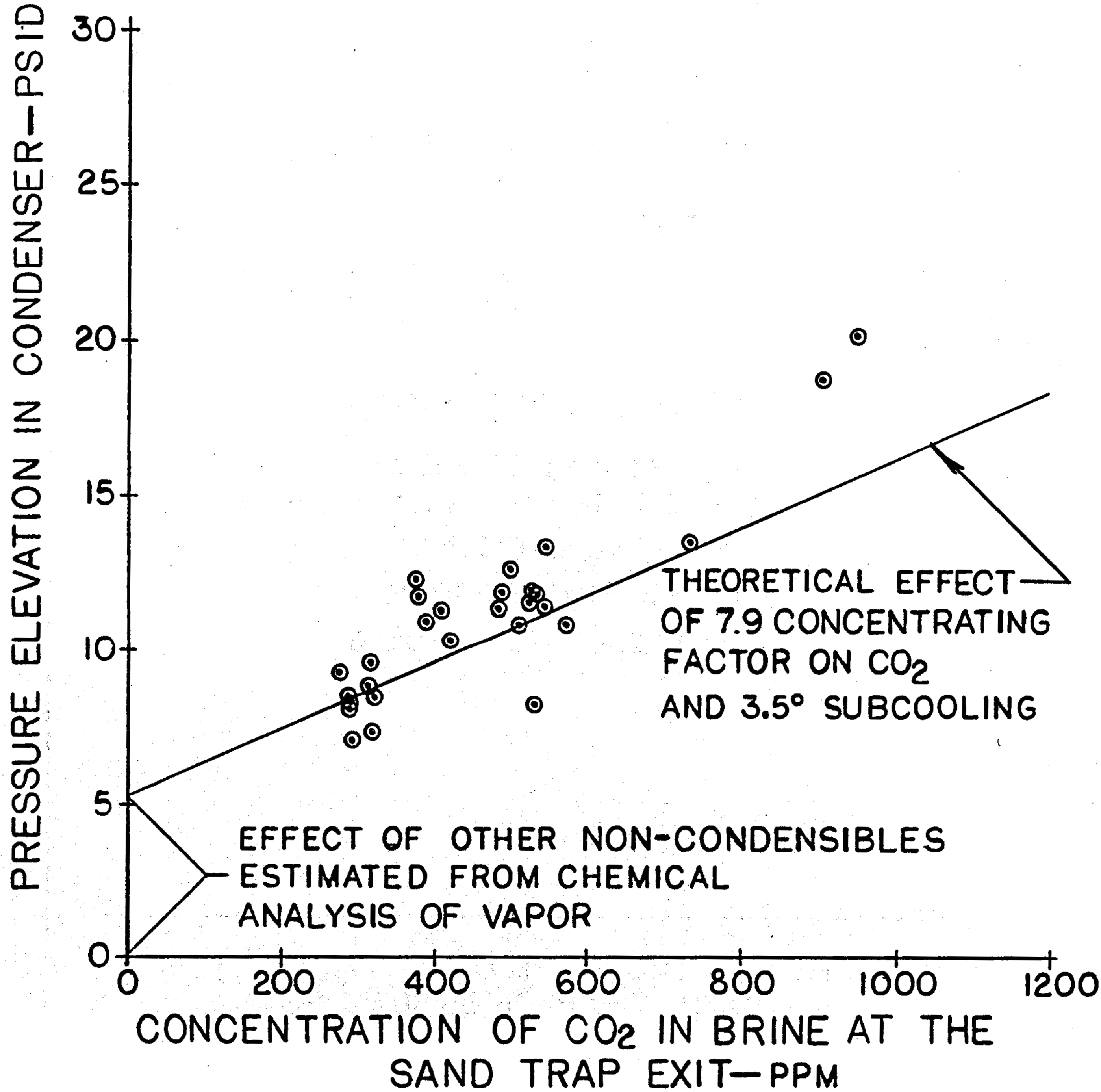

FIGURE 3.14

PREDICTED EFFECT OF SAND TRAP PRESSURE ON OVERALL PLANT PERFORMANCE

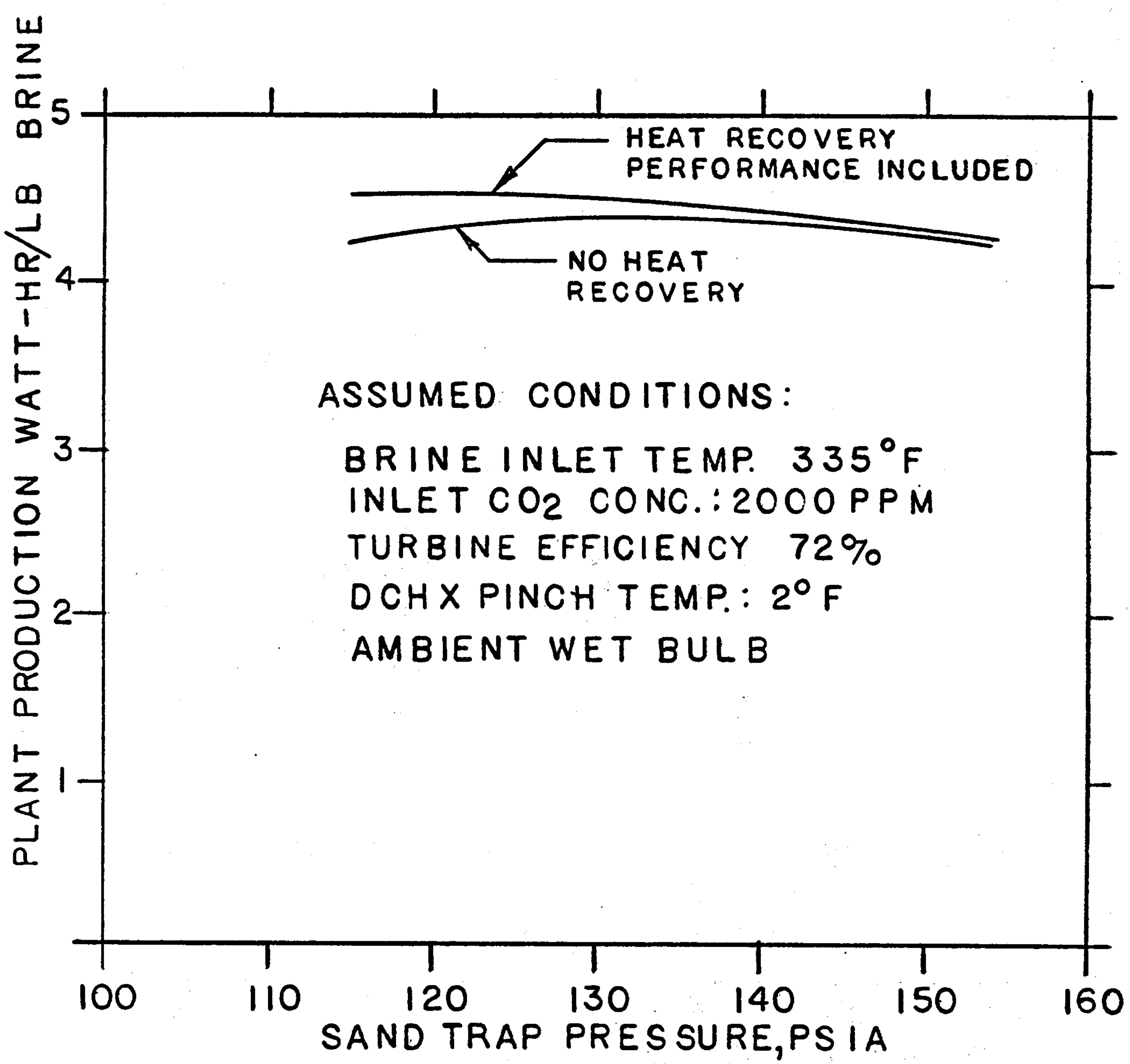

FIGURE 3.15

TURBINE FLOW CONTRIBUTED BY THE BINARY HEAT EXCHANGER AS A FUNCTION OF SAND TRAP PRESSURE

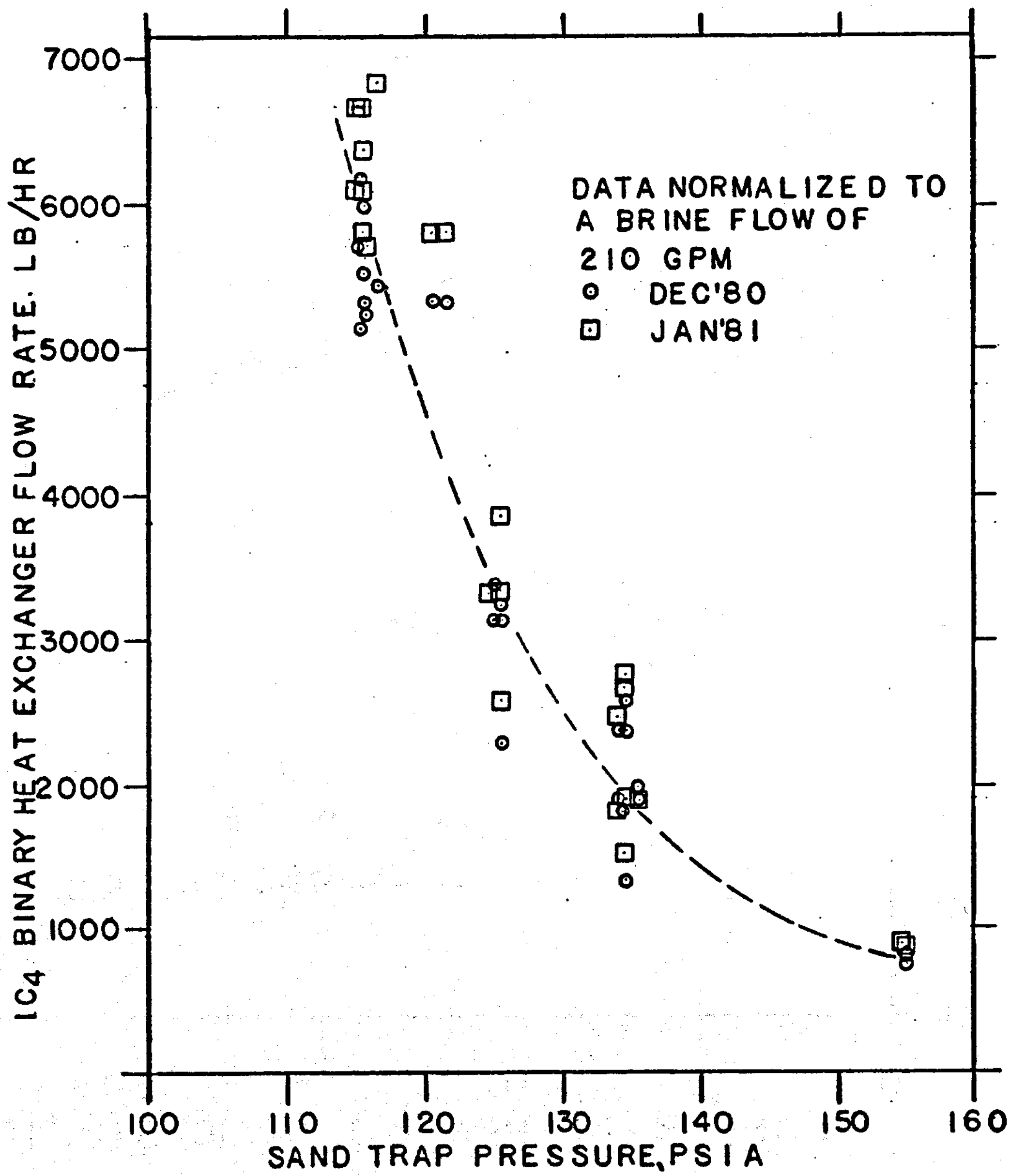

# FIGURE 3.16

PREDICTED AND MEASURED
CONDENSER PERFORMANCE

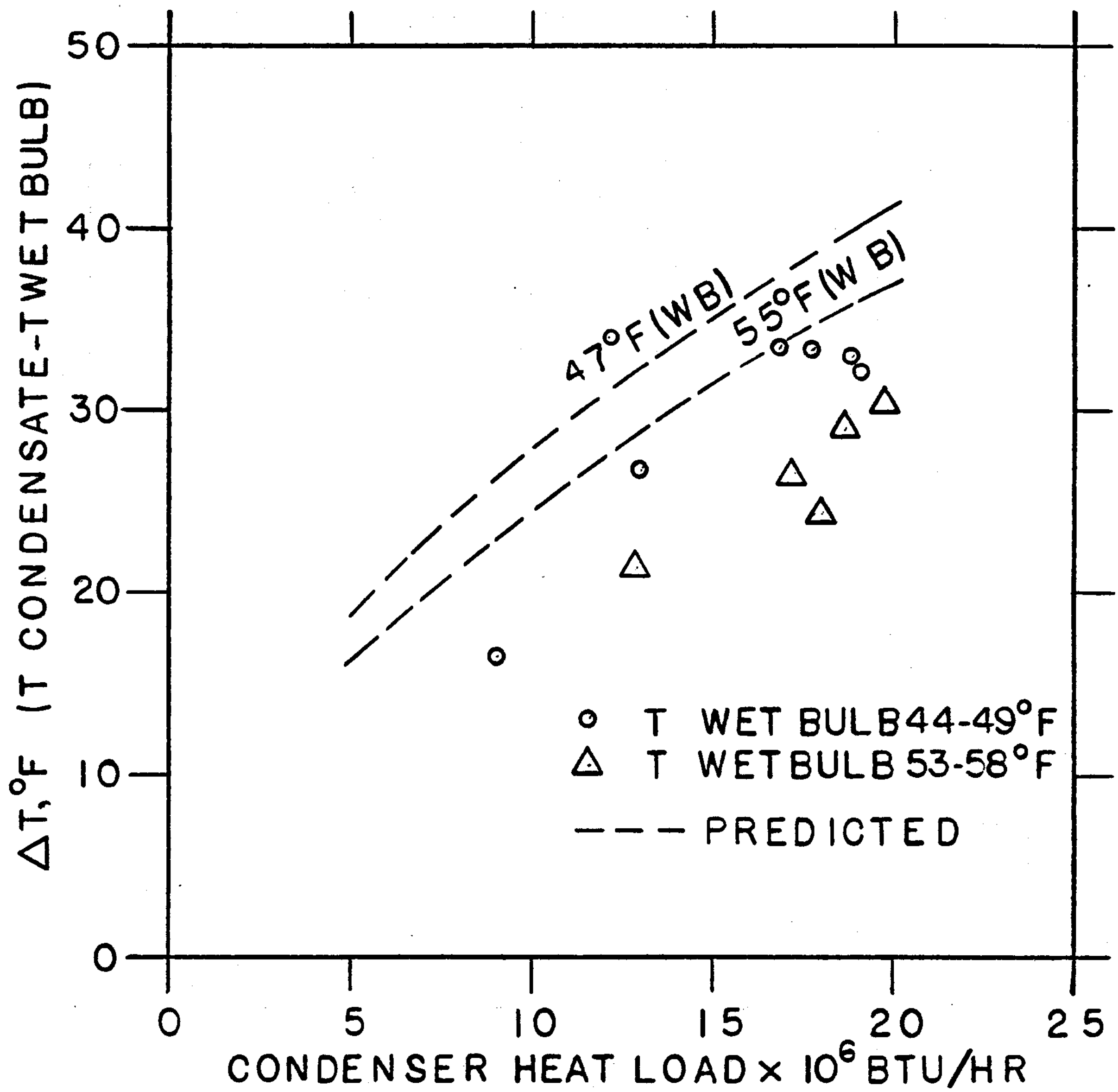

## FIGURE 3.17A

$IC_4$ WORKING FLUID DISSOLVED IN THE BRINE EXITING THE DCHX AS A FUNCTION OF OPERATING PRESSURE. LEVEL-BASED ON G.C. ANALYSIS.

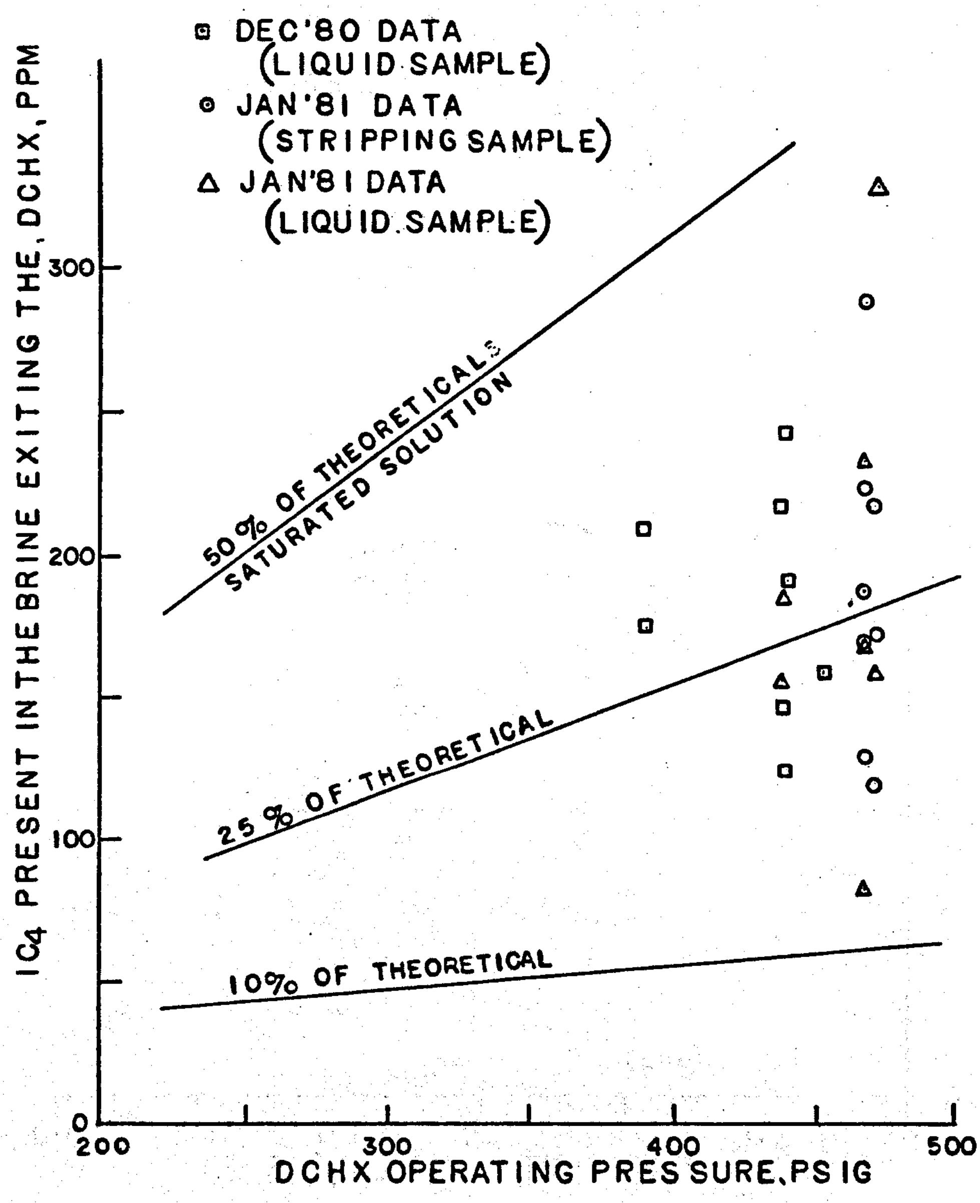

FIGURE 3.17 B

DISSOLVED IC4 AT DCHX EXIT AS A FUNCTION OF BRINE FLOW RATE

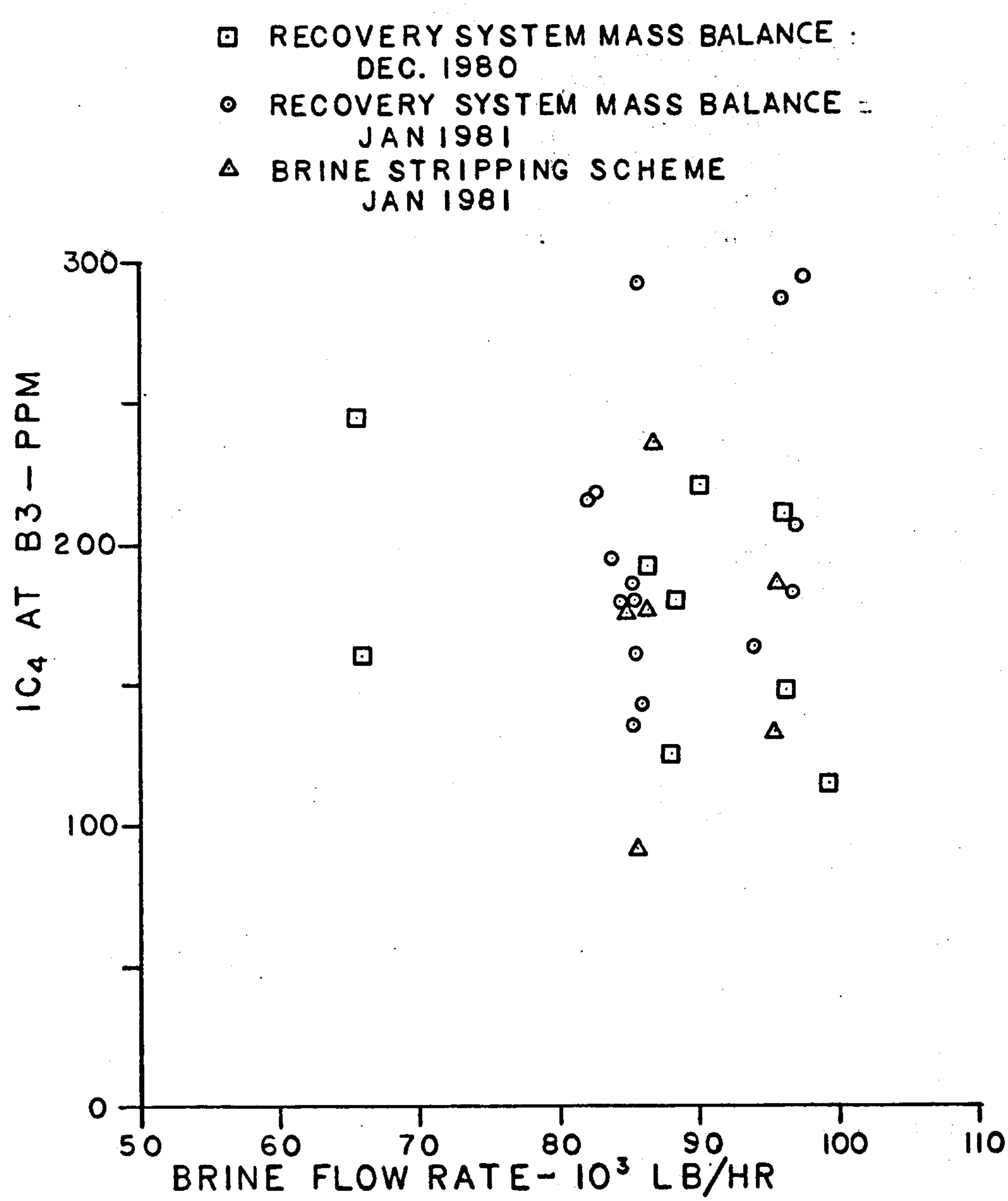

FIGURE 3.18

EFFECT OF RECOVERY TANK PRESSURE ON RESIDUAL $IC_4$ IN BRINE LEAVING PLANT.

⊙ GC DATA USING LIQUID SAMPLE
x GC DATA USING BRINE STRIPPING METHOD.

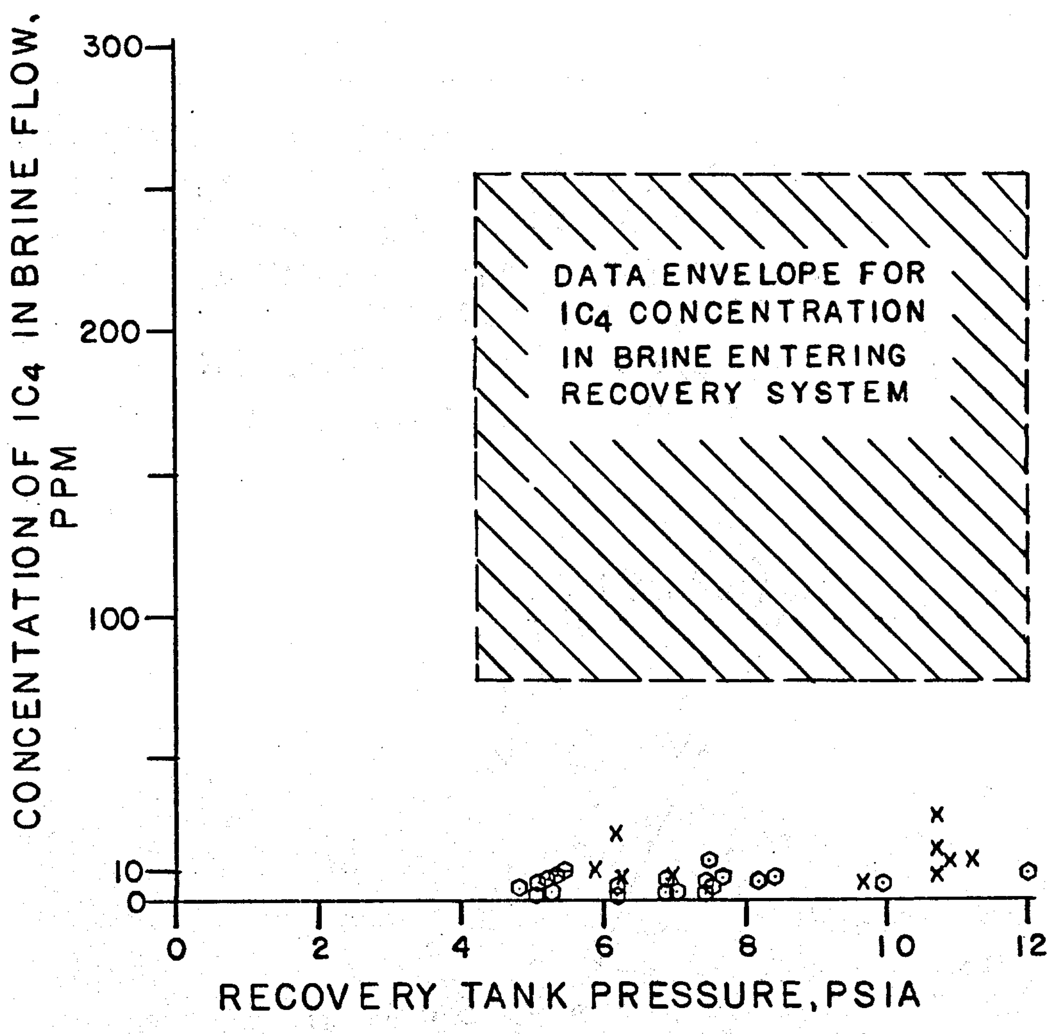

FIGURE 3.19
EFFECT OF DISSOLVED $CO_2$ ON
$IC_4$ RECOVERY

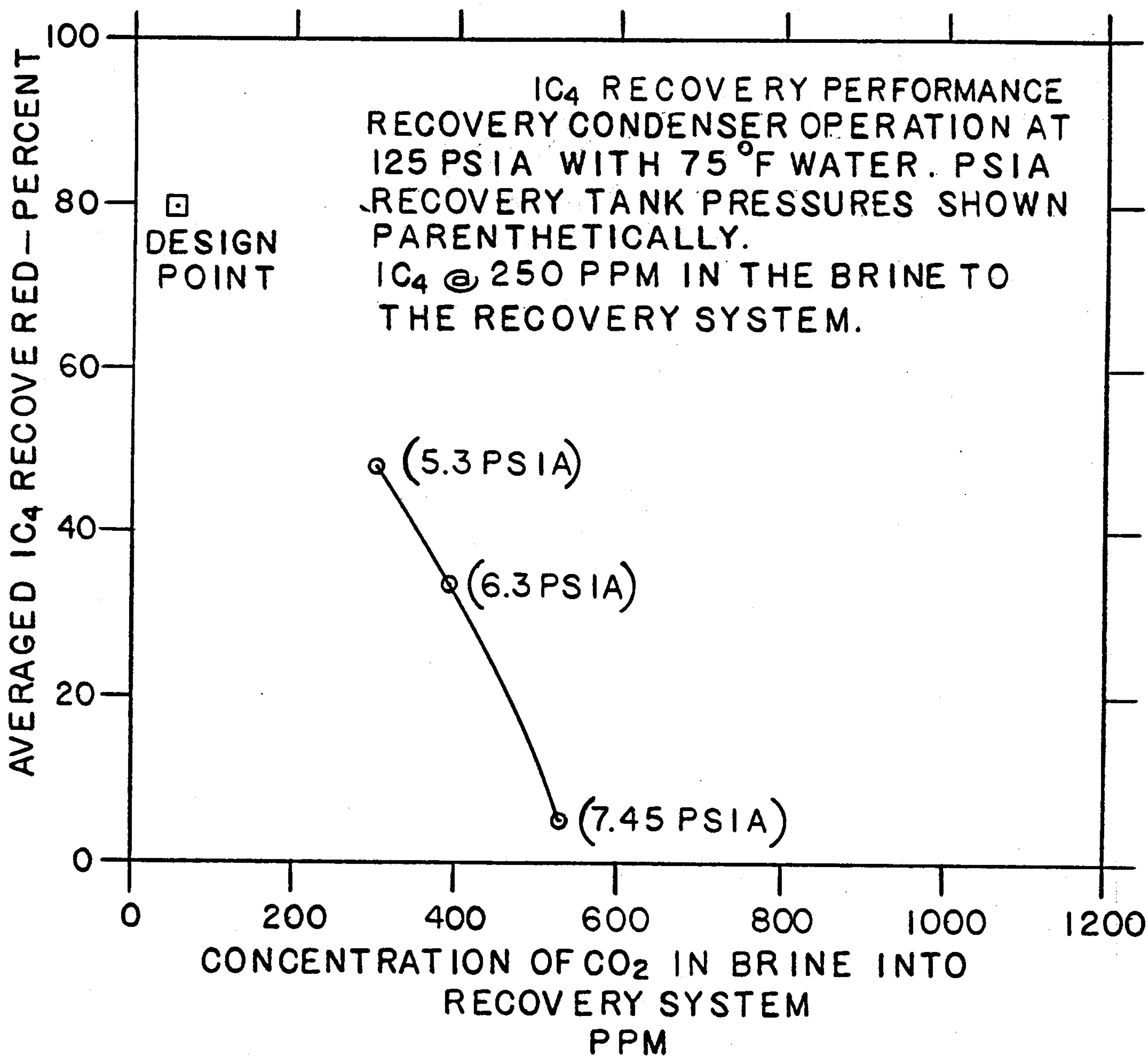

# FIGURE 3.20

VARIATION OF 500 KW PILOT PLANT UTILIZATION WITH ISO BUTANE BOILING TEMPERATURE

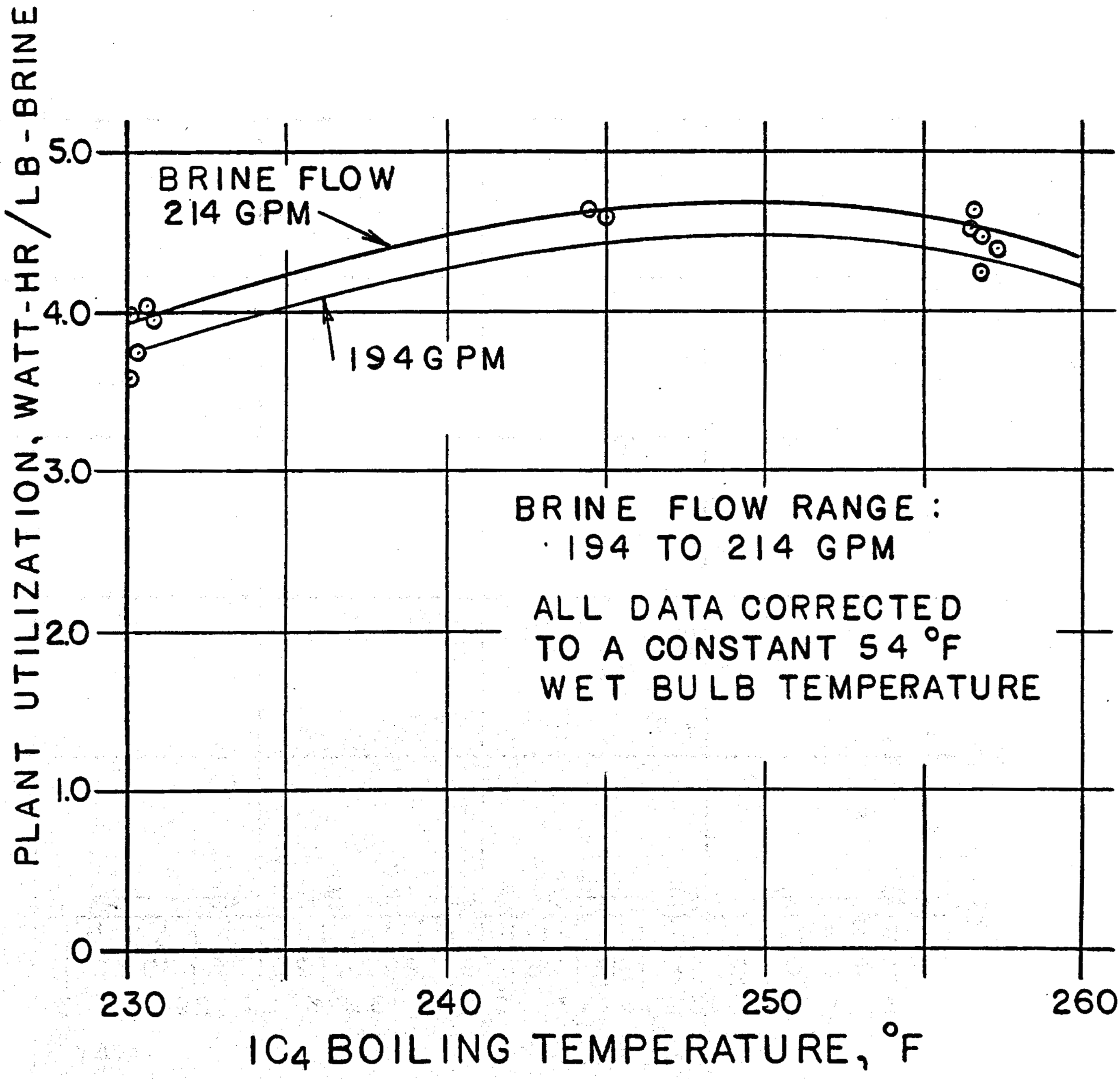

FIGURE 3.21

TURBINE EFFICIENCY VS. TIME

500 HOUR TEST

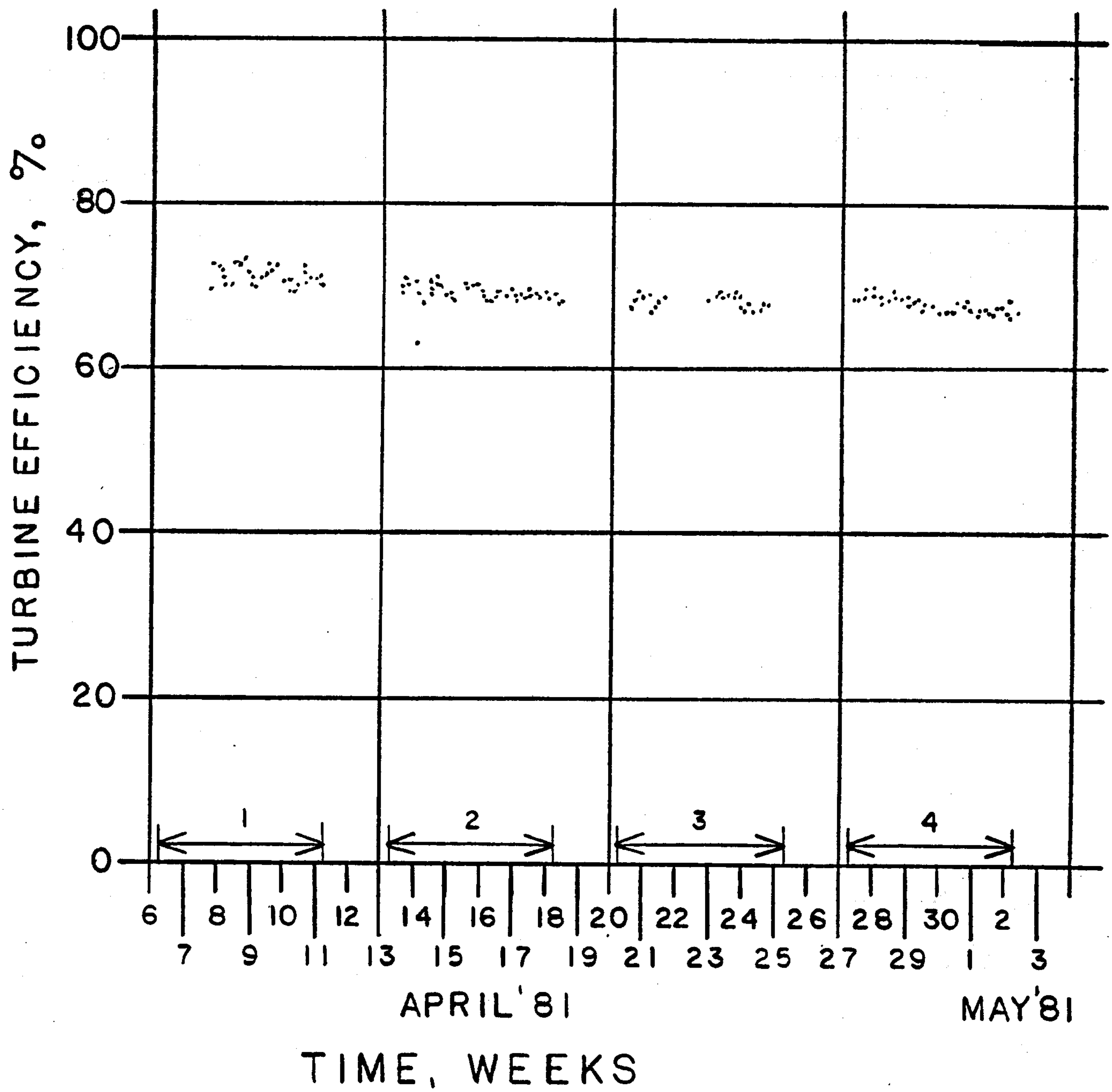

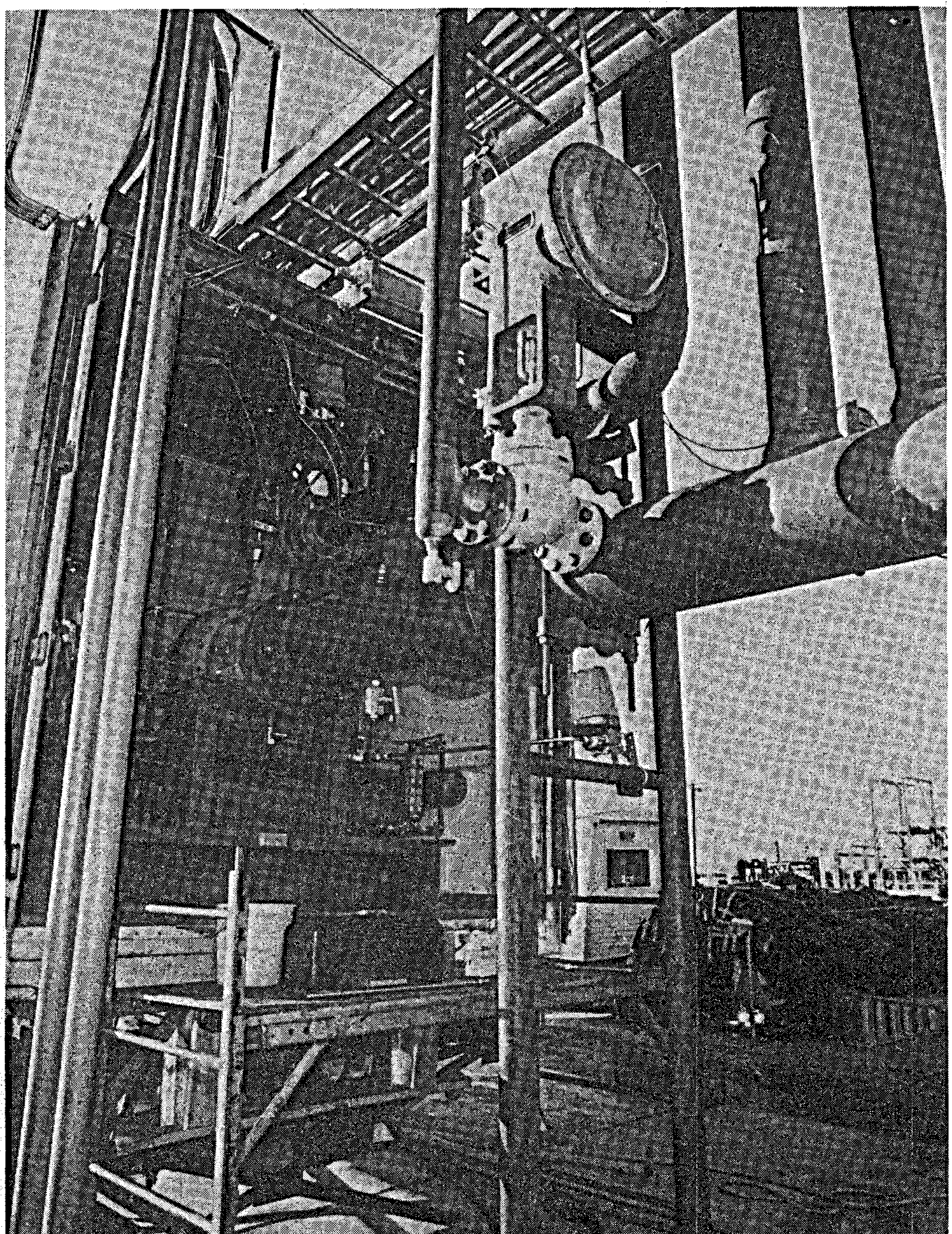

Figure 3.22 CBB 801-518
Power Turbine and Turbine Bypass Control Valve.

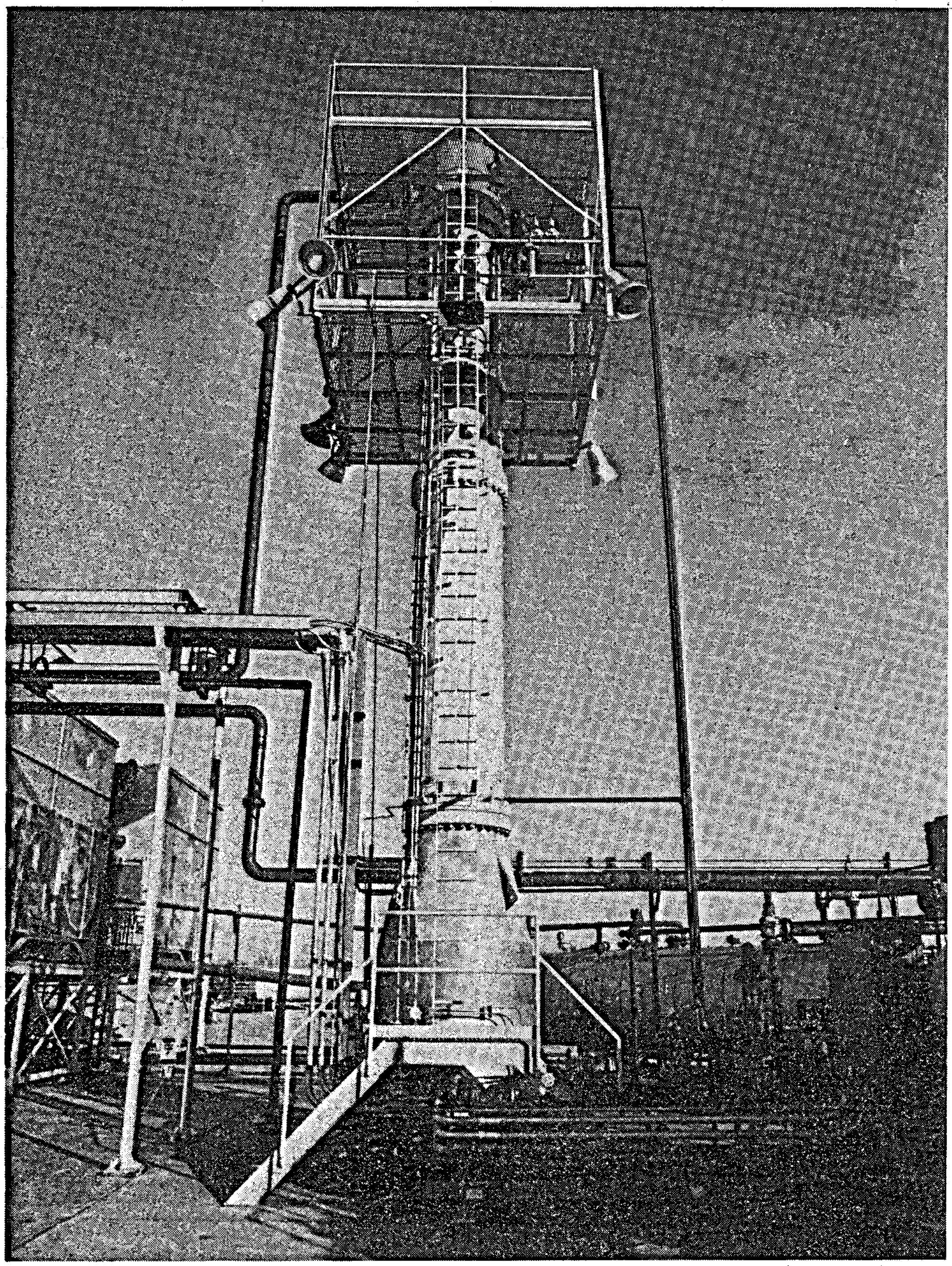

Figure 3.23 CBB 801-524
Direct Contact Heat Exchanger

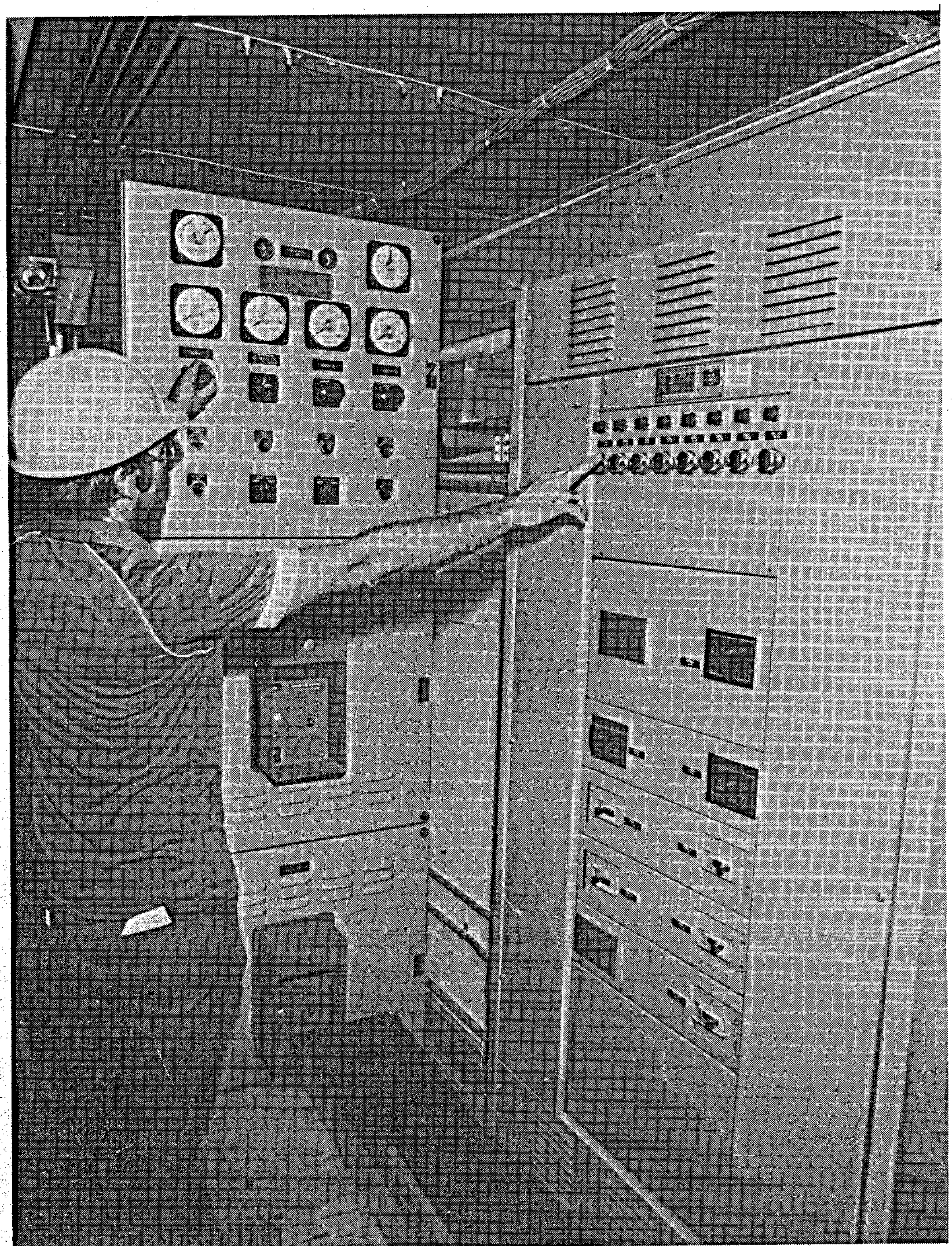

Figure 3.24 Power Trailer CBB 799-11553

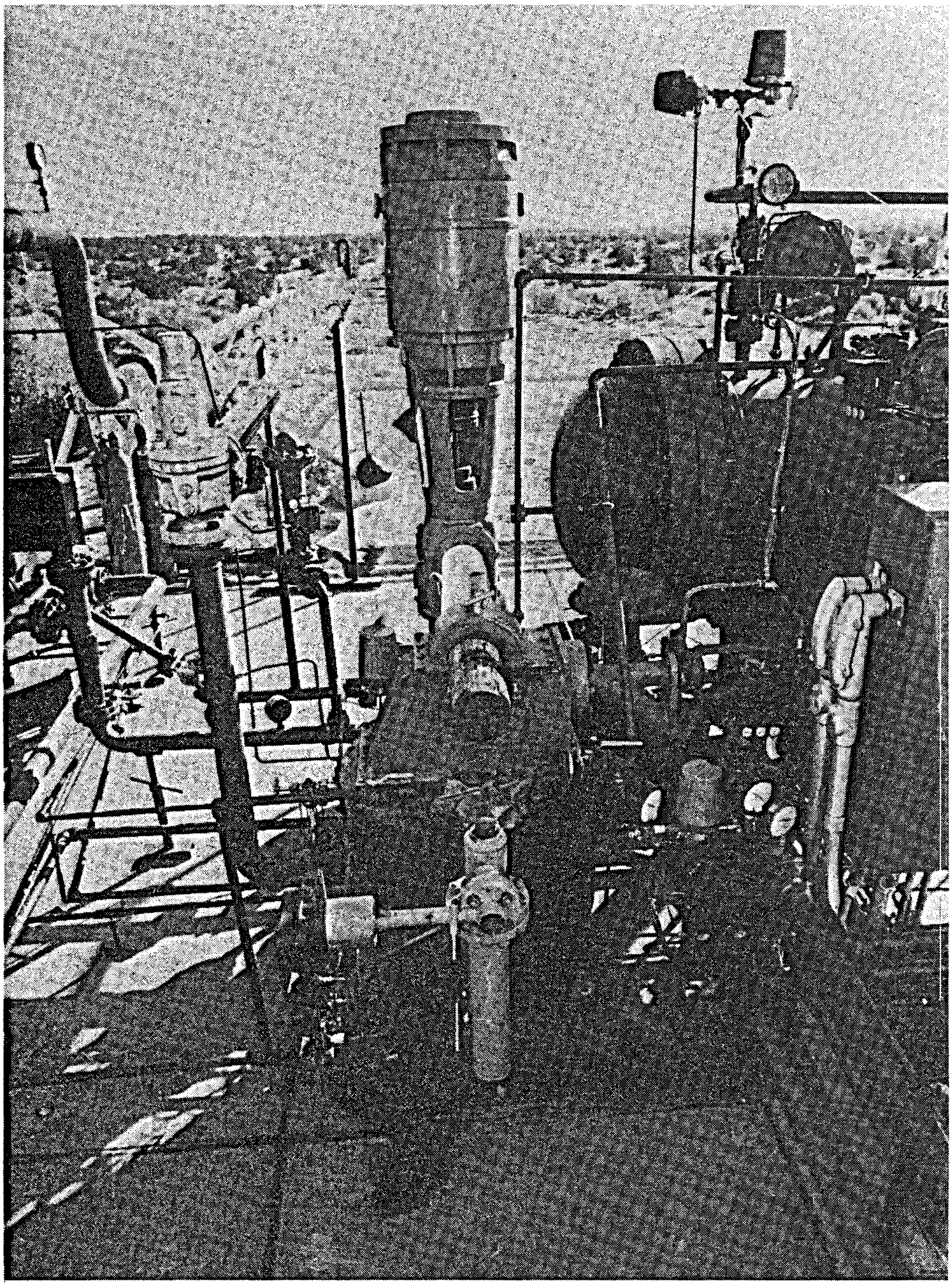

Figure 3.25 CBB 801-528
Hydraulic Turbine, Tailstock, and Brine Boost Pump.

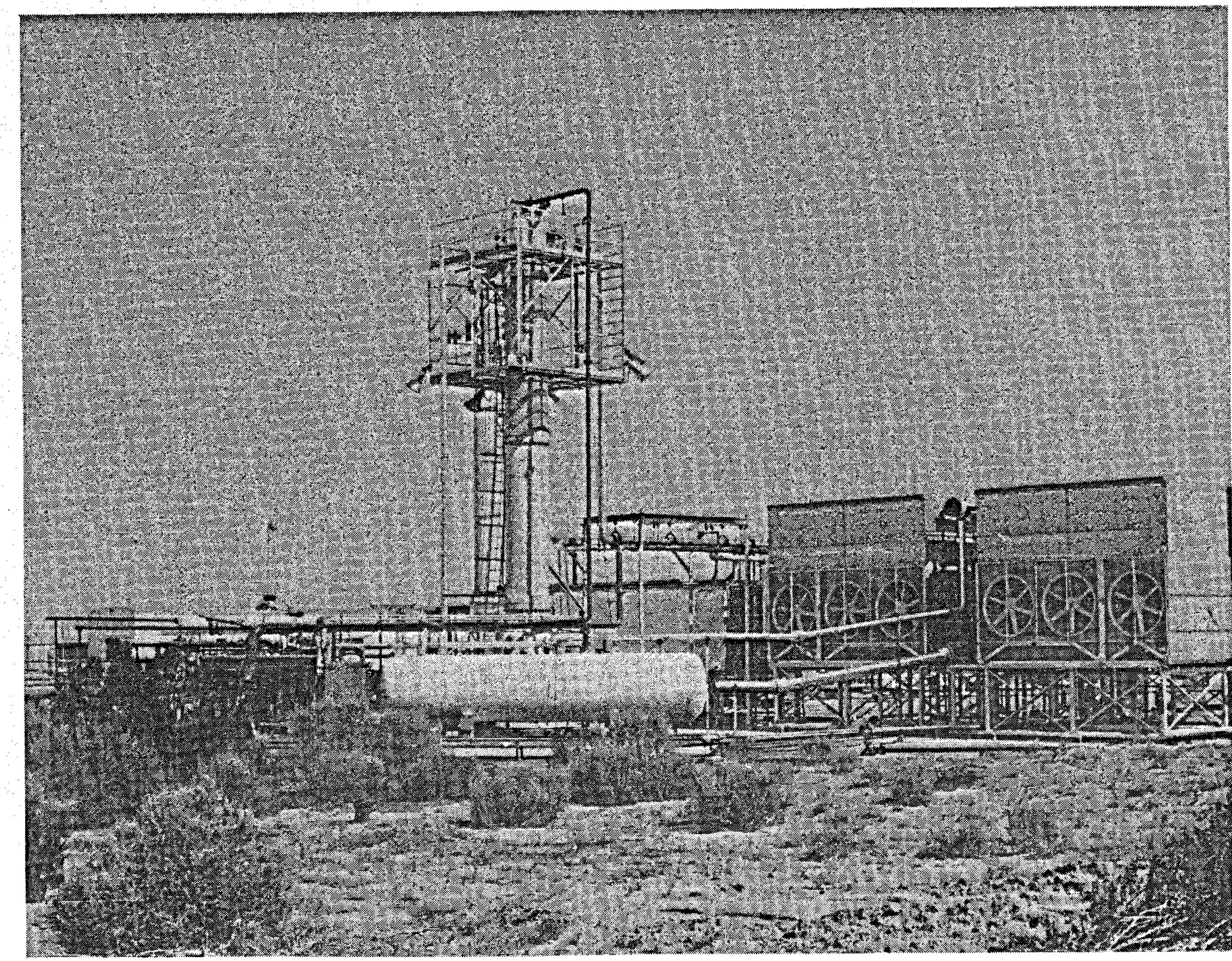

Figure 3.26 DCHX and Brine Module CBB 801-514

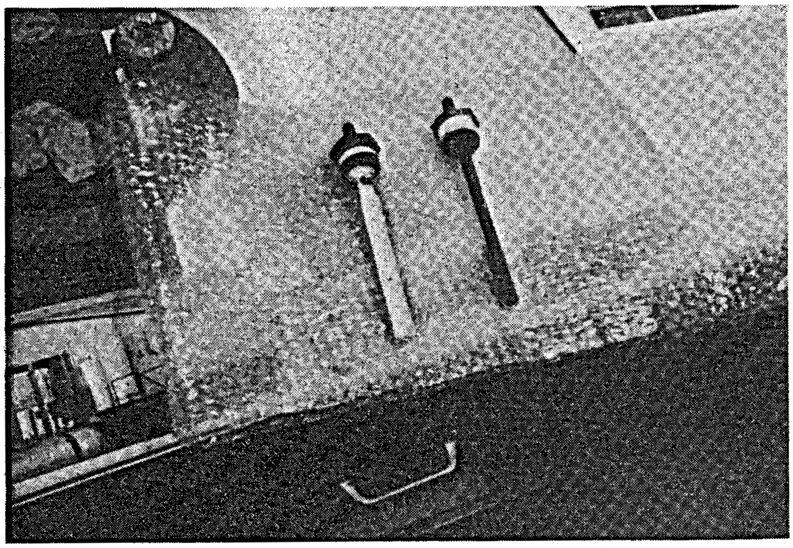

CBB 822-1086

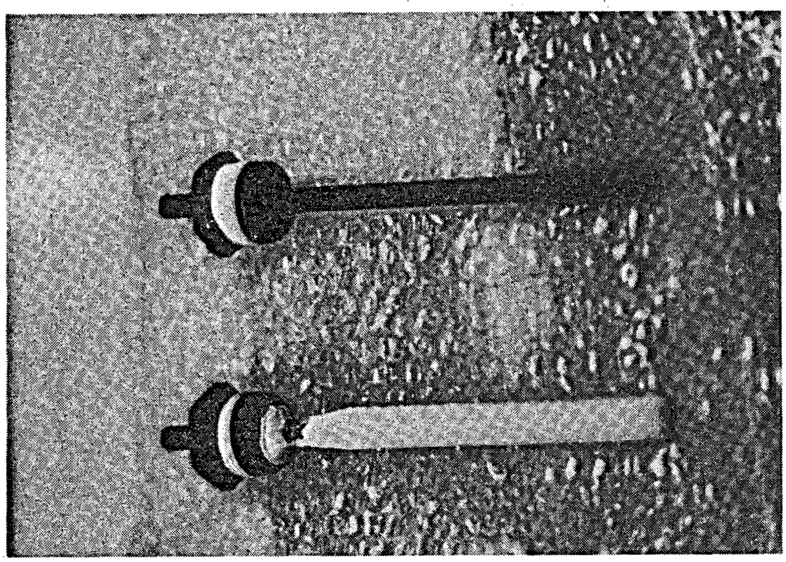

CBB 822-1084

Figure 3.27 Scale Build-up on Sample Coupons

APPENDIX A

## CALCULATION OF THE WATER TO $IC_4$ MASS RATIO IN THE WORKING FLUID LOOP

Let

$P_{IC_4}$ = partial pressure of $IC_4$ at DCHX working fluid exit - psia

$P_{H_2O}$ = partial pressure of $H_2O$ at DCHX working fluid exit - psia

$V$ = total volume occupied by gas - $ft^3$

$M^{IC_4}$ = total mass of $IC_4$ at DCHX working fluid exit - lbs

$M^{H_2O}$ = total mass of $H_2O$ at DCHX working fluid exit - lbs

$Z^{IC_4}$ = compressibility of $IC_4$ at DCHX working fluid exit

$Z^{H_2O}$ = compressibility of $H_2O$ at DCHX working fluid exit

$\bar{R}$ = universal gas constant = 1545 ft-lb/lb-mole-$^oR$

$MW^{IC_4}$ = molecular weight of $IC_4$ = 58 lb/lb-mole

$MW^{H_2O}$ = molecular weight of $H_2O$ - 18 lb/lb-mole

$T$ = temperature at DCHX working fluid exit - $^oF$

$m^{IC_4}$ = mass fraction of $IC_4$ at DCHX working fluid exit

$m^{H_2O}$ = mass fraction of $H_2O$ at DCHX working fluid exit

$v^{IC_4}$ = specific volume of $IC_4$ at DCHX working fluid exit - $ft^3/lb$

$v^{H_2O}$ = specific volume of $H_2O$ at DCHX working fluid exit - $ft^3/lb$

$P_T$ = total pressure at DCHX working fluid exit - psia

$P_{sat}^{H_2O}|_T$ = saturation pressure of $H_2O$ at DCHX working fluid exit temperature - psia

From the modified ideal gas equation of state:

$$(144)\, P^{IC_4} V = M^{IC_4} Z^{IC_4} \frac{\bar{R}}{MW^{IC_4}} T \qquad (1)$$

$$(144)\, P^{H_2O} V = M^{H_2O} Z^{H_2O} \frac{\bar{R}}{MW^{H_2O}} T \qquad (2)$$

Also $M^{IC_4} + M^{H_2O} = M_T$: $\qquad (3)$

Dividing (3) by $M_T$:

$$m^{IC_4} + m^{H} = 1 \qquad (4)$$

Combining (1) and (2):

$$\frac{P^{IC_4}}{P^{H_2O}} = \frac{M^{IC_4}}{M^{H_2O}} \frac{Z^{IC_4}}{Z^{H_2O}} \frac{MW^{IC_4}}{MW^{H_2O}} \left(\frac{M_T}{M_T}\right)$$

$$= \frac{m^{IC_4}}{m^{H_2O}} \frac{Z^{IC_4}}{Z^{H_2O}} \frac{MW^{IC_4}}{MW^{H_2O}} \qquad (5)$$

Solving (5) for $m^{IC_4}/m^{H_2O}$:

$$\frac{m^{IC_4}}{m^{H_2O}} = \frac{P^{IC_4}}{P^{H_2O}} \frac{Z^{H_2O}}{Z} \frac{MW^{IC_4}}{MW^{H_2O}} \frac{\bar{R}T}{\bar{R}T} \qquad (6)$$

Since the modified ideal gas equation of state can be written in terms of specific volumes, then

$$(144)\ P\nu = \frac{ZR}{MW}T$$

$$\nu = \frac{Z \cdot R \cdot T}{P \cdot MW\,(144)}$$

Equation (6) can be expressed

$$\frac{m^{IC_4}}{m^{H_2O}} = \frac{\nu^{H_2O}}{\nu^{IC_4}} \qquad (7)$$

Combining (7) and (4) and solving for

$$m^{H_2O} = \frac{1}{\frac{\nu^{H_2O}}{\nu^{IC_4}} + 1} \qquad (8)$$

Since the water vapor exiting the DCHX is in intimate contact with liquid brine entering, $\nu^{H_2O}$ can be assumed approximately equal to saturated vapor at the DCHX working fluid exit temperature. The specific volume of $IC_4$, $\nu^{IC_4}$ , is evaluated at the exit temperature and a partial pressure equal to $P_T - p_{sat}^{H_2O}\big|_T$.

Equation (8) is used to calculate the theoretical points of Figure 3.8.

# APPENDIX B

## CO2 CONCENTRATION MEASUREMENT ANALYSIS

Figure 3.2 shows the plant locations where samples were extracted for chemical analysis. Brine samples at B1, B2, and B3 were cooled at line pressure and collected in stainless steel bombs using the sampling train shown in Figure B-1a. A purge stream is established by fully opening needle valves V1 and V2 and throttling the flow with V3. Cooling is provided by a small shell-and-tube heat exchanger supplied with utility water. The technique yields a cooled representative sample at line pressure.

Brine samples were analyzed for dissolved $CO_2$ content using a Varian model 3700 gas chromatograph with 10 feet of 1/16 inch diamter Porapak Q** column and a thermal conductivity detector. Helium carrier gas flows of 30 ml/min and a column inlet pressure of 30 psig were used. The samples were maintained above line pressure using compressed helium and fed through a heated (120$^{o}$C) 2 ml liquid sampling valve as a liquid phase. The liquid sample vaporizes upon injection, releasing all dissolved gases to the column. Calibration was achieved by dissolving known amounts of $CO_2$ gas in deionized $H_2O$. Thermal decomposition of $NaHCO_3$ present in the brine may occur at injection temperatures causing higher than actual apparent readings. The strong correlation between theoretical $CO_2$ levels and those measured with this technique (see Section 3.2.2 and Figure 3.11) however, suggests this effect is minimal. The method yields an analytical precision of 6% or better on $CO_2$.

Samples from the working fluid loop were extracted without cooling using the scheme shown in Figure B-1b. Vapor samples from high temperature lines (WF1 and WF2) were maintained at line temperature during analysis to prevent condensation of $IC_4$ and water vapor. In addition to chromatographic analysis for $CO_2$, the working fluid loop samples were analyzed for air, $CH_4$, $C_3H_3$, $IC_4H_{10}$, and $NC_4H_{10}$. Column and detector parameters were the same as for the brine analysis. Samples were injected with a 25 - 1 vapor sampling valve. A precision of 4% on minor components was typical.

Determination of the dissolved working fluid in the brine leaving the DCHX at B3 and exiting the recovery system at B4 required a method for $IC_4$ analysis accurate in the ppm range. The liquid injection technique used for dissolved $CO_2$ determination proved unreliable for quantitative $IC_4$ determination. While the thermal conductivity detector displayed adequate sensitivity to $IC_4$ at these levels, suspected interference by the huge $H_2O$ peak that emerged just ahead of the $IC_4$ caused significant variation in the reported result of any given sample. $CO_2$, on the other hand, eluted before the $H_2O$ peak and reproduced adequately.

The liquid injection method was eventually abandoned in favor of the brine stripping scheme shown in Figure B-2. A volume-calibrated plexiglas vessel (Alltech. Assn. Model 8127) was initially purged and charged with helium at approximately atmospheric pressure. Brine was flashed into the vessel, eventually filling it to some convenient level. The helium headspace was first equilibrated with the brine through vigorous shaking and then analyzed for $IC_4$ with the gas chromatograph. Shaking allowed the helium to strip the $IC_4$ from the sample and transfer it to the headspace. The residual $IC_4$ in the brine at equilibrium was estimated from published solubility data (Ref. 4) at 1-2% of that found in the vapor. The technique yielded a precision of 10% or better in the parts-per-million range.

The $IC_4$ extracted in the tailstock and recovery vessels was sampled after it was compressed and sent to the recovery condenser (process stream 18, Figure 3.2). The composition and flow rate was monitored at RS1 to confirm the measurements at B3 using the stripping technique described above. Recovered $IC_4$ (process stream 19, Figure 3.2) was measured by counting the actuation of a liquid level float valve located in the recovery condenser. The volume of recovered fluid discharged per actuation was obtained by direct calibration.

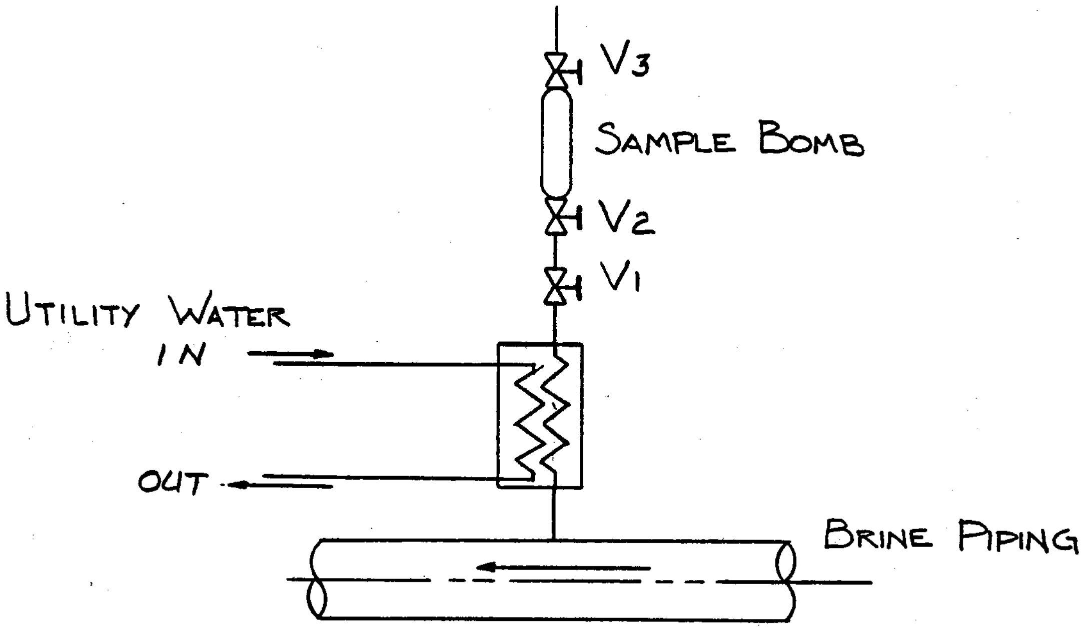


FIG B-1a BRINE SAMPLING SCHEMATIC

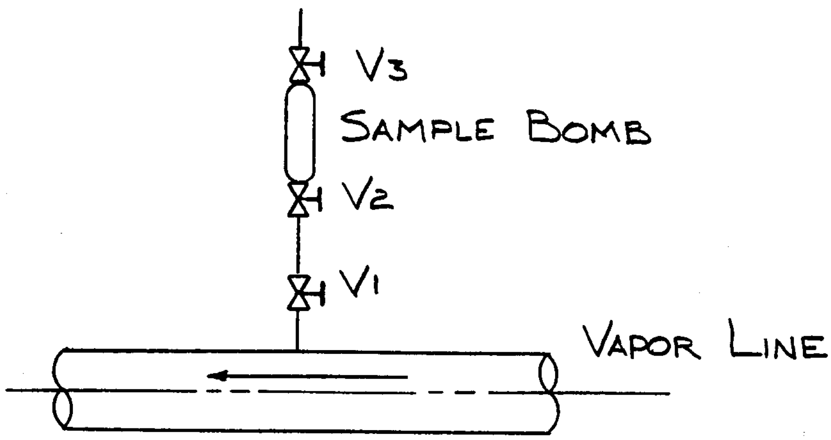


FIG. B-1b VAPOR SAMPLING SCHEMATIC

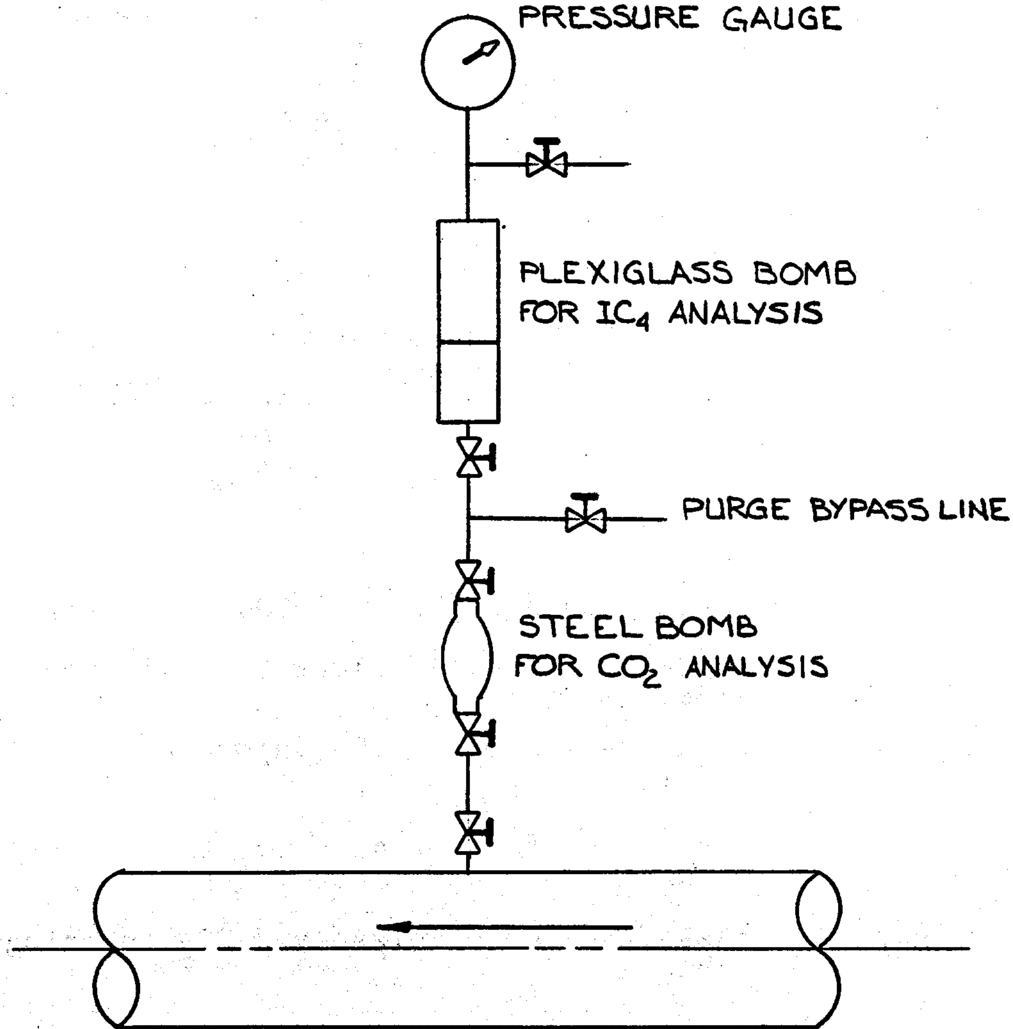


FIG. B-2: SCHEMATIC OF SAMPLE TRAIN FOR STRIPPING ANALYSIS TECHNIQUE

APPENDIX C

# A MODEL FOR THE SINGLE-STAGE ADIABATIC FLASH OF BRINE IN THE SAND TRAP

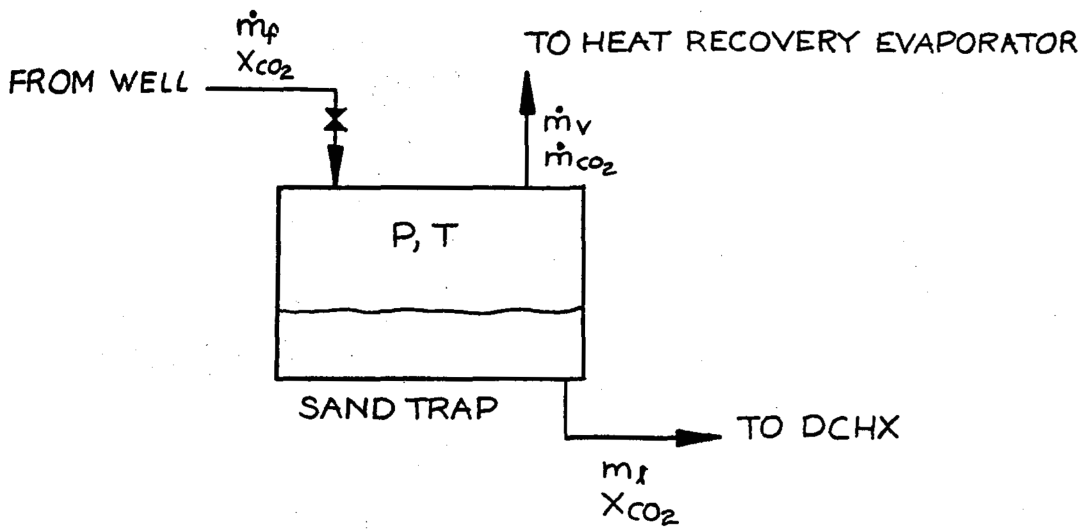


Let

$\dot{m}_f$ = total mass flow brine & $CO_2$ into flash tank, lb/hr

$\dot{m}_V$ = total mass flow of water vapor in vent flow, lb/hr

$\dot{m}_{CO_2}$ = total mass flow of $CO_2$ vapor in vent flow, lb/hr

$m_\ell$ = total mass flow brine & $CO_2$ leaving flash tank, lb/hr

$X^f_{CO_2}$ = mass fraction of dissolved $CO_2$ entering flash tank

$X_{CO_2}$ = mass fraction of dissolved $CO_2$ in brine leaving the flash tank

$Y_{CO_2}$ = mole fraction of $CO_2$ in vent

$T_{IN}$ = Temperature of brine entering flash tank (before valve), $^oF$

$P_{IN}$ = Pressure of brine entering flash tank (before valve), psia

$T$ = Temperature of 2-phase mixture in flash tank, $^oF$

$P$ = Pressure of 2-phase mixture in flash tank, psia

$p_{SAT}|_T$ = Saturation pressure of pure water evaluated at indicated temperature, psia

$h|_{T,P}$ = Enthalpy of pure water evaluated at indicated temperature and pressure, Btu/lb

$h_F|_T$ = Enthalpy of pure water saturated liquid at indicated temperature, Btu/lb

$h_S|_T$ = Enthalpy of pure water saturated vapor at indicated temperature, Btu/lb

$H|_T$ = Henry's law constant for CO2 in brine evaluated at indicated temperature, psi/mole fraction

From energy balance:

$$\dot{m}_f (1 - X^f_{CO_2}) h|_{T_{IN}, P_{IN}} = \dot{m}_V h_S|_T + \dot{m}_l (1 - X_{CO_2}) h_F|_T \qquad (1)$$

From $CO_2$ mass balance:

$$\dot{m}_f X^f_{CO_2} = \dot{m}_{CO_2} + \dot{m}_l X_{CO_2}$$

$$= \frac{\dot{m}_V}{(1 - Y_{CO_2})} \frac{Y_{CO_2}}{18} 44 + \dot{m}_l X_{CO_2} \qquad (2)$$

From Henry's law:

$$Y_{CO_2} = \frac{H(T)}{P} X_{CO_2} \frac{18}{44} \qquad (3)$$

From Raoult's rule:

$$(1 - Y_{CO_2}) = \frac{P_{SAT}|_T}{P} \qquad (4)$$

From $H_2O$ balance:

$$(1 - X^f_{CO_2}) \dot{m}_f = \dot{m}_V + \dot{m}_l (1 - X_{CO_2}) \qquad (5)$$

Case 1: $X^f_{CO_2}$, $P$, $\dot{m}_\ell$, $T_{IN}$, $P_{IN}$ are known and $X_{CO_2}$ is desired.

Substitute (5) into (2) -

$$\left\{\frac{\dot{m}_V + \dot{m}_\ell\,(1 - X_{CO_2})}{(1 - X^f_{CO_2})}\right\} X^f_{CO_2} = \frac{\dot{m}_V}{1 - Y_{CO_2}}\ \frac{Y_{CO_2}\,44}{18} + \dot{m}_\ell X_{CO_2}$$

$$\dot{m}_V \left\{\frac{X^f_{CO_2}}{(1-X^f_{CO_2})} - \frac{Y_{CO_2}}{(1-Y_{CO_2})}\ \frac{44}{18}\right\} = \dot{m}_\ell \left\{X_{CO_2} - \frac{(1-X_{CO_2})\,X^f_{CO_2}}{1 - X^f_{CO_2}}\right\}$$

$$\dot{m}_V = \dot{m}_\ell \left\{\frac{X_{CO_2} - \dfrac{(1-X_{CO_2})\,X^f_{CO_2}}{(1-X^f_{CO_2})}}{\dfrac{X^f_{CO_2}}{(1-X^f_{CO_2})} - \dfrac{Y_{CO_2}}{1-Y_{CO_2}}\ \dfrac{44}{18}}\right\} \quad (6)$$

Substitute (5) into (1) -

$$\left\{\frac{\dot{m}_V + \dot{m}_\ell\,(1 - X_{CO_2})}{\cancel{(1 - X^f_{CO_2})}}\right\} \cancel{(1 - X^f_{CO_2})}\ h\Big|_{T_{IN},P_{IN}}$$

$$= \dot{m}_V\, h_S\Big|_T + m_\ell\,(1 - X_{CO_2})\, h_F\Big|_T$$

$$\dot{m}_V = \dot{m}_\ell \left\{\frac{(1-X_{CO_2})\,h_F\big|_T - (1-X_{CO_2})\,h\big|_{T_{IN},P_{IN}}}{h\big|_{T_{IN},P_{IN}} - h_S\big|_T}\right\} \quad (7)$$

# FLOW CHART TO CALCULATE FLASH TEMPERATURE

The flash temperature is found iteratively with the following schematic. This approach is used to generate the predicted curve of Figure 3.10.

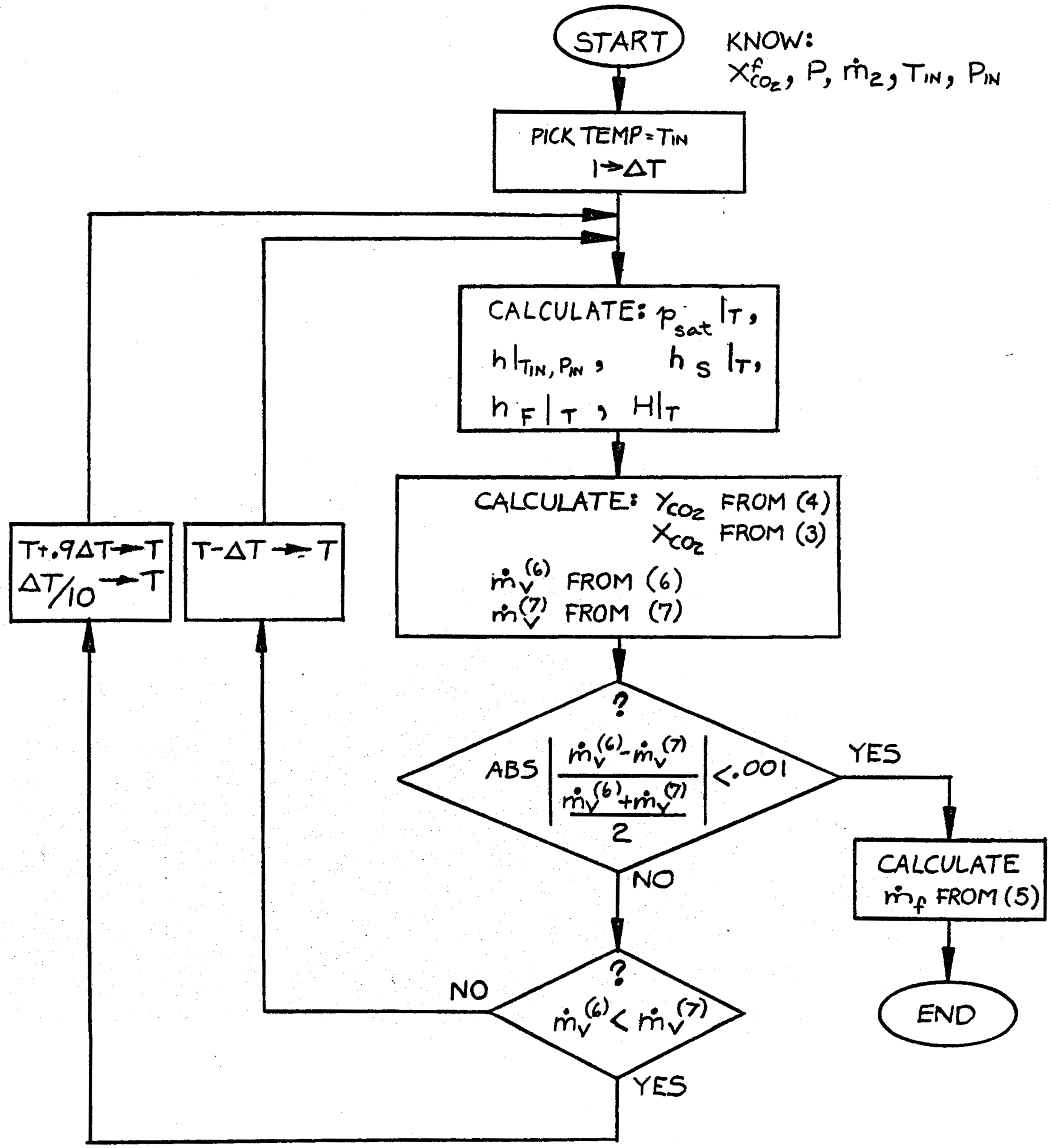

Case II: P and T are known and $X_{CO_2}$ is desired.

Combine (4) into (3) and solve for

$$X_{CO_2} = \frac{44}{18} \frac{P}{H|_T} \left(1 - \frac{p_{SAT}|_T}{P}\right) \tag{8}$$

# APPENDIX D

## A MODEL FOR THE CONDENSATION OF $H_2O$ AND $IC_4$ IN THE PRESENCE OF $CO_2$

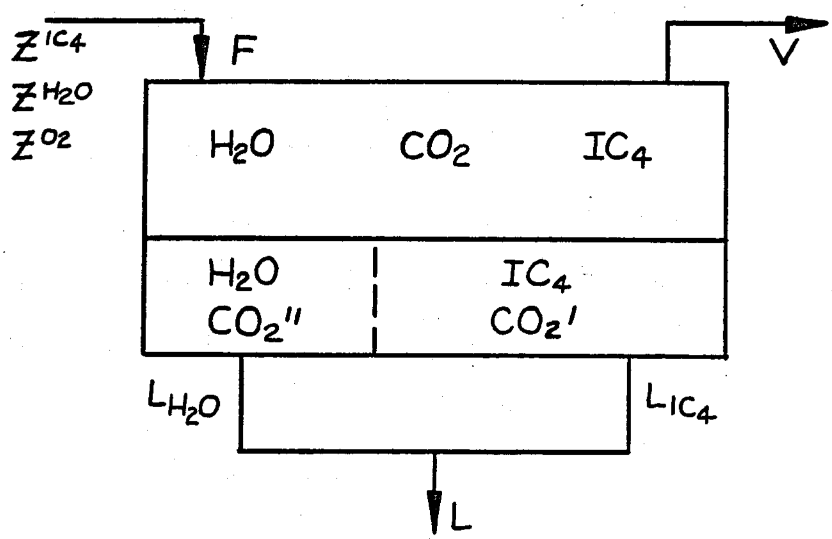


Let

$Z^{IC_4}$ = mole fraction of $IC_4$ in feed stream

$Z^{H_2O}$ = mole fraction of $H_2O$ in feed stream

$Z^{CO_2}$ = mole fraction of $CO_2$ in feed stream

$F$ = total molar flow of feed stream - moles/hr

$L_{H_2O}$ = total molar flow of water-rich condensate-moles/hr

$L_{IC_4}$ = total molar flow of $IC_4$-rich condensate-moles/hr

$L$ = total molar flow of condensate-moles/hr

$X'_{CO_2}$ = mole fraction of $CO_2$ in $IC_4$-rich condensate

$X''_{CO_2}$ = mole fraction of $CO_2$ in $H_2O$-rich condensate

$P^{H_2O}_{sat}$ = vapor pressure of saturated $H_2O$ at condensing temperature - psia

$P^{IC_4}_{sat}$ = vapor pressure of saturated $IC_4$ at condensing temperature - psia

| | | |
|---|---|---|
| $K'$ | = | phase equilibrium constant for $CO_2$ in $H_2O$ |
| $K''$ | = | phase equilibrium constant for $CO_2$ in $IC_4$ |
| $H'$ | = | Henry's law constant for $CO_2$ in $H_2O$ - psi/mole fraction |
| $H''$ | = | Henry's law constant for $CO_2$ in $IC_4$ - psi/mole fraction |
| $P_T$ | = | total pressure in condenser |
| $T$ | = | temperature of condenser |
| $Y_{IC_4}$ | = | mole fraction of $IC_4$ in vent stream |
| $Y_{H_2O}$ | = | mole fraction of $H_2O$ in vent stream |
| $Y_{CO_2}$ | = | mole fraction of $CO_2$ in vent stream |
| $V$ | = | vent flow rate - moles/hr |
| $\Delta P_{CO_2}$ | = | pressure elevation due to $CO_2$ accumulation - psia |
| $L_V$ | = | fraction of entering $IC_4$ lost through vent |

From $CO_2$ balance:

$$F \cdot Z_{CO_2} = Y_{CO_2} \cdot V + L_{H_2O} X''_{CO_2} + L_{IC_4} \cdot X'_{CO_2}$$

From Henry's law:

$$\frac{Y_{CO_2}}{X''_{CO_2}} = K'' = \frac{H''}{P_T} \qquad (2)$$

$$\frac{Y_{CO_2}}{X'_{CO_2}} = K' = \frac{H'}{P_T} \qquad (3)$$

Combining (1), (2), and (3) yields:

$$Y_{CO_2} = \frac{Z_{CO_2}}{\left(\frac{V}{F}\right) + \left(\frac{L_{H_2O}}{F}\right)\frac{P_T}{H''} + \left(\frac{L_{IC_4}}{F}\right)\frac{P_T}{H'}} \tag{4}$$

From $H_2O$ balance:

$$F \cdot Z_{H_2O} = Y_{H_2O} V + L_{H_2O}\left(1 - X''_{CO_2}\right) \tag{5}$$

or
$$L_{H_2O} = \frac{F \cdot Z_{H_2O} - Y_{H_2O} V}{\left(1 - X''_{CO_2}\right)} \tag{6}$$

From $IC_4$ balance:

$$F \cdot Z_{IC_4} = Y_{IC_4} V + L_{IC_4}\left(1 - X'_{CO_2}\right) \tag{7}$$

or
$$L_{IC_4} = \frac{F \cdot Z_{IC_4} - Y_{IC_4} V}{\left(1 - X'_{CO_2}\right)} \tag{8}$$

From Raoult's Law:

$$Y_{H_2O} \approx \frac{p_{sat}^{H_2O}}{P_T} \tag{9}$$

$$Y_{IC_4} \approx \frac{p_{sat}^{IC_4}}{P_T} \tag{10}$$

By definition:

$$Y_{H_2O} + Y_{CO_2} + Y_{IC_4} = 1 \tag{11}$$

Case 1 - Calculate the pressure elevation in the main power condenser without venting the condenser, i.e. V/F = 0

Combine (11) (10) (9) to yield:

$$y_{CO_2} = 1 - \frac{p_{sat}^{H_2O}}{P_T} - \frac{p_{sat}^{IC_4}}{P_T} \qquad (12)$$

Combining (8) (6) (4) (3) and (2) with V/F = 0 yields:

$$\frac{Z_{CO_2}}{\dfrac{Z_{H_2O}}{\dfrac{H''}{P_T} - y_{CO_2}} + \dfrac{Z^{IC_4}}{\dfrac{H'}{P_T} - y_{CO_2}}} \qquad (13)$$

Equation (12) and (13) can be solved iteratively for $P_T$ once the temperature and feed stream composition are specified.

The pressure elevation due to $CO_2$ accumulation is thus:

$$\Delta P_{CO_2} = P_T - p_{sat}^{IC_4} - p_{sat}^{H_2O} \qquad (14)$$

This procedure was used to calculate the theoretical line of Figure 3.13

Case 2 - Calculate the vent flow rate and $IC_4$ loss in the vent for condenser operation at a given pressure and temperature.

Combine (12) (8) (6) (4) (3) and (2) to yield:

$$\frac{Z_{CO_2}}{\left(V/F\right) + \dfrac{Z_{H_2O} - \left(p_{sat}^{H_2O}/P_T\right)\left(V/F\right)}{\dfrac{H''}{P_T} - y_{CO_2}} + \dfrac{Z_{IC_4} - \left(p_{sat}^{IC_4}/P_T\right)\left(V/F\right)}{\dfrac{H'}{P_T} - y_{CO_2}}}$$

$$= y_{CO_2} \qquad (15)$$

Equation (15) can be solved iteratively for V/F once T, $P_T$ and the feed stream composition are specified.

The $IC_4$ vent loss fraction can then be calculated as:

$$L_V = \frac{Y_{IC_4} \cdot V}{Z_{IC_4} \cdot F} \qquad (16)$$

APPENDIX E

## A MODEL OF THE 3 COMPONENT SINGLE STAGE FLASH IN THE $IC_4$ RECOVERY SYSTEM

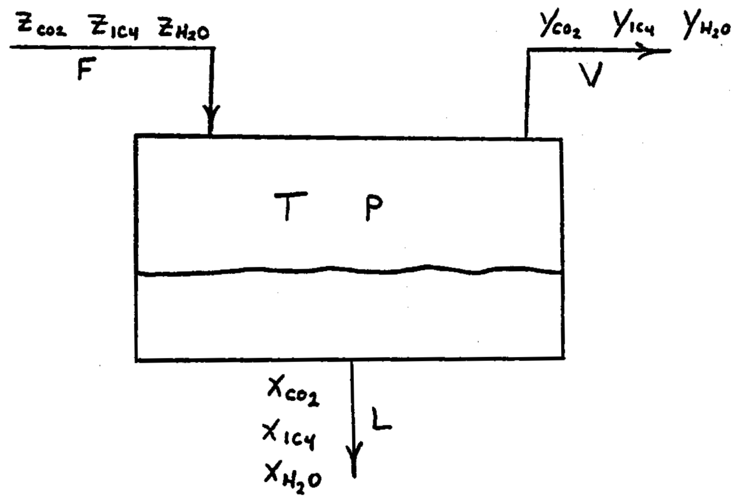


Let

| | | |
|---|---|---|
| $z_{CO_2}$ | = | the mole fraction of $CO_2$ in the flash tank feed stream |
| $z_{IC_4}$ | = | the mole fraction of $IC_4$ in the flash tank feed stream |
| $z_{H_2O}$ | = | the mole fraction of $H_2O$ in the flash tank feed stream |
| F | = | the total flow rate of feed stream - moles/hr. |
| $y_{CO_2}$ | = | the mole fraction of $CO_2$ in the Vent Stream |
| $y_{IC_4}$ | = | the mole fraction of $IC_4$ in the Vent Stream |
| $y_{H_2O}$ | = | the mole fraction of $H_2O$ in the Vent Stream |
| V | = | the total flow rate of vent stream - moles/hr. |
| $x_{CO_2}$ | = | the mole fraction of $CO_2$ in the liquid discharge stream |
| $x_{IC_4}$ | = | the mole fraction of $IC_4$ in the liquid discharge stream |
| $x_{H_2O}$ | = | the mole fraction of $H_2O$ in the liquid discharge stream |
| L | = | the total flow rate of liquid discharge stream - moles/hr. |
| T | = | Flash Tank temperature - $^{o}F$ |
| P | = | Flash Tank pressure - psia |
| $P_{sat}$ | = | saturation pressure of $H_2O$ at the tank temperature - psia. |

$H'$ = Henry's law constant for $CO_2$ in $H_2O$ - psia/mole ratio.

$H''$ = Henry's law constant for $IC_4$ in $H_2O$ - psi/mole ratio.

From an $IC_4$ balance:

$$F \cdot z_{IC_4} - x_{IC_4} \cdot L = y_{IC_4} \cdot V$$

or

$$y_{IC_4} = \frac{F \cdot z_{IC_4} - x_{IC_4} \cdot L}{V} \qquad (1)$$

From a $CO_2$ balance:

$$F \cdot z_{CO_2} - x_{CO_2} \cdot L = y_{CO_2} \cdot V$$

$$y_{CO_2} = \frac{F \cdot z_{CO_2} - x_{CO_2} \cdot L}{V} \qquad (2)$$

From an $H_2O$ balance:

$$F \cdot z_{H_2O} - x_{H_2O} \cdot L = y_{H_2O} \cdot V$$

$$y_{H_2O} = \frac{F \cdot z_{H_2O} - x_{H_2O} \cdot L}{V} \qquad (3)$$

From Equilibrium assumption:

$$\frac{y_{IC_4}}{x_{IC_4}} = \frac{H''}{P} \qquad (4)$$

$$\frac{y_{CO_2}}{x_{CO_2}} = \frac{H'}{P} \qquad (5)$$

$$\frac{y_{H_2O}}{x_{H_2O}} = \frac{P_{sat}}{P} \qquad (6)$$

From an overall balance:

$$L = F - V \qquad (10)$$

and $$Y_{IC_4} + Y_{CO_2} + Y_{H_2O} = 1 \qquad (11)$$

Combining equations 2, 4, 6, 7, 8, 9, 10, & 11 yields:

$$\frac{z_{CO_2}}{\left(\frac{V}{F}\right) + \left(1 - \frac{V}{F}\right) \cdot \frac{P}{H'}} + \frac{z_{IC_4}}{\left(\frac{V}{F}\right) + \left(1 - \frac{V}{F}\right) \cdot \frac{P}{H''}} + \frac{z_{H_2O}}{\left(\frac{V}{F}\right) + \left(1 - \frac{V}{F}\right) \cdot \frac{P}{P_{sat}}} = 1 \qquad (12)$$

Equation (12) can be solvediteratively for V if the tank pressure, temperature, and inlet flow and composition is specified.

# APPENDIX F

## 500 HOUR TEST LOG

The LBL-500 Direct Contact Pilot Plant was scheduled to make a 500-hour continuous run during the period of Monday, April 6, 1981, to Saturday, May 2, 1981, excluding the weekends. The following paragraphs present an abbreviated account of the run during the period and a summary of consumable usage.

### Week 1 - 0700 Hours, 4/6/81 to 0700 Hours, 4/11/81

Following final instrumentation adjustments and plant checks, brine from well 6-2 was brought onto the test pad at approximately 1200 hours on Monday, 4/6/81. Process flows were brought up and stabilized in a normal fashion. At 1500 hours the generator was brought up to speed but could not be synchronized with the line. The generator was shut down and the plant was run in the bypass mode through the night. At approximately 0800 hours the next morning (4/7/81), the entire site was shut down due to an electrical power outage. Brine was back on the site by 1030 hours and the plant was brought back up. At approximately 1500 hours the generator was brought up and the plant put on internal power, the problem having been found to be incorrect generator phasing wiring following repair and reinstallation. Plant operating conditions for the first week were:

| | |
|---|---|
| DCHX pressure: | Approximately 450 psia |
| Brine flow: | 210-220 gpm |
| $IC_4$ | 330-340 gpm |
| Gross output: | 570-670 kw |
| Parisitic load: | 251-279 kw |

The plant operated smoothly until it was deliberately shut down for the weekend at approximately 0700 hours on Saturday, 4/11/81.

### Week 2 - 0700 Hours, 4/13/81 to 0700, 4/18/81

Brine was brought onto the test site at 0915 hours on Monday, 4/13/81. The plant was brought up to normal fashion and switched over to internal power at 1120 hours. The plant continued to run until 2142 hours the same day, when maintenance on the display

# APPENDIX F

## 500 HOUR TEST LOG

The LBL-500 Direct Contact Pilot Plant was scheduled to make a 500-hour continuous run during the period of Monday, April 6, 1981, to Saturday, May 2, 1981, excluding the weekends. The following paragraphs present an abbreviated account of the run during the period and a summary of consumable usage.

<u>Week 1 - 0700 Hours, 4/6/81 to 0700 Hours, 4/11/81</u>

Following final instrumentation adjustments and plant checks, brine from well 6-2 was brought onto the test pad at approximately 1200 hours on Monday, 4/6/81. Process flows were brought up and stabilized in a normal fashion. At 1500 hours the generator was brought up to speed but could not be synchronized with the line. The generator was shut down and the plant was run in the bypass mode through the night. At approximately 0800 hours the next morning (4/7/81), the entire site was shut down due to an electrical power outage. Brine was back on the site by 1030 hours and the plant was brought back up. At approximately 1500 hours the generator was brought up and the plant put on internal power, the problem having been found to be incorrect generator phasing wiring following repair and reinstallation. Plant operating conditions for the first week were:

| | |
|---|---|
| DCHX pressure: | Approximately 450 psia |
| Brine flow: | 210-220 gpm |
| $IC_4$ | 330-340 gpm |
| Gross output: | 570-670 kw |
| Parisitic load: | 251-279 kw |

The plant operated smoothly until it was deliberately shut down for the weekend at approximately 0700 hours on Saturday, 4/11/81.

<u>Week 2 - 0700 Hours, 4/13/81 to 0700, 4/18/81</u>

Brine was brought onto the test site at 0915 hours on Monday, 4/13/81. The plant was brought up to normal fashion and switched over to internal power at 1120 hours. The plant continued to run until 2142 hours the same day, when maintenance on the display panel resulted in an accidental short in the control loop causing the isobutane pump to shut down and its breaker to trip. The situation was corrected, and at 2340 hours the plant was back on internal power. The plant continued to run until 1220 hours on Thursday, 4/16/81. During the early morning hours on Wednesday, 4/15/81, a minor problem was encounted with the #4 condenser. The breaker for that condenser was being intermittently tripped. This tripping had minimum impact upon the plant performance and was traced later to a safety interlock. At 1220 hours on Thursday, 4/16/81, the Reda downhole pump went down for no apparent reason (a power fluctuation was suspected), causing the test site to go down. Brine was back on the pad at 1430 hours, but it took until 1730 hours to get back to the previous operating conditions due to an instrument wiring problem on the turbine underspeed alarm. Follow- these events the plant continued to run until it was deliberately shut down at approximately 0630 hours on Saturday, 4/18/81. Plant operating conditions for the second week were as follows:

| | |
|---|---|
| DCHX pressure: | Approximately 450 psia |
| Brine flow: | 200-210 gpm |
| $IC_4$ flow: | 305-330 gpm |
| KW output (gross): | 545-660 KW |
| Parasitic load: | 251-279 KW |

During the second week, the pressure in the sand trap was run at a lower level (higher brine flash). At this pressure it was necessary to reduce brine flow in order to continue running the same pressure in the DCHX.

<u>Week 3 - 0700 Hours, 4/20/18 to 0700 Hours, 4/25/81</u>

Following minor instrumentation adjustments and repair of the hydraulic turbine drive line guard, brine was brought onto the pad at 1020 hours on Monday, 4/20/81. The plant was on internal power by 1120 hours and continued to run until 0730 hours on Tuesday, 4/21/81, when it was deliberately shut down to fix a leak from the hydraulic turbine shaft seal. Upon repair it was found that both inboard and outboard seals originally had been installed incorrectly. Both seals were replaced, and the plant was brought up at approximately 0900 hours on Wednesday, 4/22/81. Upon startup a view port on the DCHX blew a seal and it was necessary to shut the plant down again. The column was drained and a blind flange installed in place of the view port as a replacement seal was not available. The plant was started up at 1940 hours the same day and back to full internal power by 2100 hours. The plant continued to run until approximately 1545 hours on Friday, 4/24/81, when a power outage (suspected fluctuation) caused the Reda downhole pump to go down, in turn causing the test site to go down. Upon startup, the recovery compressor consistently tripped the thermal overloads, so the plant was left down for the weekend and the compressor was repaired.

Week 4 - 0700 Hours, 4/27/81 to 0700 Hours, 5/2/81

Brine was brought onto the test pad at 1100 hours on Monday, 4/27/81. At 1200 hours the plant was running on internal power and continued to run in a normal fashion until 0915 hours on Thursday, 4/30/81, when the recovery compressor kicked out, causing a high pressure level in the tailstock which, in turn, automatically shut the plant down. The reason the compressor kicked out was not found, and the plant was back on internal power by 1105 hours the same morning. At 0915 hours the next morning (Friday, 5/1/81), the recovery compressor was shut down due to oil leaks. The plant was restarted without the recovery system and continued to run until 1000 hours the same morning when the plant was shut down to patch a steam leak in the flex line between the sand trap and the binary heat exchanger. By 1200 hours the same morning the plant was back on internal power and continued to run until the final deliberate shutdown at 0700 hours on Saturday, 5/2/81. Stable plant operating conditions during the fourth week were similar to those of the second week.

General Comments

During this test period of 480 possible hours, actual total run times were as follows:

| | |
|---|---|
| Brine boost pump | 407.7 hours (84.9%) |
| $IC_4$ boost pump | 404.4 hours (84.3%) |
| Turbine | 376.8 hours (78.5%) |

In addition to those mentioned previously, problems were encountered in other areas. These were of a minor nature and did not affect the overall performance of the plant. Examples of these are:

1) Broken RTD's
2) Recovery condenser accumulator dump switch hanging up
3) Inaccurate instrument calibration
4) Chemical pumps on condensers loosing prime

These were not all of the minor problems encountered, but are presented to give the reader an idea of everyday plant operation.

It should be noted that during this four-week run, no problems due to scaling of equipment were encountered. This is attributed to the injection of the Pfizer Flocon 247 into the sand trap inlet brine line.

Consumable Usage

Consumables are defined as $IC_4$, $CO_2$, acid and inhibitor for the condensers, $N_2$, Pfizer Flocon 247, and turbine oil. Total measured $IC_4$ loss for the entire period was approximately 990 gallons. Some of this can be attributed to losses through the seals on the tailstock and the recovery compressor.

$CO_2$ usage was six 50# bottles. This usage rate is higher than normal due to losses through the tailstock seals.

Combined utility cooler and main condenser acid and inhibitor usages were approximately 85 and 40 gallons, respectively. This is to be considered normal usage.

Two nitrogen bottles were used. Since a broken burst disk in the vent system was found during the run period, this usage may be higher than normal.

Approximately 18.5 gallons of Pfizer Flocon was used during the test period. As extensive testing of this scale inhibitor has not been performed, the lowest feasible usage rate is unknown at this time.

The best estimate of turbine oil losses through the seals is 10 gallons for the entire period. For unknown reasons, most of the loss appeared to occur during the first week.